BIOLOGICAL AND CHEMICAL OXIDATION OF SULFIDIC MINERALS AT ALKALINE pH

by

Jungwoon Lee

A thesis submitted to The Robert M. Buchan Department of Mining

In conformity with the requirements for

the degree of Master of Applied Science

Queen's University

Kingston, Ontario, Canada

(December 2021)

Copyright ©Jungwoon Lee, 2021

Abstract

The oxidation of sulfidic minerals to liberate gold is currently performed with the utilization of microorganisms and chemical reagents. Biooxidation is a hydrometallurgical oxidation method which can be a pre-treatment method for gold recovery. Iron- and sulfur-oxidizing microorganisms with varying physiological characteristics liberate sulfide matrices by using reduced sulfur compounds for growth, which exposes minerals such as gold to lixiviants. Compared to conventional methods, biooxidation is an environmentally friendly and more economic pre-treatment method. The chemical oxidation of sulfide minerals has been performed in all pH ranges. However, operating in higher pH environments can decrease operating and material costs. The aim of this investigation is to test the oxidative capabilities of alkaline bacteria and chemical reagents in three pyrite concentrates. Two alkaliphilic, halo-tolerant, and chemolithoautotrophic bacteria *Thiomicrospira aerophila* (DSMZ 13739) and *Thioalkalivibrio versutus* (DSMZ 13738) were used for this study. For chemical oxidation, the carbonate effect which occurs due to the presence of sodium carbonate and bicarbonate was evaluated. Various parameters such as pH, temperature, pulp density, time, and changes in media were altered to determine the optimal oxidative parameters. Investigations with bacteria suggest that iron precipitates produced during oxidation passivated onto the particles, preventing them from attaching to the particle surface. This resulted in all experiments without the inoculation of bacteria oxidizing more pyrite than the experiments with bacteria. Therefore, chemical oxidation via the carbonate effect was investigated. Complete oxidation of the sample was observed at 11 days using 20 g/L Na_2CO_3 and 10 g/L $NaHCO_3$ with parameters of 80 °C, air supplied at 0.1 L/min, 20% pulp density, and stirred at 500 rpm. Further, qualitative, and quantitative analysis were performed on the oxidized samples to investigate physical and chemical changes in the samples. Gold leaching tests with conventional cyanidation techniques were performed on oxidized samples to determine the relationship between oxidation and gold recovery.

Acknowledgements

I would like to express my profoundest gratitude to my supervisor, Dr. Ahmad Ghahreman for his insights, continuous support and confidence in my abilities. I am grateful to be a student who learned so much from an exceptional teacher. I would also like to thank Dr. Harshit Mahandra for his support in the completion of my thesis and for his invaluable expertise. To my fellow colleagues in the Hydrometallurgy lab (especially James McNeice, Fariborz Faraji and Guillermo Alvial Hein), thank you for the continuous support and guidance over the past two years. Brooke Belfall and Larissa Smith, I am grateful for your help in improving my abilities and technical knowledge in the lab. I am thankful for Queen's University and The Robert M. Buchan Department of Mining for any assistance and support throughout my academia. To my thesis committee, I am appreciative of all your advice and suggestions throughout my defense process. Finally, thank you to my parents and friends for their patience and dedication in the completion of my graduate studies.

Table of Contents

Abstract ii
Acknowledgements iii
List of Figures vii
List of Tables ix
List of Abbreviations x
Chapter 1 Introduction 1
1.1 Background Information 1
1.2 Bacterial Oxidation 3
1.3 Chemical Oxidation 4
1.4 Scope and outline of the research project 5
Chapter 2 Literature Review 8
2.1 Mechanisms of Biooxidation 8
2.1.1 Chemolithotroph and Hydrogen Oxidation 8
2.1.2 Oxidation by Chemolithotrophic Denitrification 10
2.1.3 Contact, Non-contact and Cooperative Mechanisms of Bacterial Metal Sulfide Dissolution 11
2.1.4 Chemical Mechanisms of Bacterial Metal Sulfide Dissolution 13
2.1.5 Chemolithotrophic Oxidation of Reduced Sulfur Compounds 14
2.2 Sulfur-Oxidizing Microorganisms 15
2.2.1 Nutrients for Sulfur-Oxidizing Bacteria 16
2.2.2 Calvin-Benson-Bassham cycle 18
2.2.3 Role of Acidophilic Microorganisms in Metal Sulfide Oxidation 19
2.2.4 Role of Neutrophilic Microorganisms in Biooxidation 22
2.2.5 Role of Alkaliphilic Microorganisms in Biooxidation 27
2.2.6 Thiopaq® Process 31
2.3 Carbonate Effect 32
2.4 Bacteria Used in this Investigation 37
2.4.1 *Thiomicrospira aerophila* 37
2.4.2 *Thioalkalivibrio versutus* 38
2.4.3 Bacteria Growth Cycle 39
Chapter 3 Materials and Experimental Methods 41
3.1 Raw Materials 41
3.1.1 Ore Characterization 41

3.2 Experimental Methods 42
3.2.1 Growth and Maintenance of Bacteria 42
3.2.2 Na_2S Oxidation Studies 44
3.2.3 Bacterial Oxidation 44
3.2.4 Bottle Roll 45
3.2.5 Chemical Oxidation 46
3.2.6 Gold recovery 46
3.3 Analytical Methods 47
3.3.1 Analytical Techniques 47
3.3.2 Calculations and Error Estimation 47
3.3.3 Safety Precautions 48
Chapter 4 Results and Discussion 49
4.1 Growth Curves 49
4.1.1 Growth of *Thiomicrospira aerophila* 49
4.1.2 Growth of *Thioalkalivibrio versutus* 51
4.1.3 Growth of Mixed Cultures 54
4.1.4 Growth Studies in Other Media 56
4.2 Na_2S Oxidation 57
4.3 Oxidation of GSL 60
4.3.1 Effect of Temperature 64
4.3.2 Effect of Reduced Thiosulfate Concentration 65
4.3.3 Effect of Pulp Density 66
4.3.4 Effect of Time 67
4.3.5 Studies on other process variables 68
4.4 Oxidation of EQ2 69
4.5 Bottle Roll tests 72
4.6 Investigations on the Carbonate Effect 73
4.7 Chemical Oxidation with COREM 73
4.7.1 Effect of Temperature 74
4.7.2 Complete Chemical Oxidation 79
4.7.3 Effect of Pulp Density 80
4.7.4 Investigations with other Media 81
4.8 XRD and SEM Studies 83
4.9 Gold Recovery 87

Chapter 5 Conclusion and Recommendations 89
References 93

List of Figures

Figure 2.1. Schematic representation of the metabolism in chemolithotrophic bacteria. Chemical elements and electrons are shown as spheres: black (carbon), white (hydrogen), red (oxygen), blue (phosphorus), purple (nitrogen). 9
Figure 2.2. Schematic diagram for contact, non-contact, and cooperative bacterial leaching and oxidation of metal sulfides. 12
Figure 2.3. Schematic representation of the thiosulfate and polysulfide mechanism. Reproduced with permission from Schippers and Sand (1999). Copyright 1999, American Society for Microbiology. 13
Figure 2.4. Calvin-Benson-Bassham cycle 18
Figure 2.5: Schematic diagram of the Thiopaq® process 32
Figure 2.6: Schematic representation of the oxidation of pyrite in carbonate solutions modified from Caldeira et al. (2010) 35
Figure 2.7: Eh-pH diagrams for a metastable Fe-S-CO_3-H_2O system at 25 °C for (a) goethite and Fe (II) – carbonate complexes; (b) ferrihydrite and Fe (II) – carbonate complexes; (c) soluble iron species. Concentrations: [Fe] = 0.008 mol/L; [S] = 0.017 mol/L; [CO_3] = 0.1 mol/L (Caldeira et al., 2010). 36
Figure 2.8: Typical growth cycle for microorganisms 39
Figure 3.1: Microbial cultures in a temperature-controlled shaker 43
Figure 3.2: Apparatus used for bottle roll experiments 45
Figure 3.3: Schematic of the experimental set-up for chemical oxidation tests 46
Figure 4.1: Growth curve (A) and pH change in the medium (B) for *Tm. aerophila* at pH 10.2 and 9.5 for 7 days at 30 °C and 150 rpm. 50
Figure 4.2: Microscopic picture of *Tm. aerophila* 51
Figure 4.3: Growth curve (A) and pH change in the medium (B) for *Tv. versutus* at pH 10.2 and 9.5 for 7 days at 30 °C and 150 rpm. 53
Figure 4.4: Microscopic picture of *Tv. versutus* 53
Figure 4.5: Growth curve (A) and pH change (B) for mixed bacteria at pH 9.5 and 10.2 and thiosulfate concentrations of 10 and 20 g/L 55
Figure 4.6: Oxidation of Na_2S (A) and the changes in pH (B), ORP (C), and DO (D) at pH 10.2 for 7 days at 30 °C and 150 rpm. 59
Figure 4.7: GSL oxidation at 1% pulp density and changes in pH (B), ORP (C), and DO (D) at pH 10.2 for 14 days at 30 °C and 150 rpm. 62

Figure 4.8: Surface morphology of GSL before (A) and after partial oxidation (B) at pH 10.2, 30 °C, and 150 rpm for 14 days 63
Figure 4.9: Effect of temperature at 30 and 35 °C with GSL at 1% pulp density, pH 10.2 and 150 rpm for 14 days 65
Figure 4.10: Effect of reduced thiosulfate concentration with GSL at 1% pulp density, pH 10.2, 35 °C and 150 rpm for 14 days 66
Figure 4.11: Effect of pulp density with GSL at pH 10.2, 30 °C and 150 rpm for 14 days 67
Figure 4.12: Effect of time with GSL at 1% pulp density, pH 10.2, 30 °C and 150 rpm 68
Figure 4.13: EQ2 oxidation at 1% pulp density and changes in pH (B), ORP (C), and DO (D) at pH 10.2 for 14 days at 30 °C and 150 rpm. 71
Figure 4.14: Bottle roll tests with COREM at 5% pulp density, 500 mL solution, ambient temperature, and 40 rpm for 2 weeks. 72
Figure 4.15: Effect of temperature and changes in pH (B), ORP (C), and DO (D) of COREM at 20% pulp density, air supplied at 0.1 L/min and 500 rpm for 7 days. 77
Figure 4.16: The change in colour of COREM in solution indicating oxidation. Pictured above is oxidation of a test at 80 °C, air supplied at 0.1 L/min and 500 rpm at 0 h (A), after 1 day (B) and after 7 days (C). 78
Figure 4.17: Colour change of the dry oxidized COREM samples of tests performed for 7 days, air supplied at 0.1 L/min and 500 rpm at varying temperatures. The experiments were conducted at 25 (A), 35 (B), 50 (C), 65 (D) and 80 °C (E). 78
Figure 4.18: Complete oxidation test with COREM performed at 80 °C, 0.1 L/min air and 500 rpm for 11 days 80
Figure 4.19: Pulp density tests with COREM at 80 °C, 0.1 L/min air and 500 rpm for 3 days 81
Figure 4.20: Oxidation with other media with COREM at ambient temperature for 3 days, 10% pulp density and 500 rpm. 82
Figure 4.21: Oxidation of COREM comparing the original and altered media at 80 °C, 20% pulp density, air supplied at 0.1 L/min and 500 rpm for 7 days. 83
Figure 4.22: XRD analysis of COREM for the original ore (A), completely oxidized ore (B), and residue after HCl leaching (C). 85
Figure 4.23: Surface morphology of COREM before oxidation (A), after oxidation (B), and after acid washing (C) of the completely oxidized ore. 87
Figure 4.24: Gold recovery by cyanidation of COREM chemically oxidized at varying temperatures, 20% pulp density, air supplied at 0.1 L/min and 500 rpm for 7 days. 88

List of Tables

Table 2.1: Nutrients required for a standard biooxidation process (Rawlings and Johnson, 2007)..... 16
Table 2.2: Metal sulfide oxidizing acidophilic microorganisms (Donati and Sand, 2007)..... 20
Table 2.3: Predominate acidophilic microorganisms metal sulfide oxidizers (Bosecker, 1997; Bruynesteyn, 1989; Donati and Sand, 2007; Ewart and Hughes, 1991; Kelly and Wood, 2000; Mahmoud et al., 2017; Özkaya et al., 2007). 21
Table 2.4: Neutrophilic sulfur-oxidizing microorganisms and their characteristics 23
Table 2.5: Neutrophilic sulfur-oxidizing microorganisms used for biooxidation..... 25
Table 2.6: Characteristics of alkaliphilic sulfur-oxidizing bacteria 29
Table 2.7: Alkaliphilic sulfur-oxidizing microorganisms used for biooxidation processes..... 30
Table 3.1: Chemical analysis of the samples 41
Table 4.1: LPSA analysis of COREM oxidized at various temperatures 79

List of Abbreviations

AAS	Atomic Absorption Spectroscopy
ATP	Adenosine Triphosphate
CBB	Calvin-Benson-Bassham
CS	Carbon Sulfur
DO	Dissolved Oxygen
EPS	Extracellular Polymeric Substances
LPSA	Laser Particle Size Analyzer
NADPH	Nicotinamide Adenine Dinucleotide Phosphate
ORP	Oxidation-Reduction Potential
SEM	Scanning Electron Microscope
SOB	Sulfur-Oxidizing Bacteria
XRD	X-Ray Diffraction

Chapter 1

Introduction

1.1 Background Information

Microorganisms are of significant interest in the mining industry and in waste treatment due to their high capacity to transform various toxic sulfur compounds into stable compounds. Various waste materials such as galvanic sludge, electronic waste, medical waste, waste slag etc. are remediable in the presence of sulfur-oxidizing bacteria (SOB) (Mahmoud et al., 2017) which are well-known for their oxidative abilities to desulfurize toxic compounds and liberate sulfide from mineral matrices. The progression of knowledge on iron- and sulfur-oxidizing bacteria led to the development of an alternative pre-treatment technique called biooxidation. Biooxidation is an advantageous pre-treatment method that is more robust, economical, and eco-friendlier than processes such as pressure oxidation and roasting. Biooxidation is a hydrometallurgical oxidation method that has been applied to recover precious metals by enhancing the microbial decomposition of refractory ores. These bacteria exploit various inorganic sulfur compounds by catalyzing sulfur redox reactions that are not spontaneous at ambient conditions (Sorokin et al., 2011). Biooxidation and bioleaching have been used to extract metals such as gold, silver, copper, cobalt, nickel, zinc and uranium at high efficiencies in irrigated (heap, dump, in situ and vat) and agitated processes using bacteria (Schippers et al., 2014).

The SOB are isolated from environments with natural sulfur cycles such as soda lakes. These bacteria are characterized into different groups depending on their optimal growth temperature i.e. psychrophiles ($T_{opt} \leq 15$ ˚C), mesophiles (T_{opt} = 20-45 ˚C), thermophiles (T_{opt} = 55-65 ˚C), hyperthermophiles (T_{opt} = 85-113 ˚C) (Willey et al., 2016). Their growth and sulfur-oxidizing capabilities depend on the pH, dissolved oxygen (DO), salt concentration, nutrients, and the presence of toxic compounds. They are also characterized based on their optimal pH for growth

i.e., acidophilic, neutrophilic and alkaliphilic bacteria. Most SOB are chemolithoautotrophic prokaryotes and vary in the pathways, enzymes, and mechanisms of electron transfer in the oxidation of sulfur species. However, some are photolithotrophs which use light as their energy source and do not require oxygen for their survival or for oxidation (Poulain and Newman, 2009). Mixed cultures of SOB, based on their sulfur-oxidizing abilities, are also used for biomining processes to enhance biooxidation. Over time, the bacteria can adapt to process conditions and increase in number and metabolic capabilities, improving metal recovery efficiency (Rawlings and Johnson, 2007). Although the composition of an added inoculum may be known, the microbes at the end of a process have been found to be dramatically different. This change can be due to new bacteria from "contaminated" feed (i.e., ores, medium, air, etc.) or from mutation.

Acidophilic bacteria have been extensively explored for biooxidation in the mining industry. However, there are no significant reports on biooxidation processes using neutrophilic and alkaliphilic bacteria, although operating at neutral and alkaline pH is beneficial to the economics of a biooxidation process. In a conventional biooxidation plant, pH control represents about one-third of the operational cost (29%), including sulfuric acid, limestone and lime. Before alkaline cyanide leaching, a neutralizing agent such as limestone and slaked lime is used to produce a neutral effluent at pH 7.0-8.0 and to precipitate iron and arsenic. Biooxidation performed at elevated pH conditions will reduce the operating costs of the process by eliminating the solid/liquid separation stage between the acidic biooxidation and alkaline cyanidation process for gold recovery. Furthermore, residual acid could be present in cyanide leaching, which could lead to cyanide volatilization as HCN. The absence of information on neutrophilic and alkaliphilic microorganisms is attributable to the dominance of acidophiles in biomining. However, as current processes encounter challenges due to variations in waste and mineralogy of refractory materials, continuous optimization of biomining processes is required for them to remain sustainable and economical. The evaluation of the oxidizing capabilities of neutrophiles and alkaliphiles will assist in

broadening the fundamental knowledge on biooxidation. Understanding the potential engineering applications of microorganisms can extend beyond biomining, immensely benefiting other biotechnical fields.

1.2 Bacterial Oxidation

The term refractory applies to gold ores when the conventional cyanidation recovers only around 80% of gold after fine grinding (Nan et al., 2014). Refractory materials include the submicroscopic or occlusion of fine-grained gold, presence of tellurides, carbonaceous matter, clays, arsenic, iron and base-metal sulfides, silica encapsulation, and incomplete oxidation of elemental sulfur (Belyi et al., 2015b; Berezowsky and Weir, 2013; Fernández et al., 2000; Jha, 1987). Most refractory ores are comprised of sulfide and carbonaceous matter combined with gangue materials which prevents effective leaching by lixiviants due to preg-robbing and the occlusion of gold (Amankwah et al., 2005; Ofori-Sarpong et al., 2010). Furthermore, carbonaceous matter adsorbs the aurocyanide complex behaving like activated carbon (Adams et al., 1996). These factors result in lower lixiviant leaching efficiencies, higher lixiviant consumption and increased operating costs.

The energy consumption for the biooxidation of ores is often lower than for conventional techniques such as pressure oxidation and roasting. Furthermore, biooxidation is more advantageous for the refractory materials due to the high metal extraction in the leaching step as compared to the conventional methods. Currently, biooxidation processes for metal sulfides are inoculated with acidophilic SOB in aerobic conditions, and operate at pH=1.2-1.8 and 40-45 ˚C (Rawlings and Johnson, 2007). These processes require corrosion resistant materials and neutralization of wastewater as acid mine drainage can occur resulting in higher operating costs. Furthermore, the addition of lime is required to increase the pH for subsequent cyanidation for gold extraction as cyanide gas forms below pH 9.3-9.5 (ICMI, 2014). However, biooxidation in neutrophilic and alkaliphilic solutions can reduce or eliminate these issues, more specifically bio-

oxidation and gold leaching can occur in a singular mixed system such as a tank leaching process, or a non-mixed process such as a heap leaching process.

Acidophiles have been the dominant type of SOB utilized for biooxidation and their oxidation mechanisms have been studied intensively. However, there is little known about neutrophilic SOB and even less about alkaliphiles as compared to acidophiles.

1.3 Chemical Oxidation

Aqueous pyrite oxidation is generally described as an electrochemical reaction and can be performed in acidic, neutral, and alkaline conditions. The presence of Fe^{3+} and O_2 significantly increases the rate of pyrite dissolution, however, Fe^{3+} is more aggressive and effective as the oxidant in all pH ranges (Moses et al., 1987). The optimal oxidation parameters of iron minerals in alkaline conditions have been previously reported to be in high pH (pH = 9-13) and temperature (60-100 °C) environments (Caldeira et al., 2010; Ciminelli and Osseo-Asare, 1995; King and Lewis, 1980; Li et al., 2006; Verron et al., 2019; Wu et al., 2021).

Alkaline chemical oxidation is more advantageous than acidic oxidation for the treatment of high carbonate refractory gold ores. This avoids high acid consumption and suppresses elemental sulfur formation which accounts for agglomeration and gold loss (Bidari and Aghazadeh, 2018a). Further, the oxidative power of oxygen is amplified by reducing the production of carbon dioxide (Bidari and Aghazadeh, 2018a). Operating at high pH also reduces the chance of AMD occurring as it would buffer the generated acid from the process.

The oxidation of pyrite in alkaline solutions have been performed mainly in hydroxide, carbonate, bicarbonate, and lime media (Ciminelli and Osseo-Asare, 1995; Hossner and Doolittle, 2003; Huminicki and Rimstidt, 2009; Melashvili et al., 2016; Wu et al., 2021). Sodium hydroxide has advantages over the carbonate/bicarbonate media as it has shown an increase in oxidation due to the higher pH which results in higher gold recoveries by cyanidation (pH > 13) (Bidari and Aghazadeh, 2018a; Li et al., 2006). The addition of NaOH should be considered as expensive

relative to sodium carbonate/bicarbonate and requires higher concentrations which may cause economic problems in industrial processes. The combination of NaOH and sodium carbonate/bicarbonate media can also lead to more oxidation under specific parameters (Wu et al., 2021). Li et al. (2006) reported that a $Ca(OH)_2/Na_2CO_3$ media improves oxidation as $Ca(OH)_2$ increased the pH to 10. However, the addition of calcium can have negative effects as Bidari and Aghazadeh (2018b) reported the reduction of oxidation rate due to passivation by the presence of calcite and dolomite. Further, Senanayake (2005) noted that insoluble calcium carbonates will form (calcium ions react with free carbonate ions in solution) around gold particles leading to a significant decrease in gold extraction. Although, sodium carbonate/bicarbonate media is inferior to NaOH, it can oxidize more pyrite than NaOH between pH 10-12 as previously reported by Caldeira et al. (2010). As refractory gold ores are becoming more of an economic burden to efficiently recover gold from, an inexpensive process is required for the future of the mining industry.

1.4 Scope and outline of the research project

The motivation of this study stems from the demand of environmental and economic concerns resulting from current pre-treatment processes for refractory gold ores. In this research, new technologies utilizing bacteria and chemical reagents in alkaline environments to effectively oxidize pyrite minerals were investigated. The two alkaliphilic bacteria studied were *Thiomicrospira aerophila* and *Thioalkalivibrio versutus*. Additionally, a simplified media derived from the bacterial growth solution comprising of carbonate/bicarbonate was examined. A methodical strategy was established to understand the reactions occurring and to obtain optimized parameters for the performed experiments. The key objectives for this thesis project were:

1. To study the growth of *Thiomicrospira aerophila* and *Thioalkalivibrio versutus*
2. To analyze the oxidative abilities of *Thiomicrospira aerophila* and *Thioalkalivibrio versutus* in Na_2S and various pyrite samples

3. To understand the chemical reactions occurring during oxidation in a carbonate/bicarbonate buffered medium
4. To explore various parameters to optimize oxidation of pyrite with bacteria or chemical reagents
5. To optimize gold recovery by cyanidation in refractory gold ores following subsequent oxidation

Proposed Methodology: The structure of this investigation follows a five-chapter wise sequential layout as presented below:

Chapter 1 Introduction: This research project focuses on the oxidative abilities of bacteria and chemical reagents from sulfide materials and pyrite concentrates. The background of biooxidation and chemical oxidation are explained, and the significance of alternative pre-treatment methods are outlined.

Chapter 2 Literature Review: A comprehensive literature review was conducted on the various mechanisms of oxidation from sulfur oxidizing microorganisms, nutrients required for growth, the Calvin-Benson-Bassham cycle, acidic, neutral, and alkaline microorganisms previously used in biooxidation processes, the carbonate effect, bacteria used for this research, and a typical bacteria growth cycle.

Chapter 3 Materials and Experimental Methods: A detailed breakdown of the characterization of the three samples and experimental methods used are explained. Bacterial growth and maintenance, bacterial and chemical oxidation procedures with Na_2S and pyrite samples, analytical methods, calculations and error estimation, and safety are described.

Chapter 4 Results and Discussion: This chapter presents the results of growth curves for *Thiomicrospira aerophila* and *Thioalkalivibrio versutus*, biooxidation of Na_2S, biooxidation and chemical oxidation of pyrite, effects of various parameters on oxidation and gold recovery. Explanations of the results are presented with corresponding figures obtained from analysis if applicable.

Chapter 5 Conclusion and Recommendations: A summary of key experimental results and concluding remarks on biooxidation and chemical oxidation via the carbonate effect are described. Recommendations for future investigations in this research area are highlighted.

Chapter 2

Literature Review

2.1 Mechanisms of Biooxidation

The mechanism for bacterial oxidation on reduced sulfur compounds is unique relative to the physiology of the microorganism. Further, microorganisms can oxidize one or all of the various sulfur compounds with varying kinetics to obtain energy and electrons. Microorganisms are predominantly aerobic chemolithoautotrophs which also utilize CO_2 and O_2 as essential nutrients for survival, growth, maintenance and metabolite production (Mahmoud et al., 2017).

2.1.1 Chemolithotroph and Hydrogen Oxidation

Chemolithotrophy is the mode of metabolism (Figure 2.1) used for the oxidation of reduced inorganic compounds exclusively by prokaryotes (Amils, 2011). These prokaryotes are distributed among the Bacteria and Archaea (Oren, 2009). Chemolithotrophs use inorganic substrates such as reduced sulfur compounds (H_2S, S^0 or $S_2O_3^{2-}$), reduced nitrogen compounds (NO_2^- or NH_3), hydrogen (H_2), or iron (Fe^{2+}) as electron donors (energy) for their growth and reproduction (Amils, 2011). The main electron acceptors are oxygen (O_2) and sulphate (SO_4^{2-}), nitrate (NO_3^-), and CO_2. For sulfur oxidation, sulphate is the final product, however, sometimes elemental sulfur is stored as an alternative source of energy (Amils, 2011).

Energy obtained from electron flow of the reductant to an oxidant is conserved in the form of a proton gradient throughout the cell membrane. The proton gradient uses a membrane-bound adenosine triphosphate (ATP) synthase to initiate the phosphorylation of adenosine monophosphate to ATP (Oren, 2009). The synthesis of ATP is driven by a proton motive force generated by chemolithotrophs. Most chemolithotrophs are autotrophic utilizing CO_2 as their main carbon source. Hydrogen oxidizers can assimilate CO_2 directly from the inorganic substrate. The rest of

the chemolithotrophs use ATP and a reducing power, generally the reverse electron transport reaction, to reduce CO_2 (Amils, 2011).

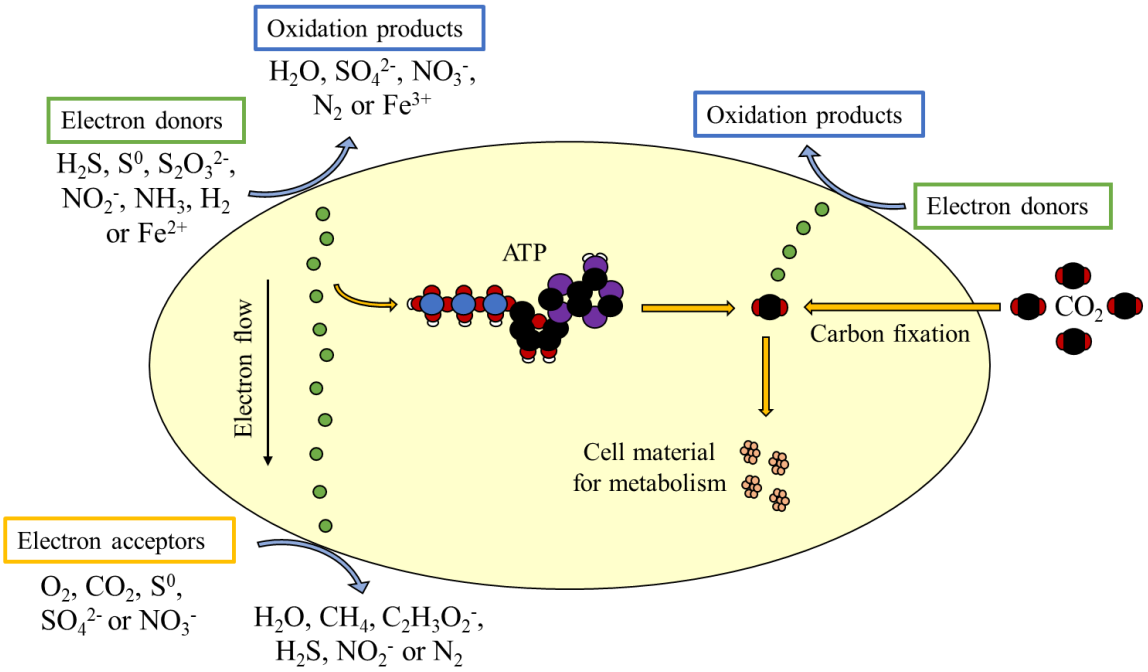

Figure 2.1. Schematic representation of the metabolism in chemolithotrophic bacteria. Chemical elements and electrons are shown as spheres: black (carbon), white (hydrogen), red (oxygen), blue (phosphorus), purple (nitrogen).

Hydrogen is an electron donor used for energy metabolism in many chemolithotrophic bacteria. The $2H^+/H_2$ couple has a very negative reduction potential (-0.41 V) which allows it to be coupled with the reduction of various electron acceptors (Oren, 2009). Therefore, aerobic bacteria can generate a large amount of energy by the oxidation of hydrogen shown below in Equation 1:

$$2\,H_2 + O_2 \rightarrow 2\,H_2O \qquad [1]$$

A variety of anerobic bacteria can generate energy by using hydrogen to provide electrons to electron acceptors such as S, $SO_4^{2-}$and NO_3^- (denitrification) (Amils, 2011; Oren, 2009). Anaerobic respiration driven by hydrogen for nitrate, sulphate, and elemental sulfur reduction are exhibited in Equation 2, 3, and 4, respectively.

$$5\,H_2 + 2\,NO_3^- + 2\,H^+ \rightarrow N_2 + 6\,H_2O \qquad [2]$$

$$4\,H_2 + SO_4^{2-} + 2\,H^+ \rightarrow H_2S + 4\,H_2O \quad [3]$$

$$H_2 + S^0 \rightarrow H_2S \quad [4]$$

Carbon dioxide is another appropriate electron acceptor for hydrogen in which the reduction reaction results in the production of methane (CH_4) or acetate ($C_2H_3O_2^-$) in Equation 5 and 6:

$$4\,H_2 + CO_2 \rightarrow CH_4 + 2\,H_2O \quad [5]$$

$$4\,H_2 + 2\,CO_2 \rightarrow C_2H_3O_2^- + H^+ + 2\,H_2O \quad [6]$$

The formation of methane as the reduction product (Equation 5) is more feasible than acetate (Equation 6) as it has a more exergonic nature than acetate ($\Delta G^{o\prime}_{CH_4} = -131$ kJ, $\Delta G^{o\prime}_{C_2H_3O_2^-} = -95$ kJ).

2.1.2 Oxidation by Chemolithotrophic Denitrification

Inorganic sulfur compounds are oxidized by some anaerobic chemolithotrophic bacteria via denitrification. Denitrifying bacteria commonly oxidize sulfide, elemental sulfur and thiosulfate (when O_2 is limiting) while reducing nitrate and other oxidized nitrogen acceptors to nitrogen gas. Sulfide oxidation results in the formation of $SO_4^{2-}$and S^0 contingent on the physiological characteristics of the SOB (Cardoso et al., 2006).

Denitrification is a technique commonly used to remove nitrate from wastewater. Microbial denitrification is considered more efficient at high nitrate concentrations and more economical compared to physico-chemical techniques such as reverse osmosis, ion exchange, electrodialysis, chemical denitrification and adsorption methods (Ahmaruzzaman and Gupta, 2011; Burakov et al., 2018; Gupta and Saleh, 2013; Kapoor and Viraraghavan, 1997; Mohsenipour et al., 2014). The oxidation of sulfide is displayed in Equations 7, 8, 9, and 10:

$$S^{2-} + 1.6\,NO_3^- + 1.6\,H^+ \rightarrow SO_4^{2-} + 0.8\,N_2 + 0.8\,H_2O \quad [7]$$

$$S^{2-} + 0.4\,NO_3^- + 2.4\,H^+ \rightarrow S^0 + 0.2\,N_2 + 1.2\,H_2O \quad [8]$$

$$S^{2-} + 4\,NO_3^- \rightarrow SO_4^{2-} + 4\,NO_2^- \quad [9]$$

$$S^{2-} + NO_3^- + 2\,H^+ \rightarrow S^0 + NO_2^- + H_2O \quad [10]$$

The elemental sulfur (S^0) that is produced biologically is hydrophilic unlike chemically produced S^0 which can be recycled into soil fertilizer or fungicide (Van Den Bosch et al., 2007). The complete denitrification reactions of elemental sulfur and thiosulfate are given in Equation 11 and 12:

$$S^0 + 1.2\,NO_3^- + 0.4\,H_2O \rightarrow SO_4^{2-} + 0.6\,N_2 + 0.8\,H^+ \quad [11]$$

$$S_2O_3^{2-} + 1.6\,NO_3^- + 0.2\,H_2O \rightarrow 2\,SO_4^{2-} + 0.8\,N_2 + 0.4\,H^+ \quad [12]$$

2.1.3 Contact, Non-contact and Cooperative Mechanisms of Bacterial Metal Sulfide Dissolution

The oxidation of iron by chemolithotrophs is mainly performed using acidophiles as Fe^{2+} is rapidly oxidized in the presence of O_2, however it is stable in acidic conditions. Therefore, the following description of the oxidation of iron sulfides applies to acidophiles while most neutrophiles and alkaliphiles are currently under investigation for their oxidative pathway.

Iron dissolution by biooxidation is initiated by the generation of Fe^{3+} ions (oxidizing agent), and the subsequent oxidation of various dissociated sulfur compounds from the sulfidic ore (Vera et al., 2013a). Metal sulfide oxidation occurs by an indirect method of chemical oxidation by “contact”, “non-contact” or “cooperative” leaching (Mahmoud et al., 2017) as illustrated in Figure 2.2. These are different chemical pathways (thiosulfate and polysulfide) for metal sulfide dissolution which are mainly dependent on the pH and the presence of different oxidants but also the mineralogy and geochemical conditions of the surrounding environment.

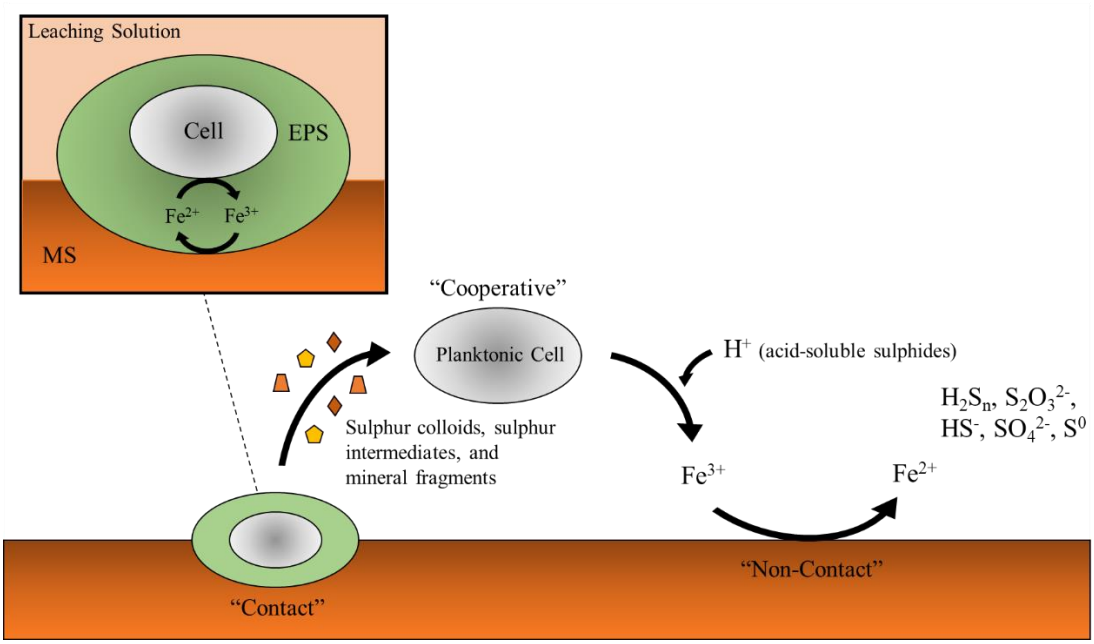

Figure 2.2. Schematic diagram for contact, non-contact, and cooperative bacterial leaching and oxidation of metal sulfides.

"Contact" leaching occurs when the majority of bacterial cells are attached to the surface of sulfide minerals with the aid of extracellular polymeric substances (EPS) which are associated with the Fe^{3+} ions. Therefore, the bacteria degrades sulfide minerals by electrochemical reactions occurring between Fe^{3+} ions and the metal sulfides at the boundary between the cells and the metal sulfide surface within the EPS (Gehrke et al., 1998; Mahmoud et al., 2017; Sand et al., 2001; Sand and Gehrke, 2006). The "non-contact" mechanism utilizes the Fe^{3+} ions produced from the oxidation of Fe^{2+} ions by planktonic bacteria (Mahmoud et al., 2017). The Fe^{3+} ions are reduced, and the cycle is repeated after they come into contact with the mineral sulfide surface. Furthermore, for acid-soluble sulfides, there is an additional attack by protons (H^+). These reactions result in the formation of various sulfur compounds such as H_2S_n, $S_2O_3^{2-}$, HS^-, SO_4^{2-}, S^0. The "cooperative" mechanism was established to describe the dissolution of sulfur intermediates, mineral fragments, and sulfur colloids by planktonic cells (Mahmoud et al., 2017; Rawlings, 2002; Rohwerder et al., 2003; Sand et al., 2001; Tributsch, 2001; Vera et al., 2013a). Attached cells from "contact" leaching release these particulates into the leaching solution where planktonic cells use them as an energy source.

2.1.4 Chemical Mechanisms of Bacterial Metal Sulfide Dissolution

Thiosulfate or polysulfide pathways oxidize sulfide minerals (Schippers, 2004). Through "contact", "non-contact" and "cooperative" leaching, these two pathways determine the oxidation reactions of sulfidic minerals, generally pyrite (FeS_2). Iron- and sulfur-oxidizing bacteria work simultaneously to oxidize metal sulfides. The mechanism proceeds when Fe^{3+} attacks the metal sulfide using electron extraction to reduce it to Fe^{2+} (Vera et al., 2013a). Metal cations (M^{2+}) and water-soluble intermediate sulfur compounds are subsequently released. Recognized iron-oxidizers, *Acidithiobacillus ferrooxidans* and *Leptospirillum ferrooxidans,* can catalyze the recycling of the Fe^{3+} ions in acidic conditions. Further, SOB such as *Acidithiobacillus ferrooxidans* and *Acidithiobacillus thiooxidans* oxidize the liberated reduced sulfur compounds. A schematic of the thiosulfate and polysulfide pathway is displayed in Figure 2.3.

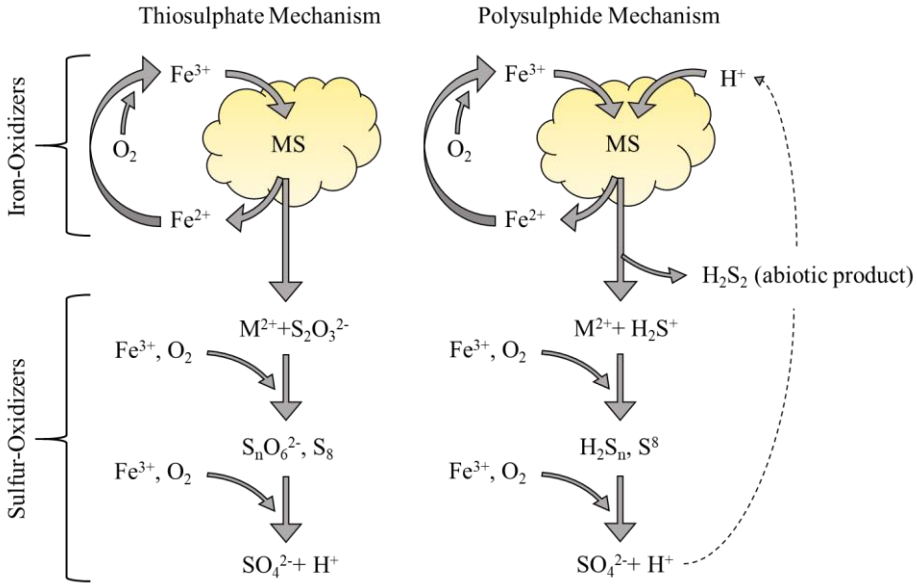

Figure 2.3. Schematic representation of the thiosulfate and polysulfide mechanism. Reproduced with permission from Schippers and Sand (1999). Copyright 1999, American Society for Microbiology.

In regard to the thiosulfate pathway, the chemical bond between sulfur and iron atoms is severed and thiosulfate is formed as the intermediate oxidative product (Luther, 1987; Moses et al., 1987). Thiosulfate then oxidizes to tetrathionate which further degrades to other intermediates which are

further oxidized to sulphate (Vera et al., 2013a). The main end product is sulfuric acid. A summary of the reaction with pyrite is shown in Equation 13 and 14.

$$FeS_2 + 6\,Fe^{3+} + 3\,H_2O \rightarrow S_2O_3^{2-} + 7\,Fe^{2+} + 6\,H^+ \quad [13]$$

$$S_2O_3^{2-} + 8\,Fe^{3+} + 5\,H_2O \rightarrow 2\,SO_4^{2-} + 8\,Fe^{2+} + 10\,H^+ \quad [14]$$

Acid-soluble metal sulfides use the polysulfide pathway as their main oxidation mechanism (Schippers and Sand, 1999). These metal sulfides include chalcopyrite ($CuFeS_2$), pyrrhotite (Fe_7S_8), galena (PbS), sphalerite (ZnS), realgar (As_4S_4) and hauerite (MnS_2) (Vera et al., 2013a). Unlike the thiosulfate pathway, the metal-sulfur bonds are severed prior to the oxidation of the sulfidic sulfur. Elemental sulfur is the main oxidative product which can be explained via polysulfides, however it can be oxidized biologically to sulfuric acid (Schippers and Sand, 1999). Equations 15, 16, and 17 exhibit the reactions of the polysulfide pathway.

$$MS + Fe^{3+} + H^+ \rightarrow M^{2+} + 0.5\,H_2S_n + Fe^{2+}\ (n \geq 2) \quad [15]$$

$$0.5\,H_2S_n + Fe^{3+} \rightarrow 0.125\,S_8 + Fe^{2+} + H^+ \quad [16]$$

$$0.125\,S_8 + 1.5\,O_2 + H_2O \rightarrow SO_4^{2-} + 2\,H^+ \quad [17]$$

The difference between the two mechanisms is that some liberated sulfur compounds in the polysulfide mechanism abiotically produce H_2S_2 after the release of metal cations. Further, the polysulfide mechanism performs an additional attack with protons which binds the valence band electrons of the sulfidic mineral.

2.1.5 Chemolithotrophic Oxidation of Reduced Sulfur Compounds

Chemolithotrophs can oxidize a variety of reduced inorganic sulfur compounds in aerobic conditions. Thiosulfate, elemental sulfur, and sulfide are common compounds oxidized by SOB which results in the formation of sulphate. The reactions are shown below in Equations 18, 19 and 20.

$$H_2S + 2\,O_2 \rightarrow SO_4^{2-} + 2\,H^+ \quad [18]$$

$$S^0 + 1.5\ O_2 + H_2O \rightarrow SO_4^{2-} + 2\ H^+ \quad [19]$$

$$S_2O_3^{2-} + H_2O + 2\ O_2 \rightarrow 2\ SO_4^{2-} + 2\ H^+ \quad [20]$$

The formation of sulphate produces sulfuric acid which decreases the pH. This can lead to corrosion of materials, health risks and acid mine drainage. The treatment of the resulting acid mine drainage is unavoidable, therefore it must be neutralized.

2.2 Sulfur-Oxidizing Microorganisms

SOB have been successfully used in the desulfurization and in the neutralization of hazardous wastewater, spent caustic and gases such as H_2S, SO_2, and HS^- in both laboratory and industrial applications. Further, the use of microorganisms for improved metal recovery including metal sulfide biooxidation in acidic conditions has been investigated extensively. Hydrogen sulfide and sulfur dioxide are toxic substances, produced from industrial and natural activities. They are present in gas or aqueous phases, have a pungent odor, and can cause respiratory problems to humans and wildlife, resulting in environmental pollution if untreated (Ndlovu, 2008; U.S. National Library of Medicine, 2107). Currently, hydrodesulfurization is the dominant desulfurization process used in the petroleum industry, however its high cost and availability of hydrogen sulfide have created interest in alternatives such as biodesulfurization (Kilbane, 2017) using SOB to remediate the toxic sulfur species in bioreactors. Biodesulfurization techniques are safer, use inexpensive reagents and are carried out at ambient temperatures unlike the conventional chemical methods (Cline et al., 2003; Janssen et al., 1994). Biodesulfurization can occur in both aerobic and anerobic conditions, however the process is considerably slower in anaerobic conditions (Sohrabi et al., 2012).

Microorganisms are categorized depending on the pH of the environment required for optimal growth. Acidophiles are the most acknowledged type of bacteria in biomining due to their versatility and demonstrated oxidative abilities. They are microorganisms that thrive in environments below pH 6.0. Neutrophilic and alkaliphilic bacteria are habitats of environments that

have a pH between 6.0 and 8.0 and above pH 8.0, respectively. The variety of these microorganisms will be discussed under the following subsections.

2.2.1 Nutrients for Sulfur-Oxidizing Bacteria

Each microorganism requires nutrients for cell growth, energy generation, and oxidative abilities. The minerals and salts found in their habitats contain a sufficient amount of nutrients to sustain the dominant population in the environment. However, when cultured in laboratories, the addition of the proper concentration of nutrients is vital. Nitrogen, phosphorous, potassium, magnesium, oxygen, and carbon are required nutrients depending on the physiology of the SOB.

Nitrogen, phosphorus and potassium are standard macronutrients added in industrial biooxidation processes for the production of microbial biomass. The nutrient addition rates and sources are displayed in Table 2.1.

Table 2.1: Nutrients required for a standard biooxidation process (Rawlings and Johnson, 2007)

Nutrient	Addition (kg/tonne of ore)	Source
Nitrogen	1.7	$[NH_4]_2SO_4$, $[NH_4]_3PO_4$, NH_2CONH_2
Phosphorous	0.9	$[NH_4]_3PO_4$
Potassium	0.3	K_2SO_4, KOH, and potassium phosphate salts (KH_2PO_4, K_2HPO_4, K_3PO_4)

The addition of an ammonium-nitrogen source is required for the synthesis of proteins, amino acids, nucleic acids and ATP (Wagnar, 2011). A phosphate-phosphorus source aids with the synthesis of ATP and nucleic acids, maintenance of homeostasis, regulating enzyme activity, and preserves the structure and function of cell membranes (Landis and Steenis, 2004). Potassium is a major monovalent intracellular cation in cells facilitating key functions such as intracellular enzyme

activity, acting as an intracellular second messenger, and maintenance of internal pH and membrane potential (Gründling, 2013). It is the least important of the three macronutrients, however it is required for the optimal growth of microorganisms.

Magnesium is another macronutrient reported to assist with the growth and maintenance of SOB. A study by Sorokin et al. (2000) investigated the effect of magnesium on the growth of *Thiomicrospira aerophila* (strain AL3) and *Thioalkalivibrio versutus* (strain AL2). The conclusion was that magnesium helped maintain the integrity of the cells for AL3 while a low concentration of Mg^{2+} (0.5-1.0 mM) significantly increased the growth rate of AL2. There have been minimal studies performed on the effects of magnesium on SOB, therefore it is uncertain if it is deemed an essential nutrient. Trace elements are metal ions required by certain bacteria in miniscule concentrations which act as cofactors for essential enzymatic reactions (Ichhpujani et al., 2008). Some examples of these metal ions are B, Co, Cu, Mn, Mo, Ni and Zn. The addition of trace elements to culture media is not necessary, however it helps the bacteria to grow more optimally.

Oxygen is the terminal electron acceptor in aerobic respiration which is required for the maintenance, metabolite production and survival of microorganisms (Mahmoud et al., 2017). Air is usually injected into biooxidation processes to ensure O_2 is not the limiting factor. The DO concentration in the process must be higher than 2 mg/L to have sufficient oxygen in solution for the SOB (Rawlings and Johnson, 2007). Carbon is another essential nutrient required to promote bacterial cell production. A 2% carbonate concentration is required for biooxidation to guarantee that an adequate amount of carbon dioxide is available (Rawlings and Johnson, 2007). Autotrophic microorganisms commonly use CO_2 as a source of carbon.

Sodium ions in the form of sodium chloride (NaCl) is a nutrient required for the growth and metabolism of some SOB. Microorganisms can be classified as halophile or halotolerant. A halophile is an organism which requires a salinity of 0.2-5.2 M Na^+ for growth. Further, Kushner and Kamekura (1988) identified halophiles as slightly halophilic (0.2-0.5 M), moderately halophilic

(0.5-2.5 M), and extremely halophilic (>2.5 M). Non-halophilic bacteria grow optimally in culture media with less than 0.2 M of dissolved salt. Unlike halophiles, halotolerant organisms can endure up to a certain concentration of NaCl but do not require it for survival. Non-tolerant bacteria, slightly tolerant, moderately tolerant, and extremely tolerant microorganisms can tolerate about 1% w/v, 6-8% w/v, 18-20% w/v, and from zero to saturation levels of NaCl, respectively (Larsen, 1986). Halophilic and halotolerant SOB are typically isolated from soda lakes, however they were also discovered in saline soils, cold saline habitats (hypersaline lakes in Antarctica), animal hides, desert salt crusts, salted food and subterranean brines (Antón, 2011).

2.2.2 Calvin-Benson-Bassham cycle

Microorganisms utilize the CBB cycle for their growth. ATP and NADPH (nicotinamide adenine dinucleotide phosphate), created from photosynthesis, are used to produce glyceraldehyde-3-phosphate (G3P) (Benson, 2019). This synthesizes the primary source of nutrients for heterotrophs, carbohydrate molecules (hexose sugars). The CBB cycle is described in three phases, carboxylation, reduction and regeneration and as shown in Figure 2.4 (Benson, 2019; Raven, 2005; Reginald and Grisham, 2008).

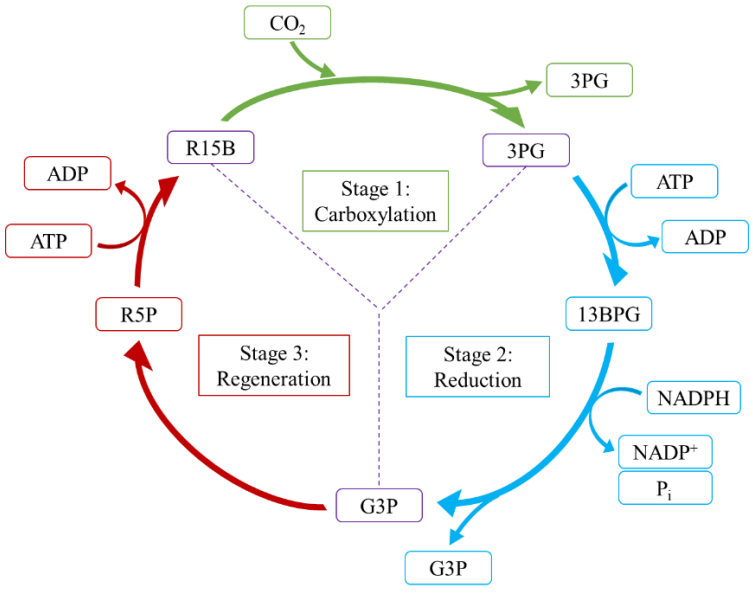

Figure 2.4. Calvin-Benson-Bassham cycle

In phase one, ribulose-1,5-biphosphate (R15B) is first phosphorylated by the enzyme phosphoribulose kinase. Then CO_2 is fixated to carboxylase R15B to produce two molecules of 3-phosphoglycerate (3PG) which is catalyzed by ribulose bisphosphate carboxylase (commonly abbreviated as Rubisco). One 3PG molecule is used for phase 2, while the other molecule is utilized in central metabolic pathways.

In phase two, 3PG is phosphorylated to 1,3-biphosphoglycerate (13BPG) with the aid of phosphoglycerate kinase. The 13BPG is reduced by glyceraldehyde-3-phosphate dehydrogenase and NADPH to form $NADP^+$, inorganic phosphate (P_i), and glyceraldehyde-3-phosphate (G3P). G3P is essential to bacteria as every sixth G3P molecule is used in the formation of glucose and other metabolic activities. Phase 3 begins with a reverse conversion of G3P to dihydroxyacetone phosphate (DHAP) by triose phosphate isomerase. Aldolase and fructose convert DHAP into fructose-6-phosphate (F6P). F6P is converted into glucose with the aid of glucose-6-phosphatase and phosphoglucoisomerase via two enzymatic steps. Further, DHAP combines with erythrose-4-phosphate to produce sedoheptulose-1,7-bisphosphate (SBP). Sedoheptulose-7-phosphate is produced by the de-phosphorylation of SBP by sedoheptulose bisphosphatase. Ribose-5-phosphate (R5P) and xylulose-5-phosphate (X5P) are formed after several rearrangement reactions by transketolase and transaldolase enzymes. Finally, R5P and X5P are isomerized by phosphopentose isomerase and phosphopentose epimerase to generate ribulose-5-phosphate (Ru5P) which re-enters the CBB cycle.

2.2.3 Role of Acidophilic Microorganisms in Metal Sulfide Oxidation

Acidophiles are the most used type of microorganisms for the oxidation of metal sulfides. A diverse set of microorganisms has been described in various industrial tank bioleaching operations and heap leaching processes (Table 2.2). The most described sulfur-oxidizing acidophiles are classified as Bacteria and are mostly mesophilic and moderately thermophilic. Archaea are the second most described microorganisms and are mostly extremely thermophilic (except for the *Ferroplasma*

genus) (Donati and Sand, 2007). All these microorganisms can oxidize Fe^{2+} and/or reduced sulfur compounds, however only a few grow chemolithoautotrophically (Donati and Sand, 2007). The microorganisms in Table 2.2 are mesophiles, moderate thermophiles, and thermophiles. There is an abundance of both iron and sulfur oxidizers which use different oxidizing and metabolic pathways. This is due to the temperature gradients within heaps and tanks which requires microorganisms with various growth temperatures that oxidize metal sulfides. Although many species and strains of microorganisms have been identified for their oxidative capabilities, the majority of the oxidation is performed by a few microorganisms. The dominant metal sulfide-oxidizing acidophiles along with their pH and temperature growth ranges are shown in Table 2.3.

Table 2.2: Metal sulfide oxidizing acidophilic microorganisms (Donati and Sand, 2007)

S. No.	Microorganisms	Bacteria or Archaea	Type
1	*Acidianus brierleyi*	Archaea	Thermophile
2	*Acidianus infernus*	Archaea	Thermophile
3	*Acidimicrobium ferrooxidans*	Bacteria	Moderate Thermophile
4	*Acidithiobacillus albertensis*	Bacteria	Mesophile
5	*Acidithiobacillus caldus*	Bacteria	Moderate Thermophile
6	*Acidithiobacillus ferrooxidans*	Bacteria	Mesophile
7	*Acidithiobacillus thiooxidans*	Bacteria	Mesophile
8	*Alicyclobacillus disulfidooxidans*	Bacteria	Mesophile
9	*Alicyclobacillus tolerans*	Bacteria	Mesophile / Moderate Thermophile
10	*Caldibacillus ferrivorus*	Bacteria	Moderate Thermophile
11	*Ferrimicrobium acidiphilum*	Bacteria	Mesophile
12	*Ferroplasma acidarmanus*	Archaea	Moderate Thermophile
13	*Ferroplasma acidiphilum*	Archaea	Mesophile
14	*Ferroplasma cupricumulans*	Archaea	Moderate Thermophile
15	*Leptospirillum ferriphilum*	Bacteria	Mesophile
16	*Leptospirillum ferrodiazotrophum*	Bacteria	Mesophile
17	*Leptospirillum ferrooxidans*	Bacteria	Mesophile

18	*Metallosphaera hakonensis*	Archaea	Thermophile
19	*Metallosphaera prunae*	Archaea	Thermophile
20	*Metallosphaera sedula*	Archaea	Thermophile
21	*Sulfobacillus acidophilus*	Bacteria	Moderate Thermophile
22	*Sulfobacillus montserratensis*	Bacteria	Mesophile
23	*Sulfobacillus sibiricus*	Bacteria	Moderate Thermophile
24	*Sulfobacillus thermosulfidooxidans*	Bacteria	Moderate Thermophile
25	*Sulfobacillus thermotolerans*	Bacteria	Mesophile / Moderate Thermophile
26	*Sulfolobus metallicus*	Archaea	Thermophile
27	*Sulfolobus yangmingensis*	Archaea	Thermophile
28	*Sulfurococcus mirabilis*	Archaea	Thermophile
29	*Sulfurococcus yellowstonensis*	Archaea	Thermophile
30	*Thiobacillus plumbophilus*	Bacteria	Mesophile
31	*Thiobacillus prosperus*	Bacteria	Mesophile
32	*Thiomonas cuprina*	Bacteria	Mesophile

Table 2.3: Predominate acidophilic microorganisms metal sulfide oxidizers (Bosecker, 1997; Bruynesteyn, 1989; Donati and Sand, 2007; Ewart and Hughes, 1991; Kelly and Wood, 2000; Mahmoud et al., 2017; Özkaya et al., 2007).

S. No.	Genus	Species	Oxidizes	pH*	Temperature* (˚C)
1	*Acidithiobacillus*	*caldus*	Sulfur	1.0-3.5 (2.0-2.5)	32-52 (45)
2	*Acidithiobacillus*	*ferrooxidans*	Iron, Sulfur	1.3-4.5 (2.5)	10-37 (30-35)
3	*Acidithiobacillus*	*thiooxidans*	Sulfur	0.5-5.5 (2.0-3.0)	10-37 (28-30)
4	*Leptospirillum*	*ferriphilum*	Iron	(1.3-1.8)	10-45 (30-37)
5	*Leptospirillum*	*ferrooxidans*	Iron	1.3-4.0 (1.5-3.0)	(28-30)
6	*Sulfobacillus spp.*	-	Iron, Sulfur	~ 0.7-5.5	~17-60

*optimum growth conditions are in brackets

The genus *Acidithiobacillus* and *Leptospirillum* are the most described acidophilic bacteria for the oxidation of metal sulfides. Specifically, *Acidithiobacillus ferrooxidans* and *Leptospirillum*

ferrooxidans are implicated as the most significant microorganisms involved in sulfide mineral oxidation (Bacelar-Nicolau and Johnson, 1999a). For processes operating above 40 ˚C and pH below 1.0, *Leptospirillum* species are more abundant than *Acidithiobacillus* (Coram and Rawlings, 2002). They are both obligate chemolithotrophs and have similar growth parameters, however *Leptospirillum ferrooxidans* cannot oxidize sulfur compounds.

Although acidophiles are widely used in biomining processes, neutrophiles and alkaliphiles may have more advantages for certain processes i.e., gold recovery from refractory ores. Therefore, potential neutrophiles and alkaliphiles with sulfur-oxidizing capabilities are identified for future research in biomining.

2.2.4 Role of Neutrophilic Microorganisms in Biooxidation

Neutrophilic microorganisms have optimal growth parameters between pH 6.0 and 8.0. Most of the neutrophilic SOB are mesophilic, however some species are moderately thermophilic. The formation of sulphate or elemental sulfur by oxidation is problematic as the accumulation of sulphate results in acidification due to sulfuric acid formation (Blais et al., 1992; Moreira and Amils, 1997). Neutrophilic bacteria have been isolated from marine, freshwater, sewage treatment processes, soils, sulfur springs and sulfur deposits. Currently, the oxidative capabilities of neutrophiles are not as recognized as acidophiles. These microorganisms belong to the genus *Citrobacter*, *Halothiobacillus*, *Nocardioides*, *Parapedobacter*, *Rhodobacter*, *Rhodopseudomonas*, *Starkeya*, *Thiobacillus*, *Thermithiobacillus* and *Thiomonas* (Table 2.4). The neutrophilic sulfur-oxidizing microorganisms utilized in biooxidation are shown in Table 2.5.

Table 2.4: Neutrophilic sulfur-oxidizing microorganisms and their characteristics

S. No.	Genus	Species	pH*	Temperature* (˚C)	Salinity (M Na^+)*	Sulphur Species Oxidized	References
1	*Citrobacter*	*youngae*	4.0-8.0	(37)	-	S^{2-}	(Purnomo et al., 2019)
2	*Halothiobacillus*	*neapolitanus*	6.5-6.9 (4.5-8.5)	28-32 (8-39)	Upper limit unknown (0-0.9 M)	S^0, S^{2-}, $S_2O_3^{2-}$, $S_3O_6^{2-}$, $S_4O_6^{2-}$	(Boden, 2017)
3	*Nocardioides*	*nitrophenolicus*	6.0-10.0 (8.0)	15-40 (30)	0-0.1	S^0, S^{2-}	(Liu et al., 2020; Yoon and Park, 2006; Yoon et al., 1999)
4	*Parapedobacter*	-	6.0-9.0	15-45	0-0.7	S^0, S^{2-}	(Kumar et al., 2015)
5	*Rhodobacter*	*capsulatus*	6.5-7.5 (7.0)	(30-35)	0-0.5 (0)	S^{2-}	(Srinivas et al., 2007)
6	*Rhodobacter*	*sphaeroides*	6.0-8.5 (7.0)	(30-34)	0-0.5 (0)	S^{2-}	(Srinivas et al., 2007)
7	*Rhodopseudomonas*	*palustris*	6.0-9.0 (6.9)	30-37 (25-40)	-	S^{2-}, $S_2O_3^{2-}$	(Imhoff, 2006; Imhoff et al., 2015; Venkata Ramana et al., 2012)
8	*Starkeya*	*novella*	5.7-9.0 (7.0)	10-37 (25-30)	-	S^{2-}, $S_2O_3^{2-}$	(Kelly and Wood, 2000)
9	*Thiobacillus*	*thioparus*	5.0-9.0 (6.6-7.2)	(28)	-	S^0, S^{2-}, SO_3^{2-} $S_2O_3^{2-}$, $S_3O_6^{2-}$, $S_4O_6^{2-}$, SCN^-	(Boden et al., 2017a; Millano and Sorber, 1986; Vlasceanu et al., 1997)

10	*Thermithiobacillus*	*tepidarius*	5.0-8.0 (7.0-8.0)	35-52 (43)	-	S^0, S^{2-}, $S_2O_3^{2-}$, $S_3O_6^{2-}$, $S_4O_6^{2-}$, $S_6O_6^{2-}$, $S_7O_6^{2-}$	(Belyi et al., 2015a; Wood and Kelly, 1985; Yang et al., 2015)
11	*Thiomonas*	-	2.0-7.8 (3.0-6.0)	40-65 (30-36, 50)	-	S^0, S^{2-}, $S_2O_3^{2-}$, $S_4O_6^{2-}$	(Kelly et al., 2007; Moreira and Amils, 1997)

*optimal growth conditions are in brackets

Table 2.5: Neutrophilic sulfur-oxidizing microorganisms used for biooxidation

S. No.	Microorganism	Material/ Method	Oxidized Species	pH	Result	References
1	*Citrobacter youngae*	Gold Tailings	FeS, $FeSO_4 \cdot 7H_2O$	5.0	Increased Au and Ag recoveries by 6.1 and 8.3%, respectively	(Purnomo et al., 2019)
2	*Halothiobacilllus neapolitanus* (NTV01)	Bio-trickling filter with gas-liquid flow	H_2S	7.0	95-100% removal	(Vikromvarasiri et al., 2017; Vikromvarasiri and Pisutpaisal, 2016)
3	*Nocardioides spp., Nocardioides nitrophenolicus, Parapedobacter spp., Thermithiobacillus tepidarius*	Bio-cake from a gold-arsenic flotation concentrate	S^0, Sb_2S_3, Sb_2S_5	7.0-8.0	Reduced S^0 and S^{2-} by 3-4%	(Belyi et al., 2015a)
4	*Rhodobacter capsulatus, Rhodopseudomonas palustris*	Airlift reactor system for synthetic and industrial waste gas	H_2S	6.2-7.6	98.5% removal	(Chen et al., 2018)
5	*Rhodobacter sphaeroides* (S and NR-3), *Rhodopseudomonas palustris*	Synthetic sewage wastewater	H_2S	-	99.8% removal	(Nagadomi et al., 2000)
6	*Starkeya novella* (SRM)	Immobilized in a	H_2S, CH_4S, C_2H_6S, $C_2H_6S_2$	7.0	100% of H_2S, 100% of CH_4S,	(Myung Cha et al., 1999)

		PVP matrix to treat organo-sulfur compounds			73% of C_2H_6S, 87% of $C_2H_6S_2$	
7	*Starkeya novella* (CH 3)	Biofilter in mixotrophic and autotrophic conditions	H_2S	7.0	Removed 99.5% mixotrophically and 97.5% autotrophically	(Chung et al., 1997)
8	*Thiobacillus thioparus* (CH11)	Immobilized with Ca-alginate for biofiltration system	H_2S	7.0	98% removal	(Chung et al., 1996)
9	*Thiobacillus thioparus* (ATCC 23645)	Biofiltration	H_2S	6.0	100% removal	(Oyarzún et al., 2003)
10	*Thermithiobacillus tepidarius* (JNU-2)	Shake flask/internal airlift loop reactor	$Na_2S_2O_3 \cdot 5H_2O$	6.0	98% removal of $S_2O_3^{2-}$	(Yang et al., 2015)
11	*Thiomonas spp.* (SS)	Biological deodorization	H_2S	6.7	90-99% removal	(Chen et al., 2004)
12	*Thiomonas spp.* (RAN5)	Synthetic and anaerobically digested gas	H_2S	6.5	90-99% removal	(Asano et al., 2012)

2.2.5 Role of Alkaliphilic Microorganisms in Biooxidation

Alkaliphiles are referred to as microorganisms with growth observed above pH 8.0 (with an optimal pH at 9.0-10.0), but they grow inefficiently at neutral pH (Horikoshi, 1999). Alkaliphiles are of great importance in the remediation of industrial wastes, epidemiology of pathogenic bacteria, and can be useful for mineral processing (Padan et al., 2005). However, investigations on the oxidative capabilities of alkaliphilic bacteria of reduced sulfur compounds are inferior in comparison to acidophilic and neutrophilic SOB.

Some alkaliphilic microorganisms are isolated from neutral environments and are able to oxidize reduced sulfur compounds such as sulfide, polysulfide, thiosulfate, tetrathionate and thiocyanate (Gonzalez-Sanchez and Revah, 2009). Nevertheless, the majority of alkaliphilic SOB are isolated from soda lakes due to their contribution to the sulfur cycle. These are referred to as haloalkaliphiles as the survival of specific bacteria are influenced by highly saline environments. Haloalkaliphiles are alkaliphilic bacteria that require a high salinity for growth and often live in more extreme environments i.e. elevated temperatures.

Alkaliphilic SOB have various advantages over acidophilic bacteria as these processes do not require corrosive-resistant material and have relatively safer systems. Furthermore, they can tolerate higher substrate and product concentrations than sulfur-oxidizing acidophiles and neutrophiles (Sorokin et al., 2011). The advantage of the use of alkaliphiles is associated with the gold leaching via a cyanidation process which requires high pH for the reaction. Applicability of alkaliphiles instead of acidophilic bacteria reduces the consumption of alkali to adjust the pH and make the process more economic and sustainable.

The bacterial strains from the genus of *Alkalilimnicola*, *Ectothiorhodospira*, *Thioalkalibacter*, *Thiomicrospira*, and *Thioalkalivibrio* in Table 2.6 have been acknowledged for their oxidative abilities on synthetic and industrial waste. Up to date to the best of our knowledge, no research has been conducted on the application of alkaliphilic bacteria for the biooxidation of ores. Table 2.7

summarizes the most recent studies of alkaliphilic sulfur-oxidizing microorganisms for biooxidation in gas and liquid matrices.

Table 2.6: Characteristics of alkaliphilic sulfur-oxidizing bacteria

S. No.	Genus	Species	pH*	Temperature* (°C)	Salinity* (M Na^+)	Sulphur Species Oxidized	References
1	*Alkalilimnicola*	*ehrlichii*	7.3-10.0 (9.3)	13-40 (30)	0.3-3.3 (0.5)	S^{2-}, $S_2O_3^{2-}$	(Hoeft et al., 2007)
2	*Ectothiorhodospira*	*magna*	8.0-11.0 (9.0-10.0)	20-45 (30-35)	0-1.4 (0.1-0.3)	S^0, S^{2-}	(Bryantseva et al., 2010)
3	*Ectothiorhodospira*	*shaposhnikovii*	6.5-10.0 (8.0-9.0)	20-45 (30-35)	0-1.2 (0.5)	S^0, S^{2-}, SO_3^{2-}, $S_2O_3^{2-}$	(Bryantseva et al., 2010; Cai et al., 2019)
4	*Thioalkalibacter*	*halophilus*	7.5-10.2 (8.5)	25-40 (30)	0.5-3.5 (1.0)	S^0, S^{2-}, $S_2O_3^{2-}$	(Banciu et al., 2008)
5	*Thiomicrospira*	-	5.9-10.0 (7.0-10.0)	3.5-42 (25-40)	0.04-3 (0.43-0.60)	S^0, S^{2-}, $S_2O_3^{2-}$, $S_3O_6^{2-}$, $S_4O_6^{2-}$	(Boden et al., 2017b)
6	*Thioalkalivibrio*	*halophilus*	7.5-9.8 (8.0-9.0)	25-47	0.2-5.0 (2.0)	S^0, S^{2-}, $S_2O_3^{2-}$, $S_4O_6^{2-}$, polysulphide	(Banciu et al., 2004)
7	*Thioalkalivibrio*	*jannaschii*	7.0-11.2	25-47 (30)	0.2-4.0 (1.0-3.0)	S^0, S^{2-}, $S_2O_3^{2-}$, $S_4O_6^{2-}$, polysulphide	(Ahn et al., 2019; Sorokin et al., 2002)
8	*Thioalkalivibrio*	*sulfidiphilus*	8.0-10.5 (10.0)	25-47 (35)	0.2-1.5 (0.4)	S^0, S^{2-}, $S_2O_3^{2-}$, $S_4O_6^{2-}$, polysulphide	(Sorokin et al., 2012)
9	*Thioalkalivibrio*	*versutus*	8.5-10.4 (9.5-9.8)	25-47 (30-35)	0.1 – 4.0 (2.0)	S^0, S^{2-}, SO_3^{2-}, $S_2O_3^{2-}$, $S_3O_6^{2-}$, $S_4O_6^{2-}$, $S_5O_6^{2-}$, polysulphide	(Ang et al., 2017; Kalantari et al., 2018; Sorokin et al., 2000)

*optimal growth conditions are in brackets

Table 2.7: Alkaliphilic sulfur-oxidizing microorganisms used for biooxidation processes

S. No.	Microorganisms	Material/ Method	Oxidized Species	pH	Result	References
1	*Alkalilimnicola ehrlichii* (MLHE-1), *Thioalkalibacter halophilus* (ALCO 1), *Thioalkalivibrio sulfidiphilus, Thioalkalivibrio versutus*	Thiopaq® process	H_2S	8.0-9.0	> 99.5% removal	(Kiragosyan et al., 2019; Sorokin et al., 2008)
2	*Ectothiorhodospira magna*	Synthetic wastewater	S^{2-}	8.0	99.9% removal	(Zhao et al., 2018)
3	*Ectothiorhodospira shaposhnikovii*	Biogas desulfurization	H_2S	-	100% removal	(Vainshtein et al., 1994)
4	*Thiomicrospira spp.*	Biogas desulfurization	H_2S	10.0	86% removal	(Van Den Bosch et al., 2007)
5	*Thioalkalivibrio halophilus, Thioalkalivibrio jannaschii, Thioalkalivibrio versutus*	Biogas desulfurization	H_2S	10.0	-	(Sorokin et al., 2008)
6	*Thioalkalivibrio versutus*	Spent caustic and synthetic sulfide in stirred tank bioreactor	S^{2-}, $Na_2S{\cdot}9H_2O$	10.2	82.7% oxidation	(Kalantari et al., 2018)

2.2.6 Thiopaq® Process

The Thiopaq® process (Figure 2.5) is a three stage biodesulfurization process developed by Paques (2014) to biologically remove H_2S from low-pressure biogas streams. A gas stream containing H_2S contacts an aqueous wash solution in the first stage of the process, the absorber. The gas is absorbed into the solution and is then transported to the bioreactor. Purified gas is released at the top of the absorber.

Sulfide is aerobically oxidized by SOB bacteria in the reactor to produce biological elemental sulfur (biosulfur). The biosulfur is hydrophilic and reduces the possibility of clogging in the system (Paques, 2014). No expensive reagents are added, however small amounts of nutrients are added to the bioreactor to ensure proper growth of the bacteria. The bioreactor is buffered with sodium hydroxide (NaOH) and operates at atmospheric pressure, between 25-40 °C, and at approximately pH 8.0-9.0. Operating under slightly alkaline conditions enables H_2S to be absorbed in the absorber to produce sodium hydrosulfide and H_2O (NATCO Group, 1999; Paques, 2014). The wash solution in the bioreactor is regenerated by the bacteria and is recycled for use in the absorber and the decanter for the next section.

Some of the wash solution is sent to the decanter (gravity settler) where the biosulfur is concentrated to 10-15 wt% and the overflow is recycled back into the bioreactor (Paques, 2014). The biosulfur leaves as a sludge which can be used for agricultural processes or purified to a high-quality sulfur cake (Schlumberger, 2016). The decanter has a small bleed stream consisting of sodium salts and biosulfur (free of sulfide) making discharge disposal easy. The Thiopaq® process results in a high removal H_2S efficiency exceeding 99.5% (Paques, 2014).

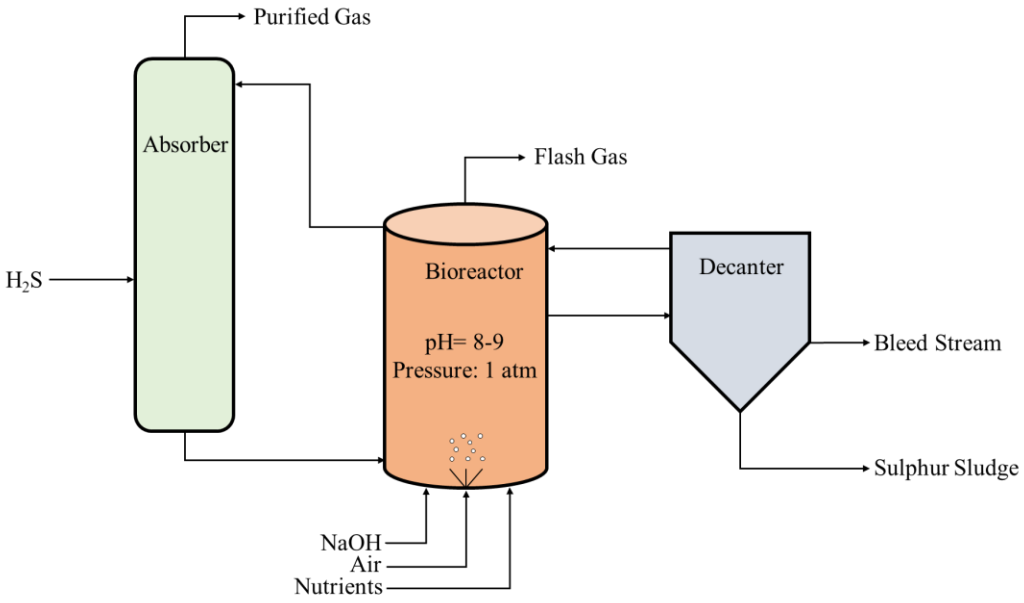

Figure 2.5: Schematic diagram of the Thiopaq® process

Thiopaq® processes have advantages over conventional desulfurization processes as they use less equipment, is simple to operate, requires minimal supervision, low-operating costs, bacteria are self-regulating, safer, and is an environmentally-friendly system (Schlumberger, 2016).

2.3 Carbonate Effect

Investigations on the oxidation of pyrite minerals in aqueous systems have been previously conducted. Oxygen and Fe(III) are the main oxidants in aqueous oxidation as shown in Equations 21, 22 and 23 (Chandra and Gerson, 2010; Descostes et al., 2002; Garrels and Thompson, 1960; Singer and Stumm, 1970).

$$\mathrm{FeS_2} + \frac{7}{2}\,\mathrm{O_2} + \mathrm{H_2O} \rightarrow \mathrm{Fe^{2+}} + 2\,\mathrm{SO_4^{2-}} + 2\,\mathrm{H^+} \qquad [21]$$

$$Fe^{2+} + \frac{1}{4}\,O_2 + H^+ \rightarrow Fe^{3+} + \frac{1}{2}\,H_2O \qquad [22]$$

$$FeS_2 + 14\,Fe^{3+} + 8\,H_2O \rightarrow 15\,Fe^{2+} + 2\,SO_4^{2-} + 16\,H^+ \qquad [23]$$

The oxidation of pyrite can be enhanced by increased temperature, pH, and injection of air. Acid mine drainage may occur if not neutralized due to the production of sulfuric acid, causing detrimental effects to the environment.

The carbonate effect is a phenomenon in which the oxidation of sulfidic minerals is enhanced in a carbonate buffered solution between pH 8-11 (Caldeira et al., 2010). The oxidation of pyrite occurs by the generation of a hydroxide radical (•OH) through the reversible adsorption of H_2O/OH^- interacting with a hole in the iron 3d t_{2g} (nonbonding pyrite orbital) at the anodic site as proposed by Mishra and Osseo-Asare (1988) and Wei and Osseo-Asare (1997). Caldeira et al. (2010) proposed that the hydroxide radical transfers to sulfur sites on the pyrite surface according to Equation 24 and 25.

$$FeS_2 + H_2O + h^+ \rightarrow Fe(\cdot OH)S_2 + H^+ \quad [24]$$

$$Fe(\cdot OH)S_2 \rightarrow FeS_2(\cdot OH) \quad [25]$$

The complete hydroxylation of the surface and oxidation of sulfur is shown in Equation 26 and 27 (Mishra and Osseo-Asare, 1988).

$$FeS_2(\cdot OH) + 3\,H_2O + 3\,h^+ \rightarrow Fe(OH)_2S_2(OH)_2 + 3\,H^+ \quad [26]$$

$$Fe(OH)_2S_2(OH)_2 + 2\,h^+ \rightarrow Fe^{2+} + S_2O_3^{2-} + 2\,H^+ + H_2O \quad [27]$$

Caldeira et al. (2010) proposed that the enhanced chemical oxidation of pyrite is due to soluble iron-carbonate complexes formed during pyrite oxidation in carbonate/bicarbonate media, buffering effect of carbonate ions, and the effect of carbonate complexation on Fe(III) solubility. Iron-carbonate complexes, $FeHCO_3^-$, $FeCO_3$, $Fe(CO_3)(OH)^-$ and $Fe(CO_3)_2^{2-}$, accelerate the Fe(II)-O_2 electron transfer reaction by favoring the oxidation of Fe(II) to Fe(III) using dissolved oxygen. The carbonate ions neutralize the protons (which form sulfuric acid) produced by maintaining a high pH environment which is optimal for pyrite oxidation. The formation of the iron carbonate complexes increases the total dissolved iron concentration which raises the redox potential of the Fe(II)/Fe(III) couple. Further, Caldeira et al. (2010) indicated that carbonate solutions had

significantly higher oxidation rates than NaOH, lime, and borate. Fe(II) bound to carbonate/bicarbonate ions form high spin complexes, requiring less energy to oxidize the Fe(II) ion (Luther et al., 1992).

Figure 2.6 represents the proposed oxidation path for pyrite oxidation in carbonate solutions by Caldeira et al. (2010). Assuming an oxygenated system containing carbonate ions, adsorbed Fe(III)-CO_3 oxidizes to Fe(II)-CO_3 by accepting electrons from the conduction band from the anodic site. Fe(II)-CO_3 is then oxidized by dissolved oxygen at the pyrite surface or in solution to Fe(III)-CO_3. This Fe(II)/Fe(III) redox couple was proposed by Moses and Herman (1991) at circumneutral pH but is suggested to also occur at alkaline pH.

At the anodic site, hydroxyl or water adsorbs on the pyrite surface and the iron 3d t_{2g} holes strengthen the adsorption of hydroxides in which the transfer of the OH radical to the sulfur species occurs as shown in Equation 24 and 25. Further hydroxylation occurs at the sulfur sites resulting in the release of thiosulfate and Fe(II)-CO_3 as shown in Equation 26 and 27. These soluble Fe(II)-CO_3 complexes favour the oxidation of Fe(II) to Fe(III), creating the oxidation cycle.

Figure 2.7 exhibits the predominant stability diagrams performed by Caldeira et al. (2010) at 25 °C in an iron, sulfur, carbonate, and water system. The precipitates produced during the carbonate oxidation of pyrite can vary. Goethite is suggested as the most probable species formed which predominates between pH 1.5-14. Ferrihydrite is the initial product of rapid hydrolysis in Fe(III) solutions, therefore it is expected to form in alkaline solutions. If ferrihydrite and $Fe(OH)_{2(s)}$ are absent, the iron carbonate complexes are stable between pH 5-11.

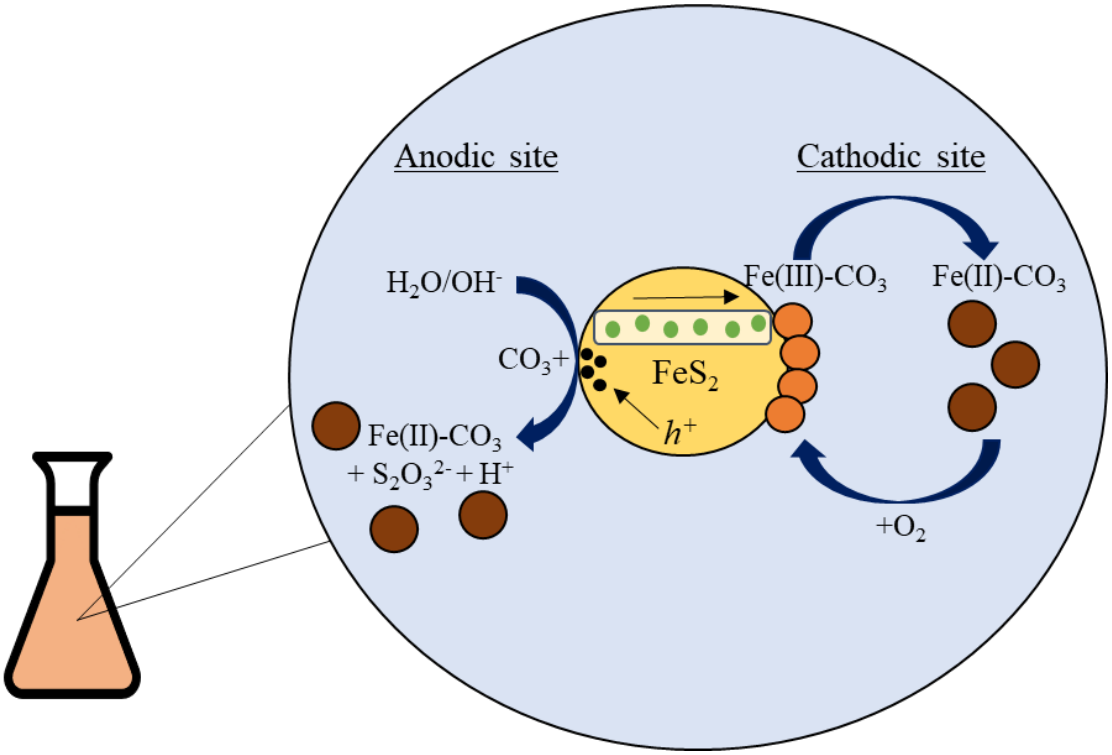

Figure 2.6: Schematic representation of the oxidation of pyrite in carbonate solutions modified from Caldeira et al. (2010).

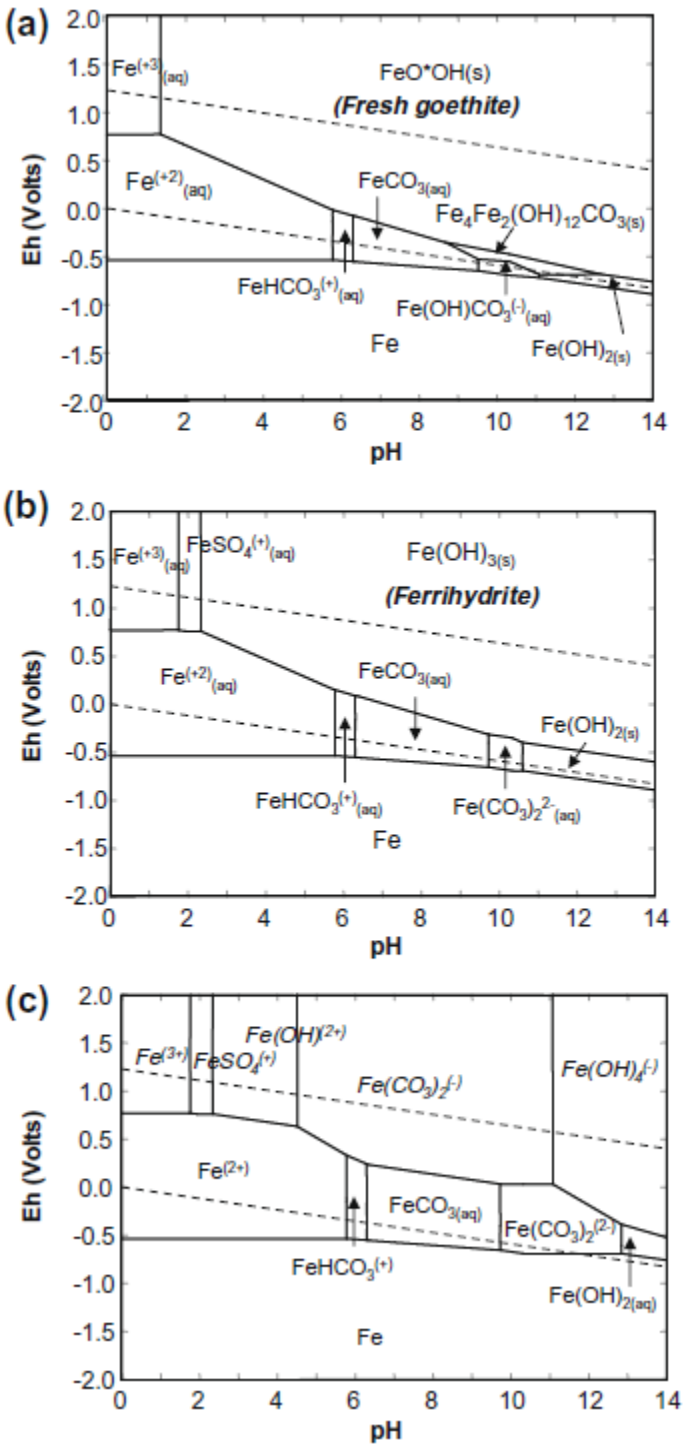

Figure 2.7: Eh-pH diagrams for a metastable Fe-S-CO_3-H_2O system at 25 °C for (a) goethite and Fe (II) – carbonate complexes; (b) ferrihydrite and Fe (II) – carbonate complexes; (c) soluble iron species. Concentrations: [Fe] = 0.008 mol/L; [S] = 0.017 mol/L; [CO_3] = 0.1 mol/L (Caldeira et al., 2010).

2.4 Bacteria Used in this Investigation

Two bacteria, *Tm. aerophila* and *Tv. versutus* were investigated in this study as they have been previously studied together for sulfur oxidation (Ang et al., 2017; Sorokin et al., 2001), and have been identified in liquid and gas desulfurization processes. The halo-tolerant bacteria studied were isolated from soda lakes which are usually located in dry climate areas that facilitate salt accumulation by evaporative concentration (Sorokin et al., 2011). These specific saline salt lakes are buffered with sodium carbonate and sodium bicarbonate, creating a high pH (9.5-10.5) environment (Sorokin et al., 2006). This environment is the only natural environment with the optimal parameters for the stable development of obligately alkaliphilic, salt-tolerant bacteria. Currently, there has been no research performed on the biological oxidation of a refractory gold ore with alkaliphilic microorganisms in a carbonate buffered media.

2.4.1 *Thiomicrospira aerophila*

Previously known as *Thioalkalimicrobium aerophilum*, the name was changed due to slight physiological differences. *Thiomicrospira* species are found in marine environments and have been exclusively associated with sulfide oxidation (Hansen and Perner, 2015). Isolated from low-saline soda lakes in Siberia and Kenya, this obligate chemolithoautotroph and gram-negative bacteria has a relatively high aerobic growth rate on a thiosulfate-limited culture (0.33 h^{-1}) (Ang et al., 2017). Depending on the strain, *Tm. aerophila* can oxidize sulfide and thiosulfate to sulfate at high rates above a pH of 8.4. The sulfur compounds are used as energy and electron donors with oxygen acting as the electron acceptor. *Tm. aerophila* can oxidize elemental sulfur however, at a much lower rate compared to other bacteria. The microbe has a high growth rate, low growth yield, can grow between pH 7.5-10.6 (optimal 10.0), at a range of 0.2-1.5 M Na^+ (optimal 0.5 M) and from ambient temperatures to 40 ˚C (optimal 30 °C) (Ang et al., 2017; Sorokin et al., 2000). This bacterium can also grow in microaerophilic conditions and has been of interest to the industry due to its ability to treat hydrogen sulfide.

Unknown bacterial species/strains from this genus were used for the removal of H_2S in a biotechnological process held at halo-alkaline conditions due to their ability to grow under extreme conditions. In a typical fed-batch experiment held at 35 ˚C, pH 10.0 and 10 mmol/h H_2S, 86% of H_2S was oxidized in 22 h (Van Den Bosch et al., 2007).

2.4.2 *Thioalkalivibrio versutus*

Initially isolated in Siberia in 1989, there are 19 known strains of *Tv. versutus* that were obtained from Siberian and Kenyan soda lakes. The cells are vibrio- or spirilla-shaped, motile, and are white colonies filled with sulfur (Sorokin et al., 2001). The bacterial species can oxidize elemental sulfur, sulfide, polysulfide, thiosulfate, sulfite and tri-, tetra- and penta-thionate (Ang et al., 2017; Kalantari et al., 2018). A nucleophilic attack of sulfide on elemental sulfur at high pH produced polysulfide which was converted to sulphate due to the instability of polysulfide at high oxygenation levels. Further, a higher DO concentration resulted in higher sulfide oxidation and sulphate production. All but one strain (ALJ 17) prefers aerobic conditions, grows optimally at 30-35 ˚C and can grow between a pH and Na^+ of 8.5-10.4 and 0.1-4.0 M, respectively (Sorokin et al., 2000). Studies have indicated that the optimal growth parameters are between pH 9.5-9.8, 2 M Na^+ and a low concentration of Mg^{2+} (0.5-1.0 mM) significantly increased the growth rate (Sorokin et al., 2000). *Tv. versutus* has been used to treat spent caustic and biogas in Thiopaq® processes (Sorokin et al., 2008). Kalantari et al. (2018) performed oxidative tests on spent caustic and a synthetic sulfide source ($Na_2S{\cdot}9H_2O$). A maximum of 82.7% oxidation of 2200 mg/L sulfide was documented in halo-alkaline conditions in a stirred tank bioreactor. Further, a DO concentration above 2 mg/L and Na^+ concentration of 0.6-2.0 M resulted in the maximum sulfide removal and sulphate production. Other sulfur compounds such as thiosulfate, polysulfides, biosulfur were observed during the tests. *Tv. versutus* was also found in desulfurization processes along with *Thioalkalivibrio jannaschii* in the subgroup operating at pH 10.0 (Sorokin et al., 2008).

2.4.3 Bacteria Growth Cycle

The growth dynamics of bacteria follow a general cycle of 4 phases: lag, exponential, stationary and death. Displayed in Figure 2.8 is the life cycle when bacteria are introduced into fresh medium.

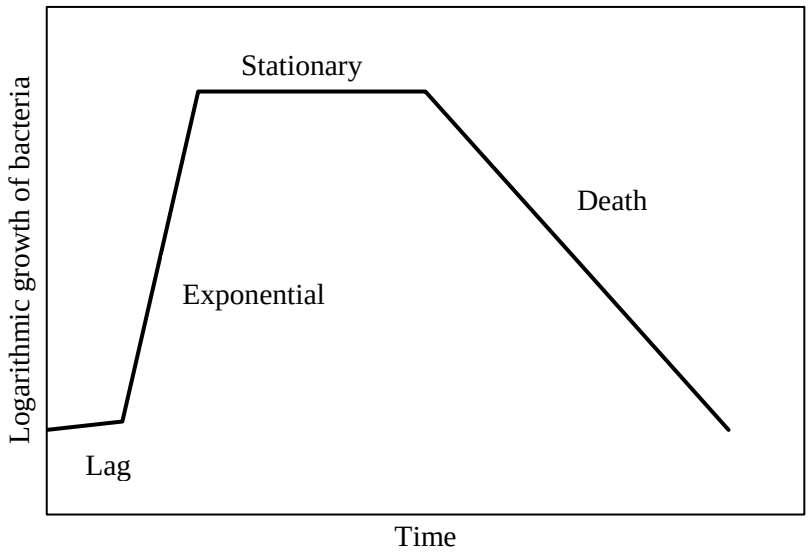

Figure 2.8: Typical growth cycle for microorganisms

The lag phase is the initial period when the bacteria are adapting to their new environment. Parameters such as the physiology of the bacteria, temperature, pH, oxygen level, and nutrients effect the pace at which the bacteria grow. Further, if the bacteria are introduced to conditions similar to its previous conditions, they will grow faster as they are already adapted to the environment. The cells may not replicate but grow in volume preparing for the exponential phase. During the lag phase bacteria commonly synthesize RNA, enzymes and essential metabolites (Bruslind, 2021).

In the exponential phase, the cells accumulate necessary nutrients for growth and divide into other cells using binary fission (Wang et al., 2015). This phase is predictable as the population doubles during this time. Optimal conditions result in more growth (steeper slopes) while non-ideal conditions will slow bacterial growth. The new cells produced are uniform and are the healthiest

compared to the cells in any other stage. Maximum growth is reached in the exponential phase and proceeds to the stationary phase.

The stationary phase occurs during the exhaustion of essential nutrients or from the inhibition by their waste products or physical space (Bruslind, 2021). The growth of the microbial population ceases as the rate of the new cells produced is equivalent to the death of the old cells. The physiology of the cells adapts to the new starvation conditions which allows them to survive longer. The cells are typically smaller in size and are weaker making them prone to more damage (Wang et al., 2015).

The final phase is from the death of the microbial population as they lose their ability to divide, and the total number of dead cells exceeds the number of live cells. The cells in this phase are generally damaged and are harder to replenish in new media.

Chapter 3

Materials and Experimental Methods

3.1 Raw Materials

Three samples identified as GSL, EQ2, and COREM were refractory gold ore pyrite concentrates utilized for this work. Varying in sulfur content, each sample was crushed, pulverized, and sieved when received and stored in air-tight bags in a 4 °C fridge to prevent oxidation. All samples were used for investigations involving biological oxidation and only COREM was used for the chemical oxidation experiments.

3.1.1 Ore Characterization

The elemental analysis of the samples is displayed in Table 3.1 and the concentrations were determined using several techniques. The total carbon and sulfur contents were measured using the Eltra CS 2000 carbon sulfur determinator. The gold concentration was measured using a conventional fire assay method. The remaining elements were determined using a PerkinElmer ELAN 9000/NexION instrument for Inductively Coupled Plasma – Optical Emission Spectrometry. X-Ray diffraction (XRD) analysis was performed on the samples GSL and COREM. EQ2 was not analyzed because it was only used for a few tests. GSL had high concentrations of quartz and pyrite with traces of albite and orthoclase. COREM was composed of quartz, pyrite, illite and traces of magnetite and kaolinite.

Table 3.1: Chemical analysis of the samples

Element	GSL	EQ2	COREM
Al (%)	3.9	8.5	5.2
Au (ppm)	1.6	1.2	1.7
As (ppm)	102	3350	182
Ca (%)	0.2	0.6	0.1
Cu (ppm)	522	1990	646

Fe (%)	20.1	12.6	4.5
K (%)	3.2	2.9	1.6
Mg (%)	0.2	0.6	0.2
Pb (ppm)	41	770	234
Total C (%)	0.1	0.2	0.1
Total S (%)	23.4	11.0	5.7

The particle size of the samples was measured using a Laser Particle Size Analyzer (LPSA). The initial P_{80} of GSL, EQ2, and COREM were 38, 32 and 55 µm, respectively.

3.2 Experimental Methods

All methods involving the presence of bacteria were performed under sterile conditions. A 70% ethanol solution was used to disinfect one's hands and the lab area. All glassware in contact with bacteria were autoclaved at 121 °C for 35 mins for sterilization. To further ensure sterilization, the addition of media, bacteria and ore into flasks were performed under a propane flame.

3.2.1 Growth and Maintenance of Bacteria

Before the oxidation of sulfide minerals could be examined, the bacteria used for the experiments had to be investigated for their growth capabilities. *Thiomicrospira aerophila* (DSMZ 13739) and *Thioalkalivibrio versutus* (DSMZ 13738) are risk group 1 bacteria obtained from the Deutsche Sammlung von Mikroorganismen und Zellkulturen (DSMZ). The frozen bacteria cultures were recovered at room temperature and suspended into fresh DSMZ 925 media in 10 mL vials. The bacterial cultures were grown and maintained in autoclaved 250 mL baffled flasks in a 30 °C incubator at 150 rpm. 100 mL of fresh medium was added to the flask and 5% (v/v) of a previous liquid culture was inoculated. Fresh cultures were prepared every week. The flasks used caps with a 0.45 µm filter to ensure sterilization while providing air for the bacteria as they are aerobic microorganisms. To avoid any loss of bacteria, they were also stored in long-term storage in Biobeads at -80 °C and in short-term storage in 4% agar plates at 4 °C.

For batch cultivation, the carbonate buffered medium containing (g/L) Na_2CO_3 (20); $NaHCO_3$ (10); NaCl (5); K_2HPO_4 (1); $MgCl_2 \cdot 6H_2O$; KNO_3; 2 mL/L of trace mineral solution containing (g/L): EDTA (0.5); $MgSO_4 \cdot 7H_2O$ (3); $MnSO_4 \cdot H_2O$ (0.5); NaCl (1); $FeSO_4 \cdot 7H_2O$ (0.1); $Co(NO_3)_2 \cdot 6H_2O$ (0.1); $CaCl_2$ (0.1); $ZnSO_4 \cdot 7H_2O$ (0.1); $CuSO_4 \cdot 5H_2O$ (0.01); $AlK(SO_4)_2$ (0.01); H_3BO_3 (0.01); $Na_2MoO_4 \cdot 2H_2O$ (0.01); Na_2SeO_3 (0.001); $Na_2WO_4 \cdot 2H_2O$ (0.01); $NiCl_2 \cdot 6H_2O$ (0.02), using thiosulfate as the energy source was used (DSMZ, 2009). *Tm. aerophila* and *Tv. versutus* required 20 g/L and 10 g/L of $Na_2S_2O_3 \bullet 5H_2O$, respectively. The carbonate buffer maintained the pH of the solution at pH 10.2. 2N HCl was used to decrease the pH of the medium for investigations at lower pH. The medium was passed through a 0.2 µm Thermo Scientific Nalgene Rapid-Flow filter unit which removed any contaminants in the solution.

Figure 3.1: Microbial cultures in a temperature-controlled shaker

All the tests with bacteria were performed in the incubator pictured in Figure 3.1 unless noted otherwise.

To generate growth curves for the bacteria, Ultraviolet-visible spectroscopy at an optical density of 600 nm was used. This method was previously used by Ang et al. (2017) to measure bacterial growth by their biomass. Kinetic samples were collected at 0, 1, 2, 4, 8, 12, 24, 48, 72, 120, 168 h intervals. Growth was measured at pH 10.2 and 9.5 to determine the optimal parameters. Photographs of the bacteria were taken on a Rebel Microscope, Echo.

3.2.2 Na_2S Oxidation Studies

To test the oxidation potential of the bacteria, oxidation tests with Na_2S were conducted for 7 days. The experiments were performed in the incubator at 30 °C and agitated at 150 rpm. Na_2S with an initial sulfide concentration of 1000 mg/L S^{2-} was used for these experiments. The salt was added to the flasks at two different times, initially before the bacteria was inoculated and after the bacteria reached their maximum growth. This was to determine if the bacteria could grow in the presence of Na_2S and if oxidation was enhanced at maximum growth. The bacteria culture medium was constant for all bacterial tests with Na_2S and pyrite unless stated otherwise.

3.2.3 Bacterial Oxidation

To evaluate the oxidative abilities of *Tm. aerophila* and *Tv. versutus*, pyrite concentrates were added to the sterile flasks with a pulp density of 1% (w/v). The experiments were maintained in an incubator at 30-35 °C and agitated at 150 rpm with a retention time of 2 weeks. Duplicate tests were performed without the inoculation of bacteria, which will be referred to as "control" experiments in this thesis. The process variables that were investigated include temperature (30 and 35 °C), thiosulfate concentration (4 – 20 g/L), pulp density (1 - 10%), time (7 – 30 days) and pH (9.5 and 10.0).

After 2 weeks, the ore was separated from the solution via centrifugation at 5500 rpm for 5 min using 50 mL Falcon tubes. The ore was placed in a vacuum-sealed oven at 40 °C for 2-3 days to ensure no more oxidation occurred. The centrifuge tubes were weighed, and the solids were

pulverized using a pestle and mortar. The ore was then acid washed in a 10% HCl solution at 65 °C for 1 h. The acid wash removes any sulfates produced during oxidation. Once washed, the ore is centrifuged again to remove the acid and rinsed with deionized water. The centrifuge tubes are then placed into the vacuum-sealed oven until completely dry. The ore is then weighed, pulverized, and used for analysis.

3.2.4 Bottle Roll

Biooxidation tests were carried out with COREM ore in an autoclaved 1 L reactor (Figure 3.2) with a working volume of 500 mL and 5% pulp density. The bioreactor revolved at 40 rpm and at ambient temperature for a total experimental time of 2 weeks. The bacteria were grown to their maximum population and were transferred into the reactor with the pyrite sample. After 1 week, the bacterial solution and ore were separated through centrifugation using 50 mL Falcon tubes. Once the solid was completely separated from the previous bacterial solution, it was replaced by a fresh bacterial solution at maximum growth. The solids were added back into the reactor using a vortex mixer. The tests were restarted for another week to finish the 2-week tests. When finished, the solids were dried, acid washed and analyzed.

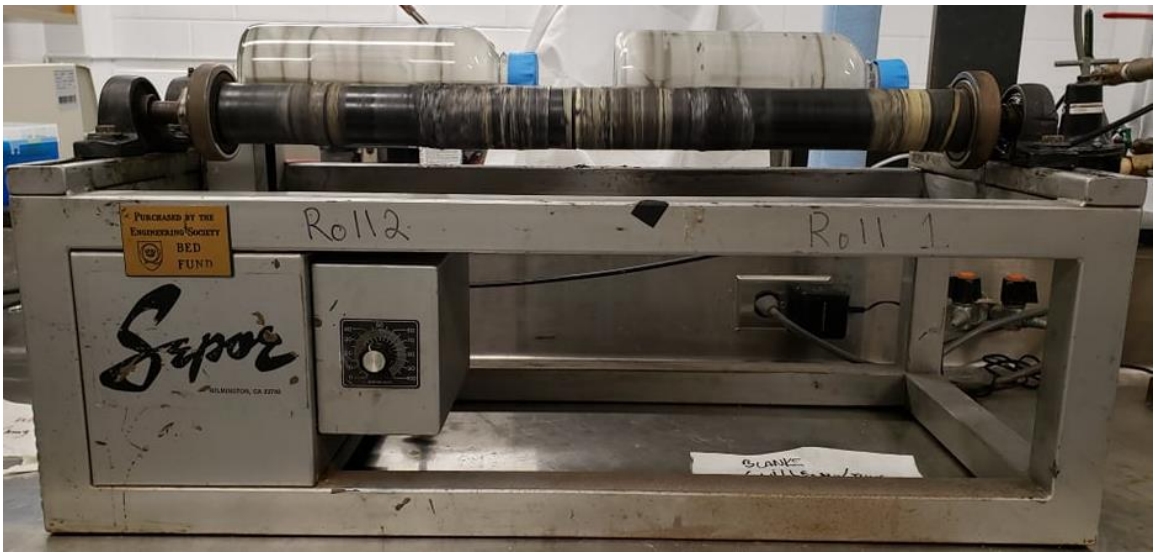

Figure 3.2: Apparatus used for bottle roll experiments

3.2.5 Chemical Oxidation

Experiments with COREM using only chemical reagents were conducted to determine the parameters necessary to achieve maximum oxidation and the effects of gold recovery following subsequent oxidation. Sodium carbonate and bicarbonate were the main constituents in the chemical oxidation tests. Tests were scaled up in 500 mL Erlenmeyer flasks with 225 mL of solution and were agitated at 500 rpm using a magnetic stir bar. Air was supplied at 0.1 L/min and a temperature probe connected to a heat plate was used to maintain the temperature in the system. To determine the optimal oxidation parameters, the temperature (25 – 80 °C), pulp density (10 – 30 %), and concentration of reagents in the media were varied in the experiments. Kinetic sampling was performed at 24 h and 48 h subsequently until the end of the test. The residence time was 3-11 days and when finished, the solids were separated from the solution using a vacuum filter. The solids were dried, acid washed and analyzed similarly to the bacterial oxidation tests. However, sterilization was not necessary for these tests as there was no presence of bacteria. The apparatus for the tests is shown in Figure 3.3.

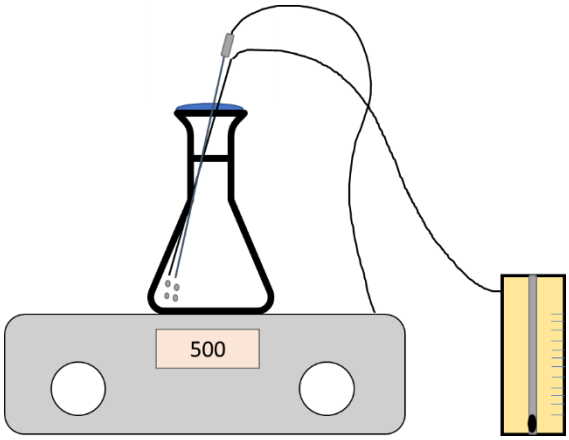

Figure 3.3: Schematic of the experimental set-up for chemical oxidation tests

3.2.6 Gold recovery

Conventional cyanidation leach experiments were performed for the chemically oxidized samples. 100 mL of 1000 ppm cyanide solution was placed in 250 mL Erlenmeyer flasks with the oxidized ore (15 – 20% pulp density) for 24 h at ambient temperature. The slurry was mixed with a magnetic

stir bar at 500 rpm. The cyanide concentration was measured using a Metrohm, 916 Ti-Touch titrator with a silver electrode. The solids were separated using a gravity filter and were washed with NaOH then DI water to remove any remaining cyanide. The samples were dried, pulverized and sent for fire assay analysis.

3.3 Analytical Methods

3.3.1 Analytical Techniques

All aqueous samples were measured for the pH, oxidation-reduction potential (ORP) and dissolved oxygen (DO) concentration. A pH/ORP probe equipped with a sympHony™ H30PCO handheld meter was used to record the pH and ORP of solutions. A Thermo Orion Star A213 DO meter and probe were used to measure the oxygen concentration in the samples. Kinetic aqueous samples were passed through a 0.45 μm Sarstedt non-pyrogenic sterile syringe filter before analysis.

For experiments examining oxidation, measurements were taken before and after each test by an iodometric titration method for sulfide concentration in solution (Holm et al., 2000) for Na_2S and by the Eltra CS 2000 carbon sulfur determinator for pyrite samples.

XRD, scanning electron microscopy (SEM), and LPSA were used to analyze the ore mineral for some pyrite samples. XRD and SEM were sent to analytical labs on campus (at Geological Sciences and Geological Engineering) and fire assay was sent for analysis to external service laboratories.

3.3.2 Calculations and Error Estimation

There were a variety of factors that may have affected the data due to the unpredictable nature of the bacteria. Therefore, all experiments with regards to growth curves and oxidation were repeated twice at minimum to generate consistent results.

Pyrite oxidation was calculated using values obtained from the Eltra CS 2000 carbon sulfur determinator and inserted into Equation 28.

$$\frac{W_I S_I - \frac{W_A S_F}{W_P / W_F}}{W_I S_I} * 100 \quad [28]$$

where, W_I is the initial weight of sample, S_I is the initial sulfur content, W_A is the weight of sample after acid wash, S_F is the final sulfur content after acid wash, W_P is the weight of ore added to the acid wash solution, and W_F is the final weight after oxidation. Since only a portion of the sample was washed with acid solution, an equation had to be developed to correlate the weight loss with the entire oxidized sample. Kinetic oxidation values were calculated using the same equation; however the total weight of the sample (W_F) was adjusted to account for the ore removed from the experiment.

Gold recovery was calculated using Equation 29 from values acquired from fire assay analysis. Analysis was performed on samples before and after oxidation, and after cyanidation.

$$\frac{C - c}{C} * 100 \quad [29]$$

where, C is the initial gold concentration and c is the final gold concentration.

Error bars for the gold recovery graphs/charts were produced based on the average of gold concentrations in samples analyzed by fire assay. The average was approximately 3.25% for the upper and lower limit which will be used as the fixed error value for all gold recovery plots.

3.3.3 Safety Precautions

Laboratory work was performed using precautionary measures to maintain a safe working environment. A lab coat, safety glasses, and proper gloves and footwear were always worn. As both bacteria are risk group 1 microorganisms, sterilization and disposal were performed using 10% freshly prepared bleach solution. Tests with acid or cyanidation were performed in their respective fume hoods with a H_2S or HCN gas detector. All chemicals and contaminated equipment were properly disposed in waste containers labelled with all elements and pH range. A shower and eye wash station was nearby in case of an emergency.

Chapter 4

Results and Discussion

4.1 Growth Curves

Growth curves were produced for *Tm. aerophila* and *Tv. versutus* for 7 days using DSMZ 925 media at 5% (v/v) inoculation. The bacteria were incubated at 30 °C and agitated at 150 rpm. Kinetic samples were collected at 0, 1, 2, 4, 8, 12, 24, 48, 72, 120, 168 h intervals at pH 10.2 and pH 9.5.

4.1.1 Growth of *Thiomicrospira aerophila*

As observed in Figure 4.1, the growth of *Tm. aerophila* gradually increased until 48 h and then was stationary for the entire 7-day period. At both pH 9.5 and 10.0, maximum growth was recorded on the 5th day of the tests. Optimal growth was measured at pH 9.5 where the maximum OD_{600} value was 0.39. Growth at pH 10.2 was slightly lower with the maximum OD_{600} value recorded at 0.34. For pH 10.2 and 9.5, the pH initially decreased reaching its lowest pH values at 48 h and 24 h, respectively. After these times, the pH steadily rose to approximately 9.7-9.8. The correlation between the growth and pH plot indicates the pH drops during initial growth and starts to increase as the population of the bacteria is maintained. The decrease in pH is due to the initial growth spurt where a large amount of sulfuric acid is produced as the thiosulfate is converted into sulfate. The increases in pH were due to the reduced production of sulfuric acid due to the buffering effects of carbonates. For oxidation experiments conducted with *Tm. aerophila*, the bacteria were grown for 48 h before being utilized for the tests.

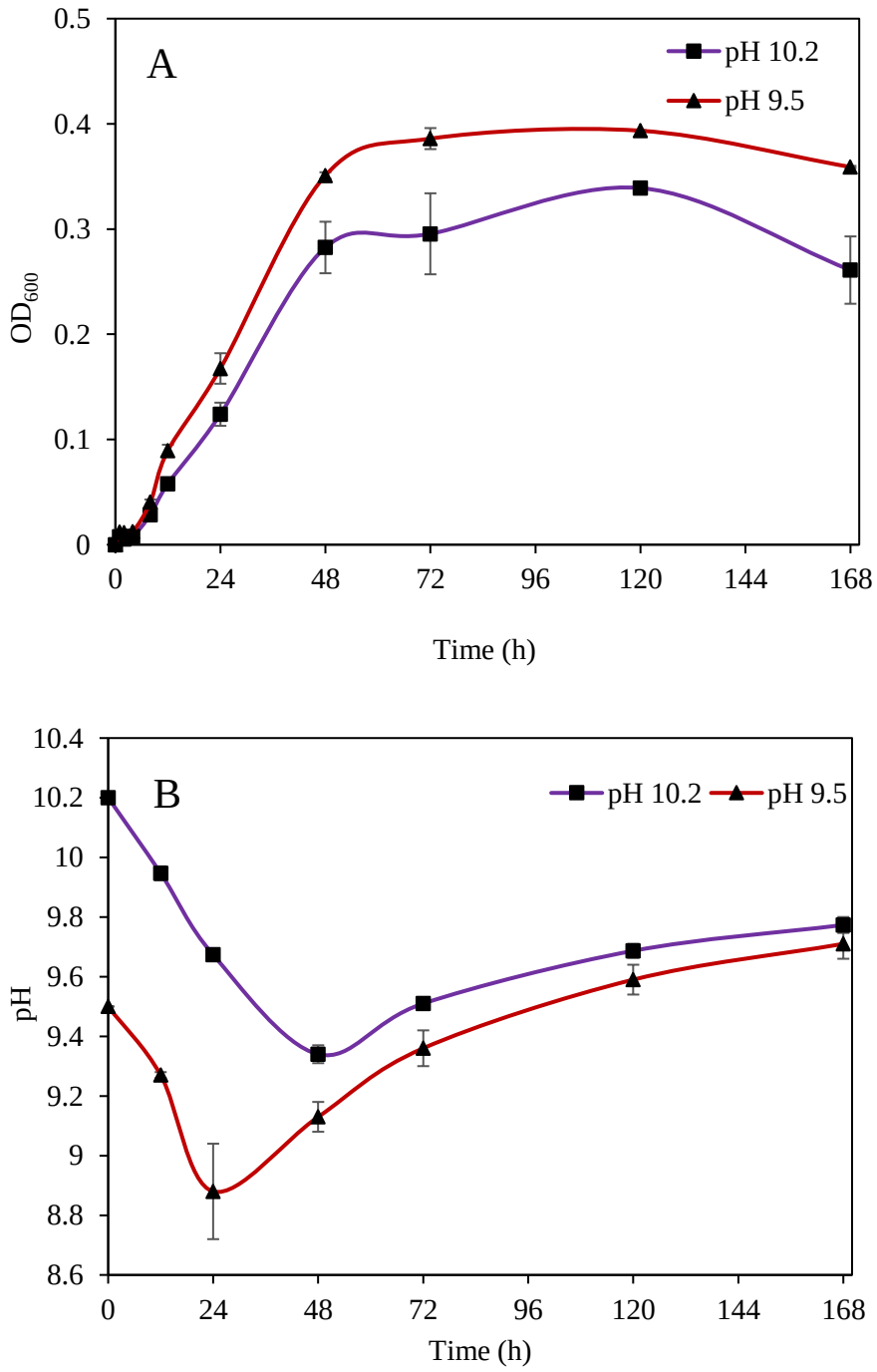

Figure 4.1: Growth curve (A) and pH change in the medium (B) for *Tm. aerophila* at pH 10.2 and 9.5 for 7 days at 30 °C and 150 rpm.

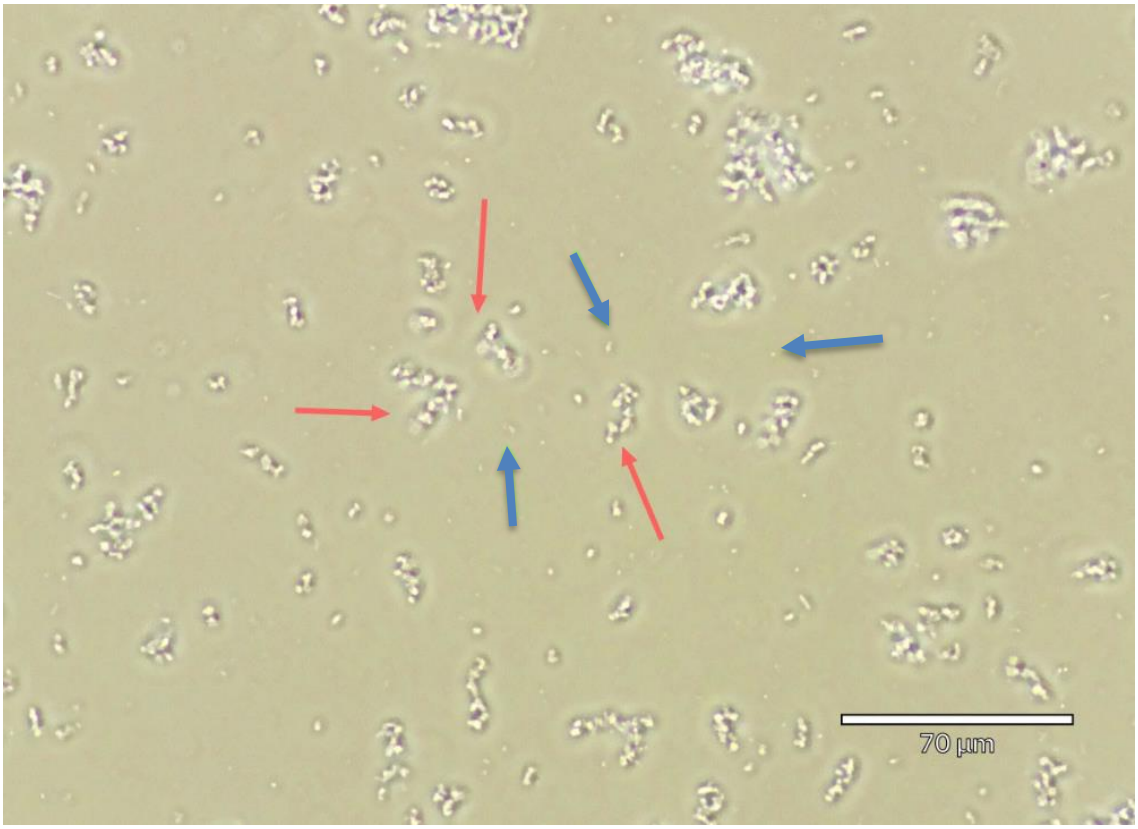

Figure 4.2: Microscopic picture of *Tm. aerophila*

Figure 4.2 exhibits a microscopic picture of the bacteria at maximum growth. The red and blue arrows indicate clusters or singular bacteria. They are known to form compact colonies and each cell is approximately 0.5 x 1.5 µm (Sorokin et al., 2001).

4.1.2 Growth of *Thioalkalivibrio versutus*

The growth patterns of *Tv. versutus* are different from those of *Tm. aerophila* as there was significant bacterial growth at 24 h as presented in Figure 4.3. The bacterial population then decreased and was maintained until the end of the 7 days. The optimal growth was observed at pH 9.5 at a maximum OD_{600} value of 0.75. Although growth at pH 10.2 had a lower maximum OD_{600} value of 0.49, the population was maintained higher than at pH 9.5 after 48 h. This may be due to the correlation of their death rate with their prior growth conditions. Biselli et al. (2020) performed

studies with Escherichia coli with observations of slower growth leading to an exponentially slower death rate as the maintenance rate of the cells decreased.

The pH of the solution during growth was similar to the patterns observed for *Tm. aerophila*. The pH decreased until the maximum growth at 24 h for pH 9.5 and 48 h for pH 10.2 then steadily increased to pH 9.7-10.0. The decrease in the pH was correlated with the growth of bacteria due to the formation of sulfuric acid. For the oxidation experiments conducted with *Tv. versutus*, the bacteria were grown for 24 h before being utilized for the tests.

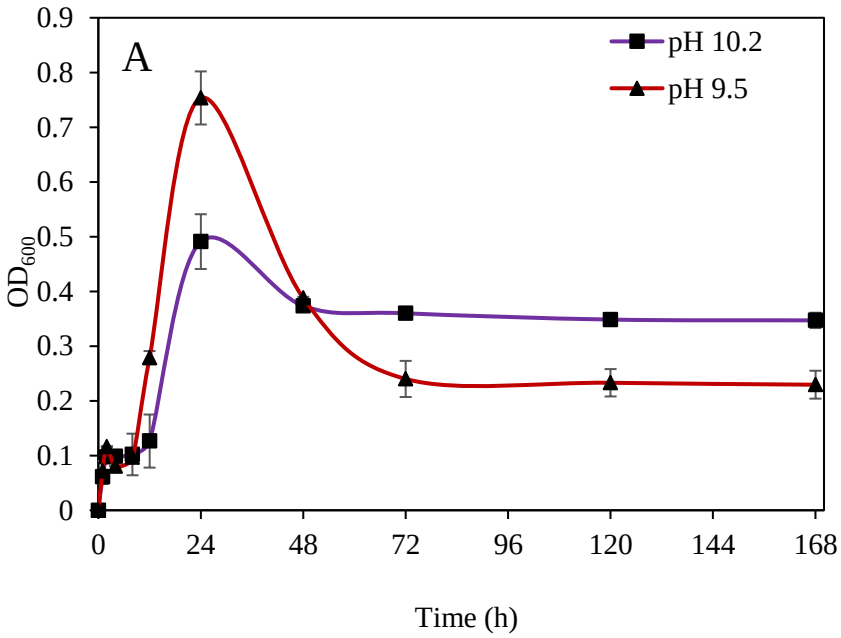

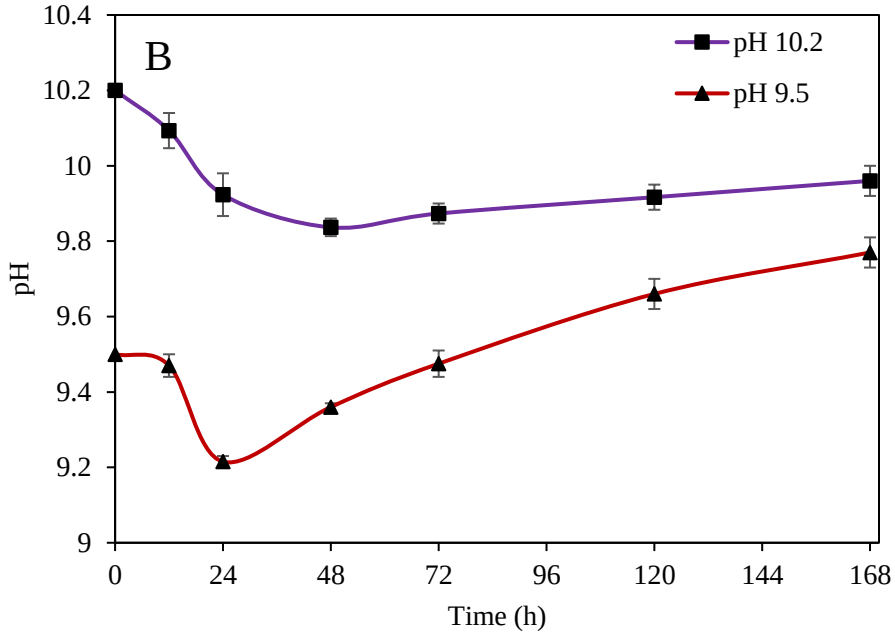

Figure 4.3: Growth curve (A) and pH change in the medium (B) for *Tv. versutus* at pH 10.2 and 9.5 for 7 days at 30 °C and 150 rpm.

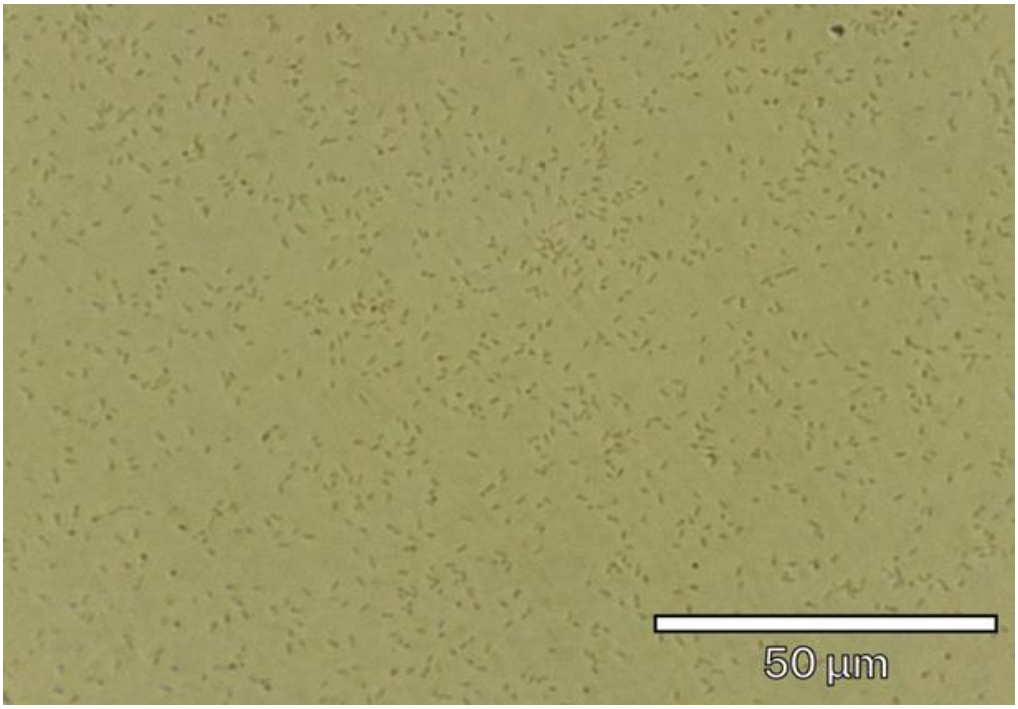

Figure 4.4: Microscopic picture of *Tv. versutus*

A microscopic image shown in Figure 4.4 is of *Tv. versutus* at maximum growth. The cells are approximately 0.7 x 2.0 µm (Sorokin et al., 2001) in size. Halo-bacteria usually have carotenoids to protect them from high light and oxygen radicals. However, *Tv. versutus* produced yellow pigments instead of carotenoids as the colony grew older. Previous studies have reported this function to protect them by providing an additional ion barrier for the membrane (Foti et al., 2006; Takaichi et al., 2004).

4.1.3 Growth of Mixed Cultures

Biooxidation processes typically utilize various microorganism because of their unique oxidizing characteristics and bacterial synergism (Bacelar-Nicolau and Johnson, 1999b; Mahmoud et al., 2017). For sulfur compounds, microorganisms oxidize different reduced sulfur species which can lead to increased oxidation. Therefore, growth using a mixed culture of *Tm. aerophila* and *Tv. versutus* were investigated from a 2.5% (v/v) inoculum from each bacterium.

Since both bacteria used different concentrations of thiosulfate (20 g/L and 10 g/L of $Na_2S_2O_3.5H_2O$) for growth, growth curves were performed at both concentrations and at pH values of 9.5 and 10.2 which are displayed in Figure 4.5.

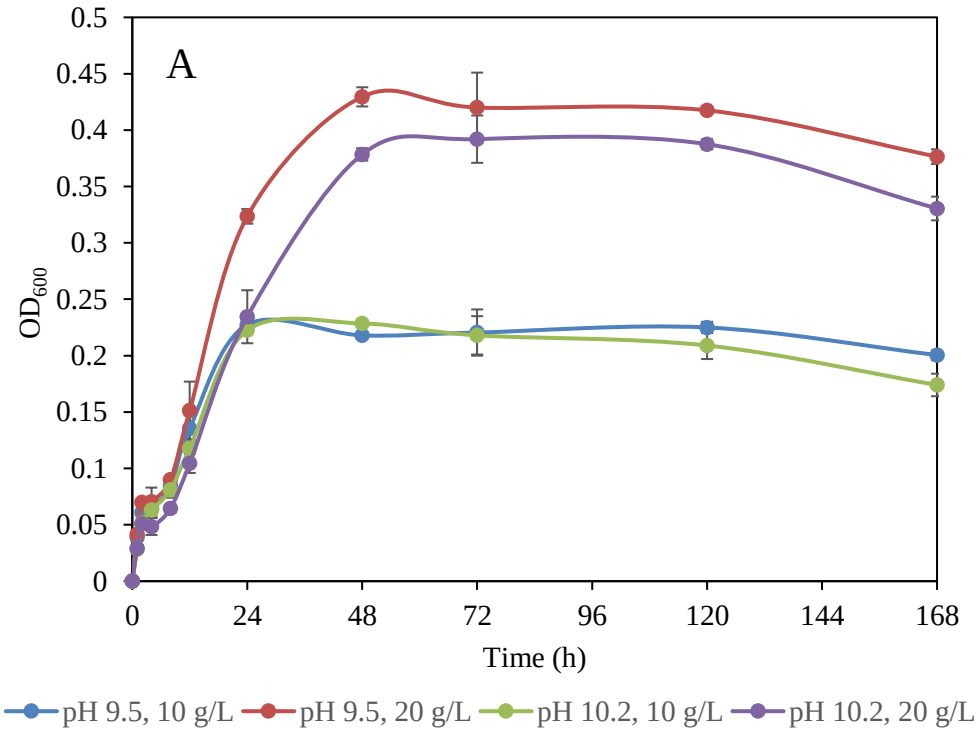

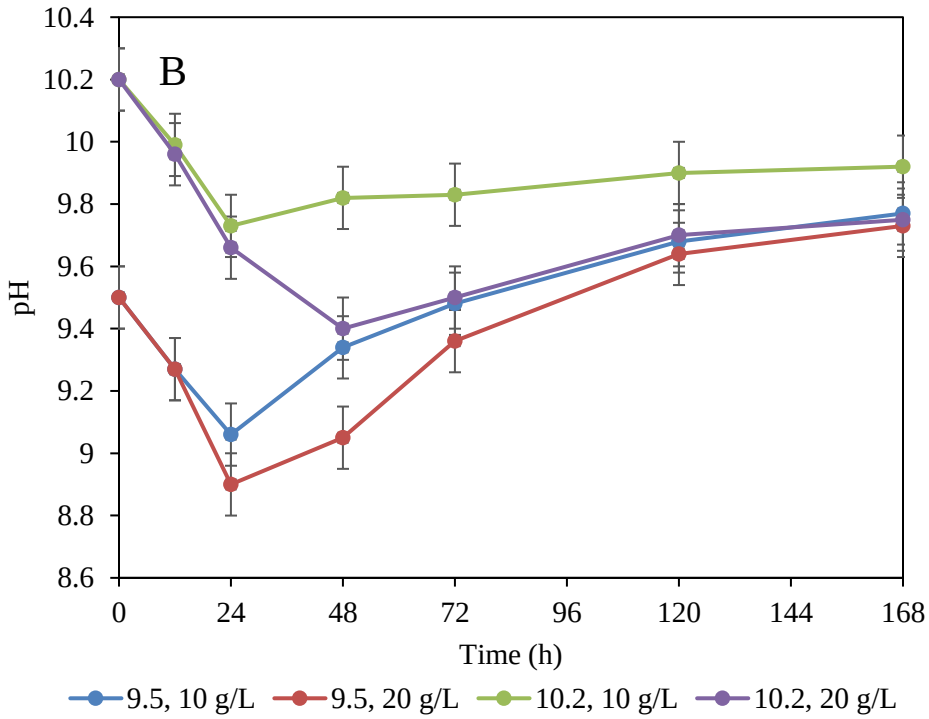

Figure 4.5: Growth curve (A) and pH change (B) for mixed bacteria at pH 9.5 and 10.2 and thiosulfate concentrations of 10 and 20 g/L

The optimal growth condition for the mixed culture was at pH 9.5 and 20 g/L with an OD_{600} value of 0.43 at 48 h. Higher growth was observed at pH 9.5 regardless of the concentration of thiosulfate. Tests with the medium at pH 10.2 were measured at approximately half the OD_{600} value of tests at pH 9.5. The mixed culture resembled the growth pattern of *Tm. aerophila* (Figure 4.1A) with an initial increase in population which is then maintained. Similarly, the pH decreased until 24 - 48 h and increased to pH 9.7-9.9 by the end of the 7-day period.

4.1.4 Growth Studies in Other Media

Bacterial growth with a modified DSMZ 925 media were performed to test if both bacteria can survive in buffers other than carbonate/bicarbonate. Phosphate, ammonium, and a glycine-sodium hydroxide were considered. However, experiments with phosphate and ammonium buffers were not performed as the phosphate buffer did not reach pH 10.0 and both bacteria grow in concentrations of ammonium less than 2 mM (Sorokin et al., 2000). Therefore, growth tests were investigated at pH 10.0 with a glycine-sodium hydroxide buffer (AAT Bioquest Inc., 2020).

The growth tests were unsuccessful as *Tv. versutus* did not grow in the modified media and *Tm. aerophila* had limited growth. The pH of the media with *Tm. aerophila* dropped below 8 in 24 h and dropped again below 7 after 48 h. This was below the growth pH threshold for the bacteria (Sorokin et al., 2000). This suggests bacteria cannot survive for long and the buffer was not strong enough. pH adjustments were made by adding more media, however they were also unsuccessful as the pH consistently dropped between 6-24 h after inoculation.

Experiments were also conducted at varying inoculation percentages, 2.5, 5 and 10% (v/v). Increasing the inoculation affected their initial growth, however the difference in the population during the stationary phase was minimal.

4.2 Na_2S Oxidation

Investigations on the biological oxidation capabilities by *Tm. aerophila* and *Tv. versutus* were performed. The bacteria were grown to their maximum population and 1000 mg/L of sulfide as Na_2S was added. The oxidation tests were conducted for 7 days in a 30 °C incubator at 150 rpm. The experiments containing bacteria were compared to the "control" tests in which only Na_2S was added to the DSMZ 925 media (no bacteria). As shown in Figure 4.6A, both bacteria were able to oxidize approximately 96% of the sulfur compared to the control test in which approximately 38% was oxidized. This suggests that the bacteria were responsible for approximately 58% of the oxidation performed by utilizing sulfur as an energy source. Their growth in a sulfur medium had been investigated previously by Ang et al. (2017). Experiments with the addition of Na_2S before inoculation were also conducted to determine if the amount of oxidation was affected. However, differences in the oxidation of Na_2S were negligible regardless of when the salt was added to the system. For Tv. versutus, their growth in the solution was observed to be high at 24 h followed by good growth for the remainder of the test, like their growth curve. However, *Tm. aerophila* was observed to have slow growth in 24 h, followed by significant growth at 48 h which it maintained for the remainder of the experiment.

Figure 4.6B exhibited a drop in pH due to the production of sulfuric acid due to the growth of the bacteria (using Na_2S and thiosulfate as energy sources). Although most of the sulfur was oxidized, Tm. aerophila had a larger decrease in pH than Tv. versutus due to their growth characteristics. This was evident by comparing the pH changes in their growth in Figure 4.1B and Figure 4.3B. The control test had a slight drop in pH resulting from the chemical oxidation as there was no presence of bacteria. The ORP (Figure 4.6C) increased for all experiments and was positive in the bacterial tests, however the control tests remained negative suggesting less oxidation occurred. Therefore, the pH and ORP helped to confirm that both bacteria can oxidize Na_2S in aqueous

systems. The DO (Figure 4.6D) in the solution was similar before and after for the tests inoculated with bacteria but was lower in the control tests.

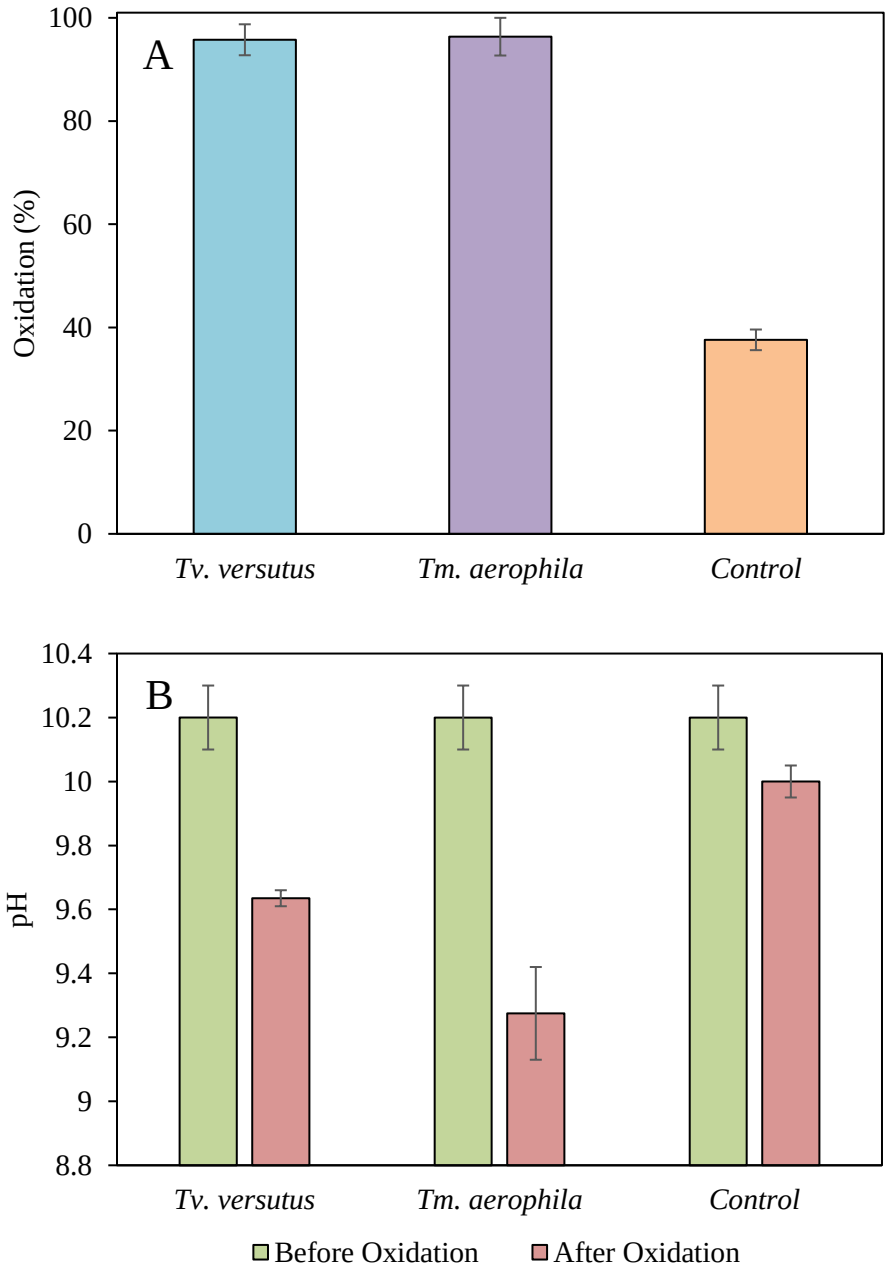

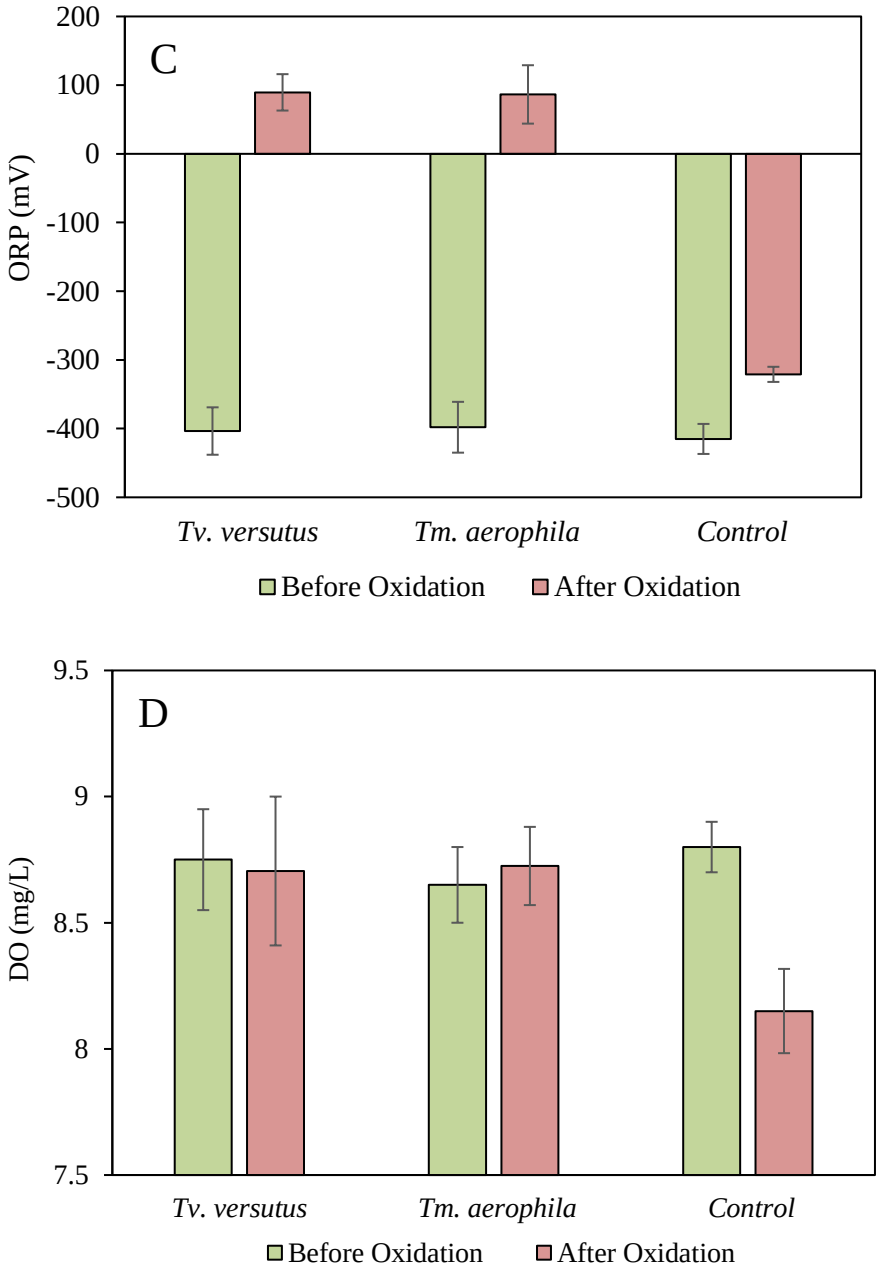

Figure 4.6: Oxidation of Na_2S (A) and the changes in pH (B), ORP (C), and DO (D) at pH 10.2 for 7 days at 30 °C and 150 rpm.

4.3 Oxidation of GSL

The differences in pyrite oxidation due to biological and chemical oxidation were investigated with GSL. This sample had the highest sulfur content (23.4%) compared to the other pyrite concentrates (EQ2 and COREM had 11% and 5.7%, respectively). Bacteria were grown to their maximum OD_{600} value before the addition of ore.

Figure 4.7 displays the oxidation of GSL at 1% pulp density with the changes in pH, ORP and DO. *Tv. versutus*, *Tm. aerophila*, and the control test oxidized approximately 34, 23, and 37% of pyrite, respectively. Although it was difficult to determine the pH change in the bacterial inoculated tests due to the reduction of pH during their growth, the final pH and ORP indicated that the highest oxidation occurred in the control tests. Unlike the Na_2S tests, the control tests had lower pH and a positive ORP compared to the biooxidation tests. Therefore, this suggests more oxidation occurred in the control tests than with the tests inoculated with sulfur-oxidizing bacteria. This may be explained by the high sulfur content in the concentrate which can create a toxic environment for the microorganisms (Pirieh and Naeimpoor, 2019). The growth of the bacteria may be inhibited by the addition of the ore due to the new environment, or it currently cannot utilize the sulfur in pyrite as an energy source.

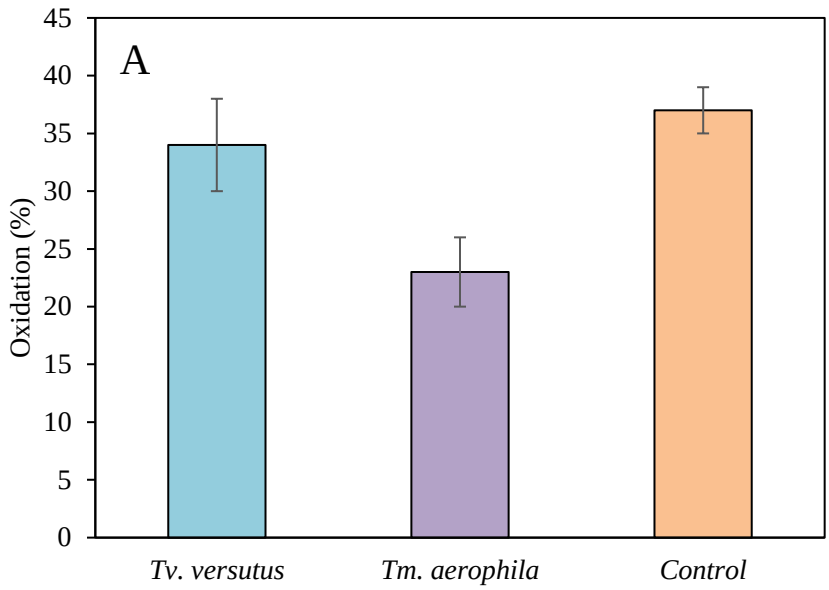
A
Oxidation (%)
45
40
35
30
25
20
15
10
5
0
Tv. versutus
Tm. aerophila
Control

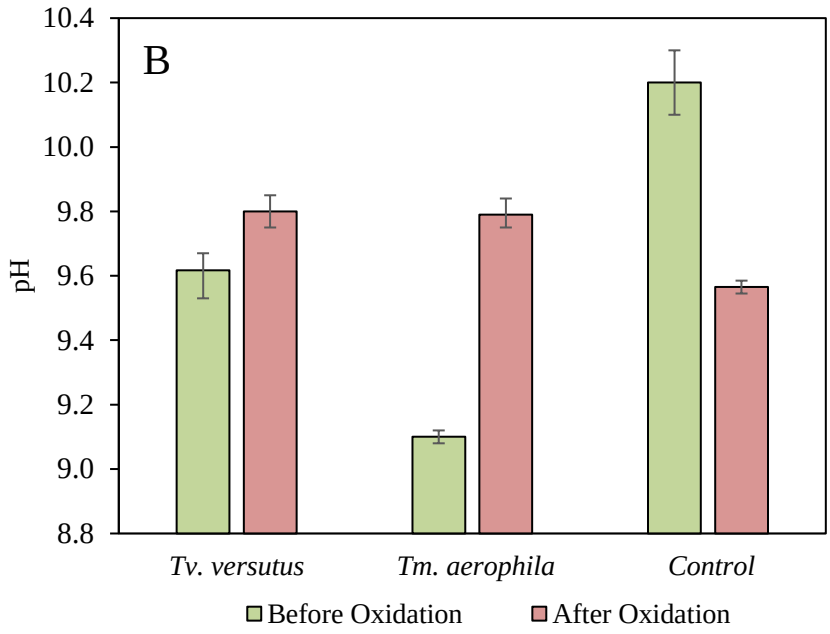
B
pH
10.4
10.2
10.0
9.8
9.6
9.4
9.2
9.0
8.8
Tv. versutus
Tm. aerophila
Control
Before Oxidation
After Oxidation

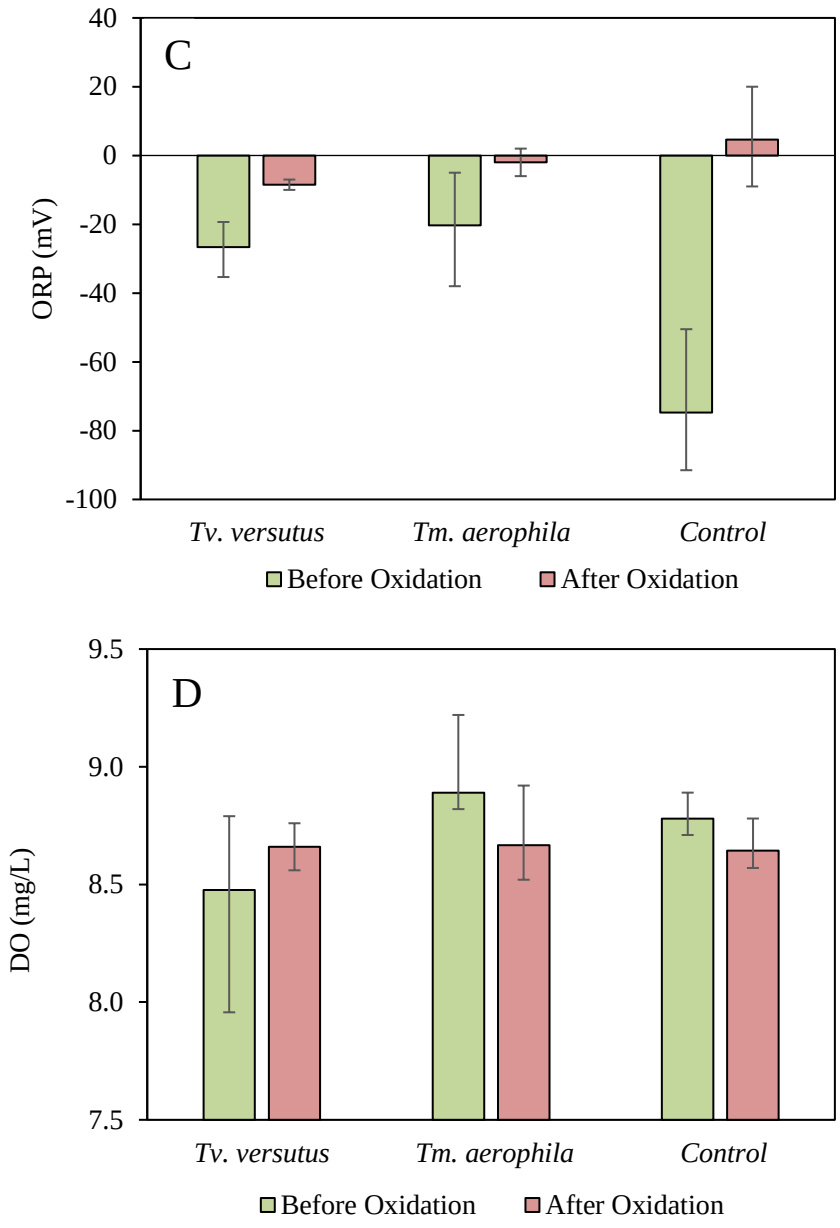

Figure 4.7: GSL oxidation at 1% pulp density and changes in pH (B), ORP (C), and DO (D) at pH 10.2 for 14 days at 30 °C and 150 rpm.

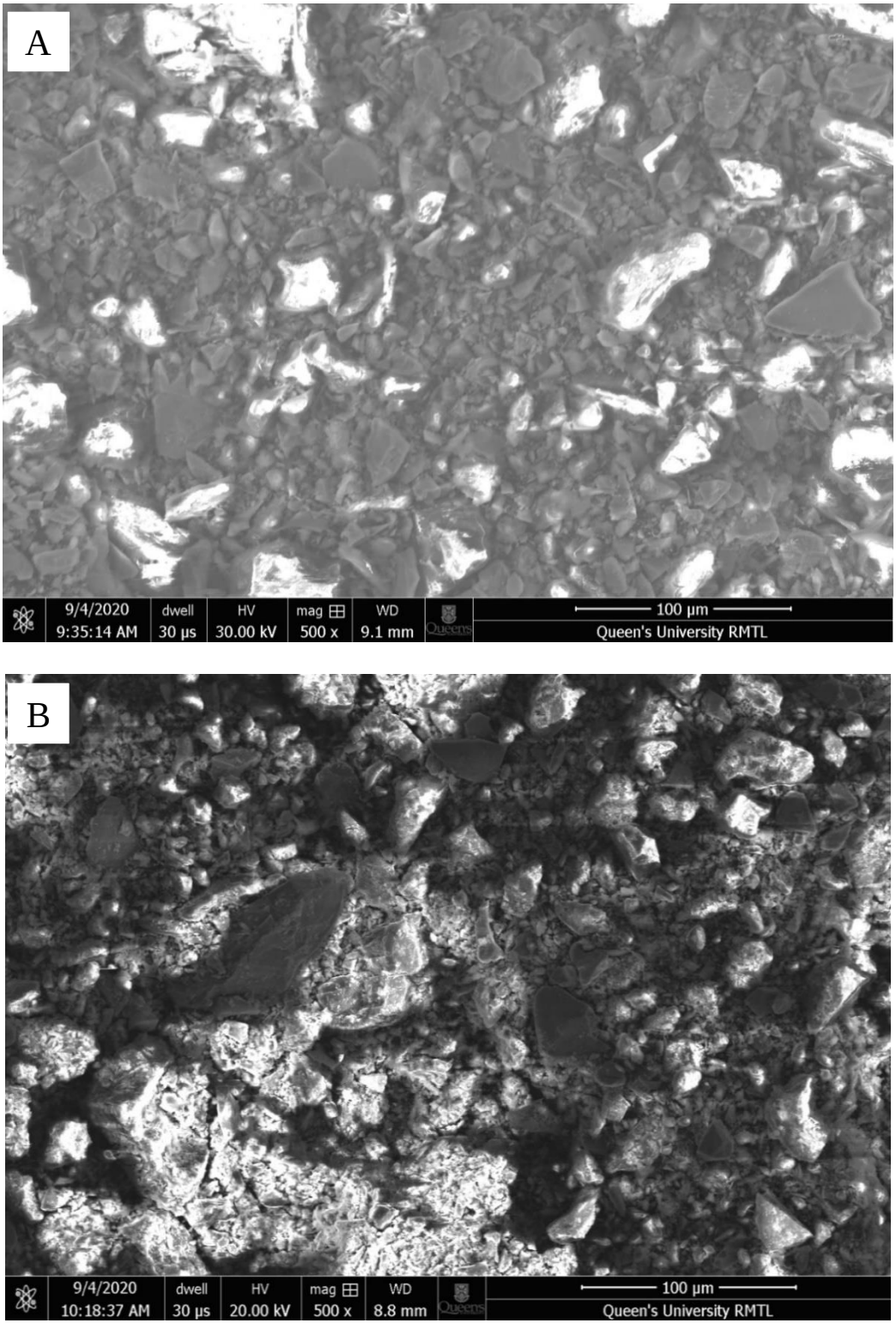

Figure 4.8: Surface morphology of GSL before (A) and after partial oxidation (B) at pH 10.2, 30 °C, and 150 rpm for 14 days

Grain edges and corners, defects, solid and fluid inclusion pits, cleavages and fractures are formed in sites with specific sites of high surface energy (Chandra and Gerson, 2010; McKibben and Barnes, 1986). This is demonstrated on the surface of GSL before and after oxidation as observed in Figure 4.8. As seen in Figure 4.8A, the pyrite surface is generally flat. Figure 4.8B indicated oxidation occurred as the surface was rougher with deep cuts into the ore. The figures indicate the removal of sulfide matrices which may increase metal recovery by exposing the metals to lixiviants.

4.3.1 Effect of Temperature

Investigations on increasing temperature to improve pyrite oxidation is well established (Moses et al., 1987; Moses and Herman, 1991; Schoonen et al., 2000; Wang et al., 2019). To test the biological and chemical oxidation potential, experiments at 35 °C were performed. Tests at higher temperatures were not investigated as both bacteria have good growth parameters only until 35 °C. The oxidative performances by *Tv. versutus*, *Tm. aerophila*, and the control test are displayed in Figure 4.9 as 35, 30 and 42% were oxidized, respectively. This resulted in a 0.5% increase in oxidation for *Tv. versutus*, 6.5% for *Tm. aerophila* and 5% for the control test compared to the experiments at 30 °C. The increase of oxidation for *Tm. aerophila* may be due to its physiological oxidation abilities which might be enhanced at higher temperatures. As observed previously, the control tests oxidized more than both bacteria at 30 and 35 °C.

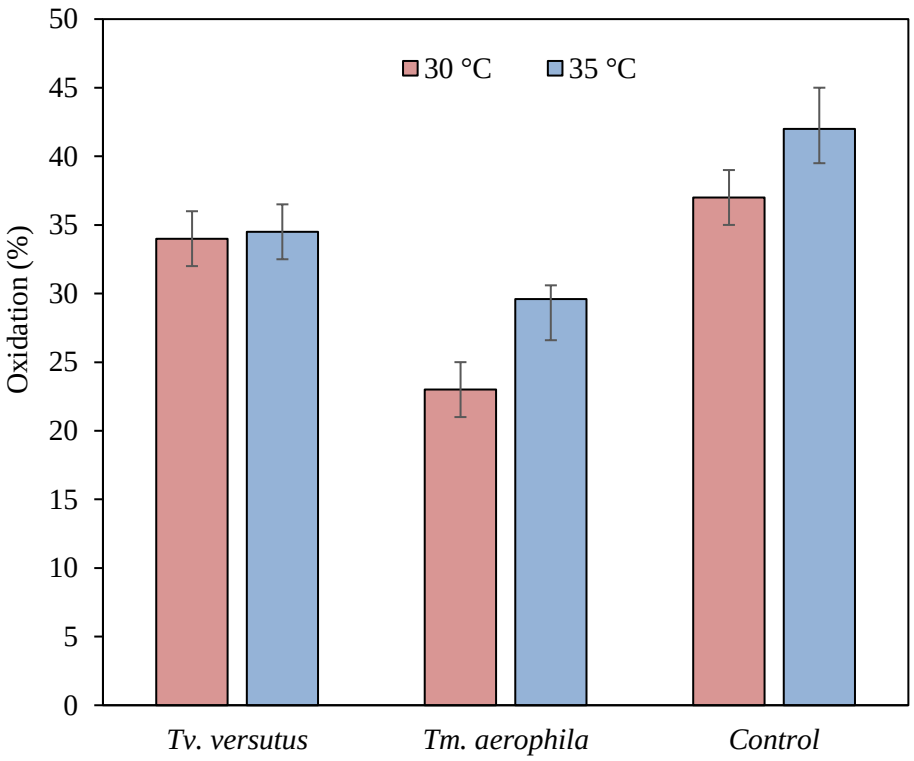

Figure 4.9: Effect of temperature at 30 and 35 °C with GSL at 1% pulp density, pH 10.2 and 150 rpm for 14 days

4.3.2 Effect of Reduced Thiosulfate Concentration

To reduce the bacteria's dependence on the supplied thiosulfate and to increase oxidation, a strategy by Mubarok et al. (2017) to significantly reduce thiosulfate in the media was investigated. Further, studies have shown that adapting microorganisms to certain environments can promote their dependance on other energy sources (i.e. sulfur in pyrite) (Astudillo and Acevedo, 2008; Haghshenas et al., 2009; Wang et al., 2014; Xia et al., 2008). The thiosulfate concentration in the media was reduced by 80%. Figure 4.10 exhibits the oxidative results with reduced thiosulfate media at 35 °C. Pyrite was oxidized by *Tv. versutus*, *Tm. aerophila* and the control test at 44.2, 41.3 and 50%, respectively. This was a significant increase relative to the tests without reduced thiosulfate media as over 8% more oxidation occurred for all three cases.

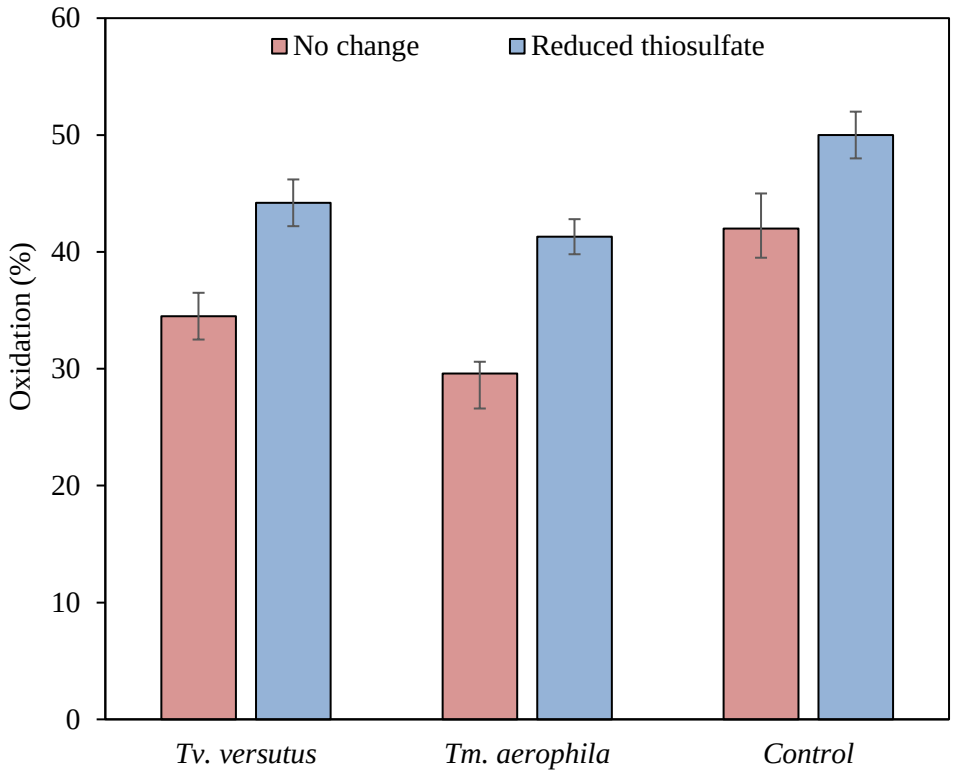

Figure 4.10: Effect of reduced thiosulfate concentration with GSL at 1% pulp density, pH 10.2, 35 °C and 150 rpm for 14 days

4.3.3 Effect of Pulp Density

To understand the role of chemical oxidation in sulfur materials, oxidation experiments without bacteria were performed at various pulp densities. As seen in Figure 4.11, there was a decrease in oxidation as the pulp density increased. At 0.5, 1, 5, and 10%, pyrite oxidation was observed to be 42, 37, 26, and 14% respectively. Increasing pulp density decreases the iron solubility which results in lower oxidation (Acevedo et al., 2004; Pathak et al., 2014).

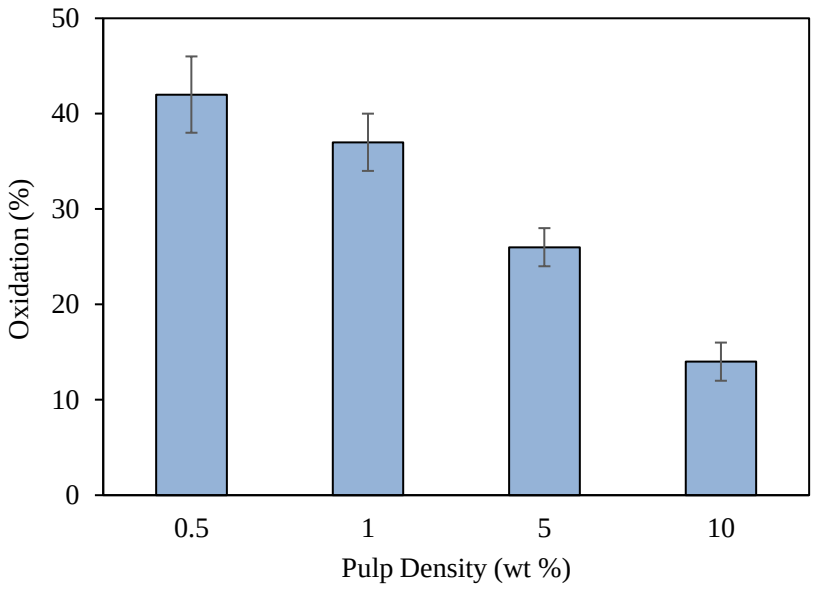

Figure 4.11: Effect of pulp density with GSL at pH 10.2, 30 °C and 150 rpm for 14 days

4.3.4 Effect of Time

Experiments were also performed over a 7 and 30-day period to investigate the effect of time on oxidation without the inoculation of bacteria. As indicated in Figure 4.12, there was a positive correlation in the time and in the oxidation of GSL with 14, 37 and 64% oxidized for 7, 14 and 30 days, respectively. There were no significant differences in the pH, ORP, and DO values between the experiments.

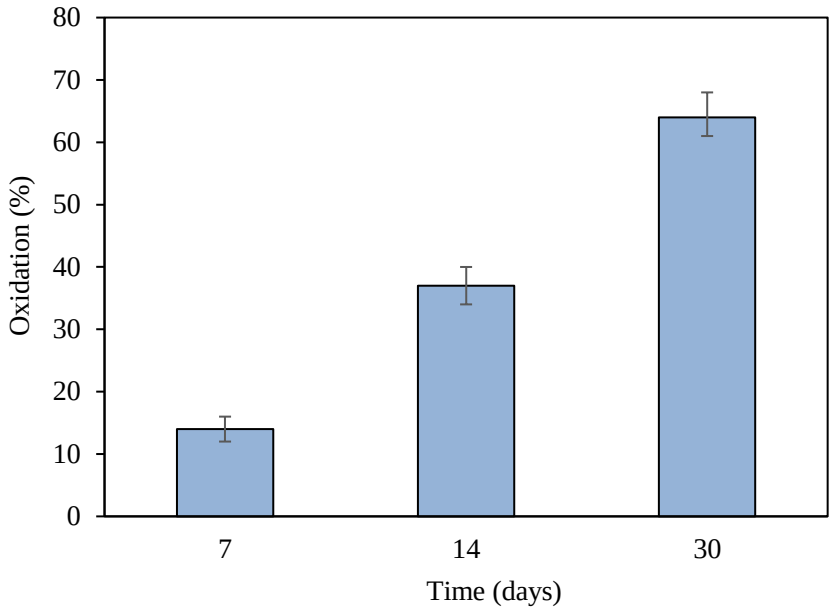

Figure 4.12: Effect of time with GSL at 1% pulp density, pH 10.2, 30 °C and 150 rpm

4.3.5 Studies on other process variables

Variations to the process were investigated to determine if oxidation by bacteria could surpass the oxidation occurring in the control tests. Methods such as using a mixed culture, lowering the pH to 9.5, and a 2-phase technique were used to improve the oxidation of the ore. A mixed culture of bacteria was tested because it could lead to increased oxidation due to the combination of their oxidizing characteristics and bacterial synergism (Bacelar-Nicolau and Johnson, 1999b; Mahmoud et al., 2017). However, both tests were only able to oxidize approximately 23%. Lowering the pH to 9.5 where their maximum growth was achieved, was to test if more bacterial growth increased oxidation. These tests were also unsuccessful as approximately 22% and 12% of the ore was oxidized with *Tv. versutus* and *Tm. aerophila*, respectively. A 2-phase technique to initially oxidize the pyrite abiotically to transform the toxic sulfur compounds to less toxic intermediates was performed. Subsequently, biotic oxidation was performed by microorganisms to more easily utilize the sulfur intermediates to increase oxidation (De Graaff et al., 2012; Pirieh and Naeimpoor, 2019). Oxidation was significantly lower for *Tv. versutus*, however *Tm. aerophila* had approximately 26%

oxidation, 3% higher than the original test seen in Figure 4.7A. Although higher oxidation was achieved, the control tests were still more effective at oxidizing GSL.

Further, methods such as limiting oxygen to the system and eliminating any potential contaminants by washing the ore with ethanol and thymol (bactericide), were investigated with no success.

4.4 Oxidation of EQ2

Investigations with another pyrite concentrate were conducted to understand the enhanced oxidation in the control experiments which are presented in Figure 4.13. EQ2 was another pyrite ore with approximately half the sulfur content as GSL (11%). However, the problem persisted as the experiments revealed that the control tests consistently had higher oxidation efficiencies than the bacterial tests. The control tests had chemically oxidized 54% of the pyrite compared to *Tv. versutus* and *Tm. aerophila* tests which had oxidized approximately 44% and 42%, respectively. This may be explained due to the high sulfur content or from the high concentration of arsenic (3350 ppm) which is toxic to most microorganisms (Cervantes et al., 1994; Das et al., 2013; Podol'skaya et al., 2002). The changes in the pH, ORP, and DO were similar to the results from GSL. Both bacteria increased their pH while the control test reduced pH after oxidation. This suggests that the bacteria continued to grow which increased pH and sulfuric acid reduced pH in the control test. The ORP and DO values followed the same trends as the tests from GSL, however, ORP was higher at the end of the tests for EQ2. These differences may be due to the minerology of the ore as EQ2 contained half of the sulfur content of GSL which resulted in higher oxidation occurring readily.

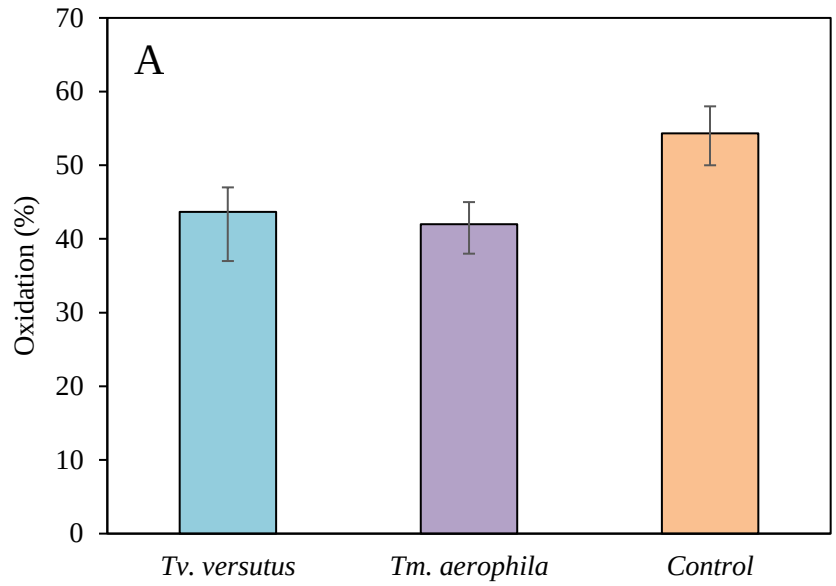
A
Oxidation (%)
70
60
50
40
30
20
10
0
Tv. versutus
Tm. aerophila
Control

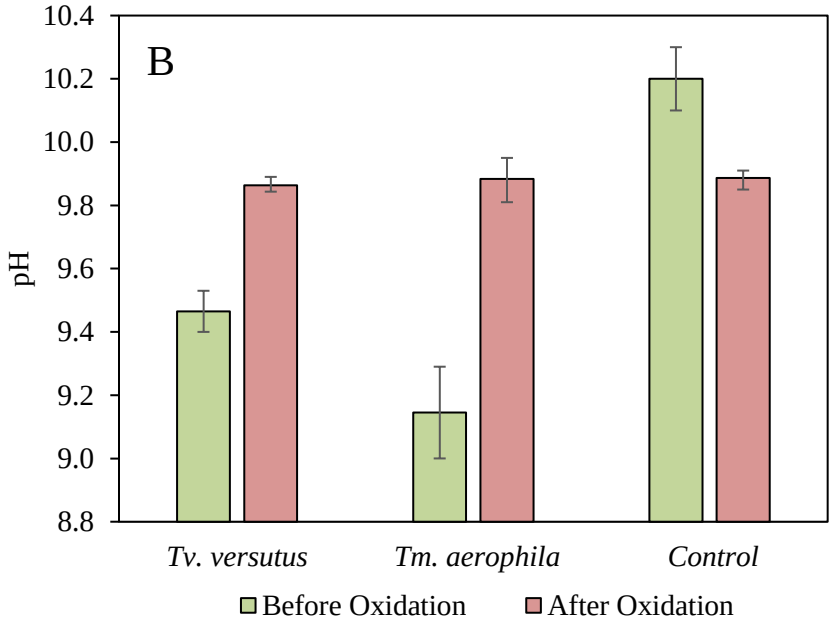
B
pH
10.4
10.2
10.0
9.8
9.6
9.4
9.2
9.0
8.8
Tv. versutus
Tm. aerophila
Control
Before Oxidation
After Oxidation

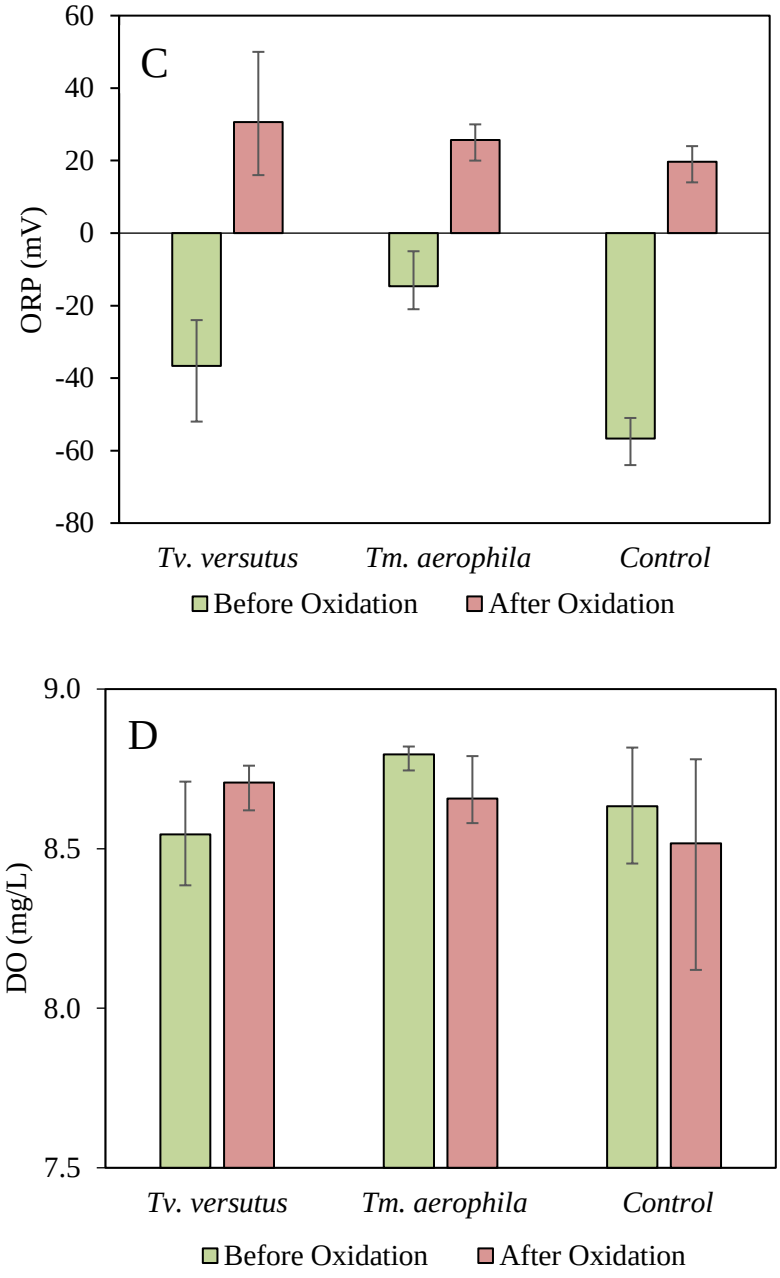

Figure 4.13: EQ2 oxidation at 1% pulp density and changes in pH (B), ORP (C), and DO (D) at pH 10.2 for 14 days at 30 °C and 150 rpm.

4.5 Bottle Roll tests

To further comprehend the enhanced oxidation in the control tests, bottle roll tests were performed with COREM. This pyrite concentrate had the lowest total sulfur content (5.7%) which should have the least toxic impact on the bacteria. These experiments were scaled-up to 5% pulp density in 1 L sterile reactors, were run for 2 weeks at ambient temperature, and rolled at 40 rpm. The media was replaced after one week with new fully grown bacteria. However, the same pattern was observed in Figure 4.14 as enhanced oxidation was observed in the control tests. The oxidations of the ore were approximately 21, 16, and 19% for the control, *Tv. versutus* and *Tm. aerophila*, respectively. However, unlike the previous experiments, *Tm. aerophila* had better results than *Tv. versutus*. This may be due to their physiological characteristics regarding dissolved oxygen as the reactor was sealed during the experiment. Therefore, it is proposed that the chemical oxidation performed by the carbonate effect predominates in the oxidation of pyrite minerals in the presence of sulfur-oxidizing bacteria.

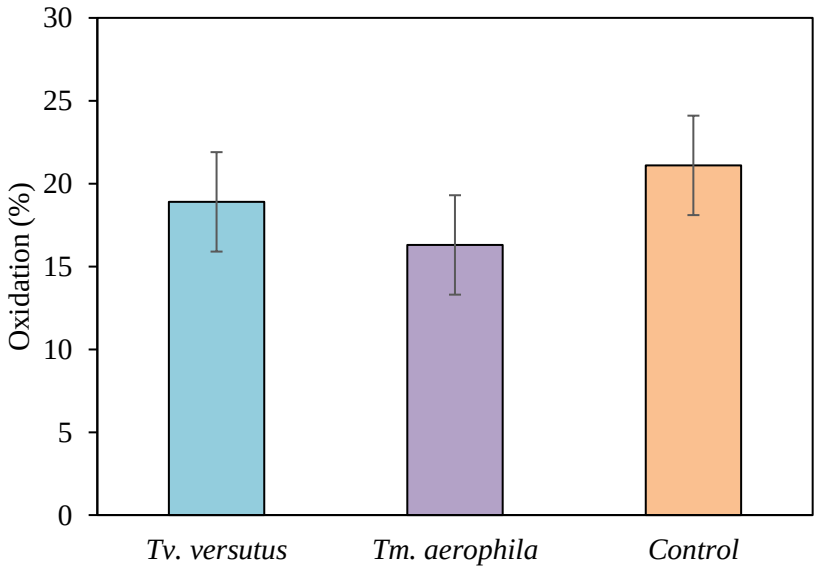

Figure 4.14: Bottle roll tests with COREM at 5% pulp density, 500 mL solution, ambient temperature, and 40 rpm for 2 weeks.

4.6 Investigations on the Carbonate Effect

The results previously mentioned demonstrate the reduced oxidation of pyrite in carbonate solutions in the presence of alkaliphilic sulfur oxidizing bacteria. It is proposed in this study that the bacteria attach to the surface of pyrite preventing the "carbonate effect" to occur to its full extent. "Contact leaching" refers to the attachment of sulfur-oxidizing microorganisms onto the pyrite surface due to their extracellular polymeric substances (Dong et al., 2020; Gehrke et al., 1998; Mahmoud et al., 2017; Sand et al., 2001; Sand and Gehrke, 2006; Vera et al., 2013b). This layer of bacteria would hinder the oxidation of pyrite reducing the exposure of the surface to chemical oxidizing constituents and by blocking oxidant diffusion. The passivation of precipitates (iron oxides) resulting in low oxidation yield from pyrite in carbonate solutions has been previously reported (Caldeira et al., 2003; Descostes et al., 2002; Evangelou and Zhang, 1995).

Chandra and Gerson (2010) confirmed that goethite (FeOOH) and hematite (Fe_2O_3) passivates on pyrite surfaces under neutral and alkaline conditions. However, at both high pH (pH 8 – 11) and carbonate concentrations (0.1-1 mol/L $NaHCO_3$), there is a continuous removal of the passivation layer due to the presence of soluble ferrous iron carbonate complexes ($Fe(CO_3)_2^{2-}$ and $Fe(CO_3)(OH)^-$) (Caldeira et al., 2010; Descostes et al., 2002; Evangelou and Zhang, 1995; Wu et al., 2021). These are the main species in Fe(II) oxidation in carbonate/bicarbonate solutions, which prevent the coating of complexes (Caldeira et al., 2010; Descostes et al., 2002). This was the environment the ore was exposed to as the initial pH and carbonate/bicarbonate concentration of the solution was approximately 10.0 and 0.3 M, respectively. Therefore, it is suggested that the continuous removal of the passivation layer from the carbonate effect may also prevent the coating of bacteria on the pyrite surface, preventing biooxidation from occurring.

4.7 Chemical Oxidation with COREM

COREM ore with a total sulfur content of 5.7% and gold concentration of 1.7 ppm was used to investigate the carbonate effect and gold recovery after oxidation. The experiments were performed

on heat plates in 500 mL flasks with 225 mL of solution agitated at 500 rpm. Air was supplied at 0.1 L/min to provide oxygen to the system and since no bacteria were present, various temperatures (25 – 80 °C) and pulp densities (10 – 30 %) were studied.

Initial studies on the carbonate effect were conducted by eliminating constituents in the DSMZ 925 media to determine if their presence affected oxidation. All reagents (excluding sodium carbonate/bicarbonate) had minimal effects on pyrite oxidation except for thiosulfate, which reduced oxidation. Thiosulfate was more readily oxidized than sulfide because it was soluble in water and has an easier oxidation pathway as it is an intermediate product before forming sulfate as depicted in Equation 13 and 14. Therefore, the media was simplified to only sodium carbonate and bicarbonate in concentrations of 20 and 10 g/L, respectively.

4.7.1 Effect of Temperature

Experiments to investigate the effect of temperature were performed at 20% pulp density and at 25, 35, 50, 65 and 80 °C for 7 days. As shown in Figure 4.15, temperature is a significant parameter in pyrite oxidation and a clear correlation is exhibited. Considerable oxidation was achieved in the first 24 h at all temperatures followed by minor oxidation for the remainder of the test. The most oxidation occurred at 80 °C in which 89% of COREM was oxidized in 7 days. Temperatures at 25, 35, 50, and 65 °C oxidized 42, 47, 55 and 74%, respectively. Experiments at 90 °C were attempted, however the high loss of solution made it difficult to maintain a proper volume. The relationship between temperature and pyrite oxidation in carbonate solutions was in agreement with other studies (Ciminelli and Osseo-Asare, 1995; Li et al., 2006). Due to the buffering effect of the carbonates, the pH did not vary much for temperatures below 50 °C as shown in Figure 4.15B. However, there was a slight decrease in pH at 65 °C at the end of the test and a significant decrease at 80 °C at 120 h. Additional media was added to the experiments at 80 °C to raise the pH as more oxidation occurred as pH the was increased (Caldeira et al., 2010; Ciminelli and Osseo-Asare, 1995; Li et al., 2006; Wu et al., 2021). No significant changes were seen in the ORP and DO plots

in Figure 4.15C and D, respectively. The ORP was positive indicating oxidation occurred and the DO generally decreased which correlated with the oxygen uptake required for oxidation.

Further, the samples could be analyzed qualitatively by their colour both during and after oxidation. The iron precipitates formed during oxidation changed the solution to a reddish orange colour which became darker as higher oxidation was achieved. Figure 4.16 demonstrates the change in colour for a test at 80 °C as A was after 1 day (original colour of ore in solution), B after 2 days, and C after 7 days. Figure 4.17 shows the incremental colour differences in the final dry samples as the temperatures in the tests were increased. The precipitates were washed with HCl which removed the reddish orange colour, returning the sample to its grey colour.

The particle size of the ore oxidized at various temperatures was investigated using LPSA analysis. The results shown in

Table 4.1 presents a relationship as particle size decreased as higher oxidation was attained. This can be explained by the removal of sulfide matrices during oxidation. The starting particle size of COREM was 55 µm which was reduced to 44, 39, 39, 37 and 34 µm for the experiments at 25, 35, 50, 65 and 80 °C, respectively. Although the difference in oxidation between 35 and 80 °C was approximately 47%, the particle size only decreased by 5 µm.

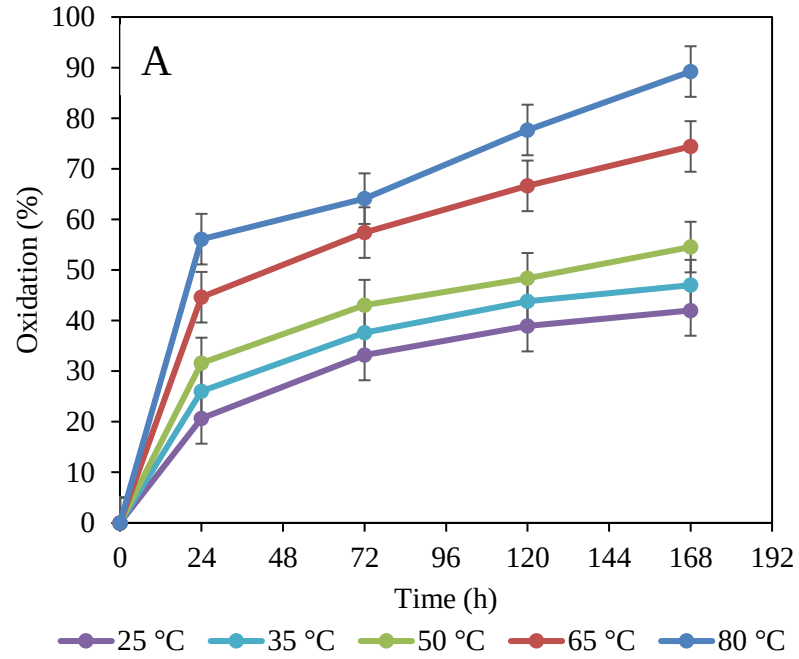
A
Oxidation (%)
100
90
80
70
60
50
40
30
20
10
0
0
24
48
72
96
120
144
168
192
Time (h)
25 °C
35 °C
50 °C
65 °C
80 °C

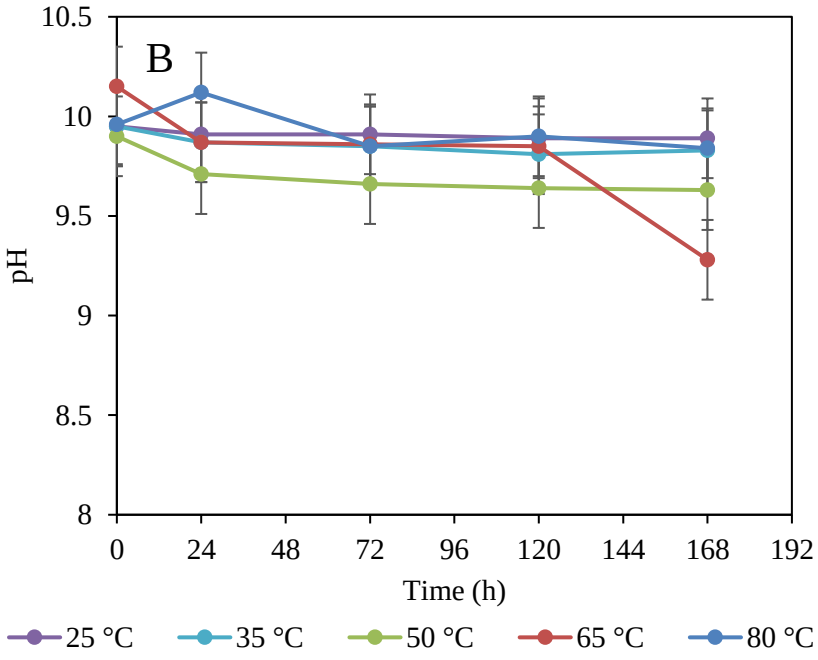
B
pH
10.5
10
9.5
9
8.5
8
0
24
48
72
96
120
144
168
192
Time (h)
25 °C
35 °C
50 °C
65 °C
80 °C

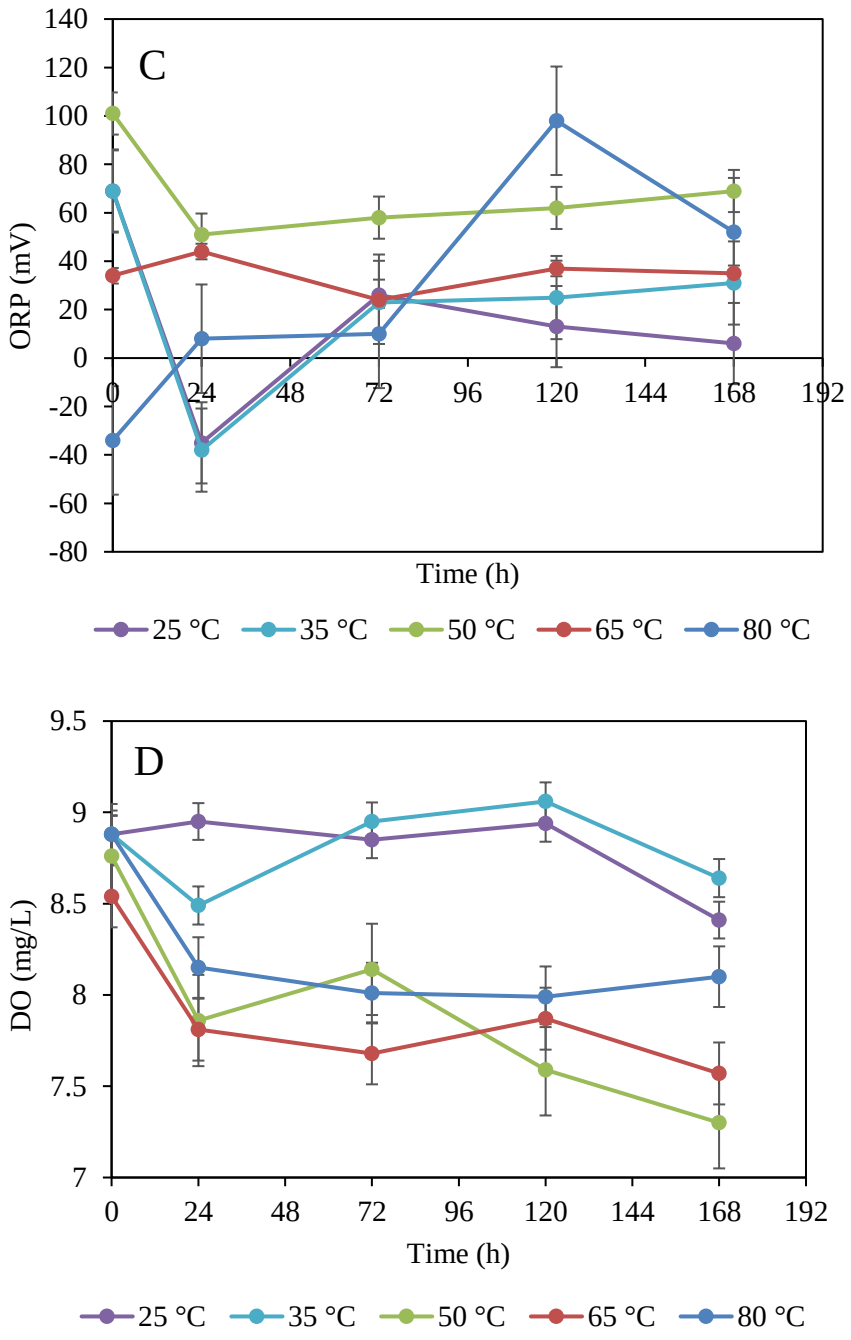

Figure 4.15: Effect of temperature and changes in pH (B), ORP (C), and DO (D) of COREM at 20% pulp density, air supplied at 0.1 L/min and 500 rpm for 7 days.

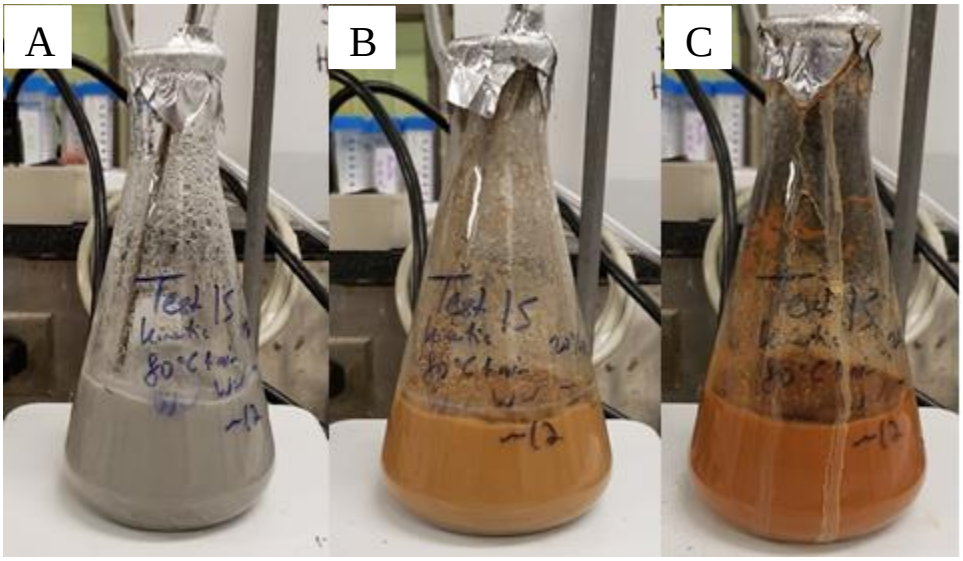

Figure 4.16: The change in colour of COREM in solution indicating oxidation. Pictured above is oxidation of a test at 80 °C, air supplied at 0.1 L/min and 500 rpm at 0 h (A), after 1 day (B) and after 7 days (C).

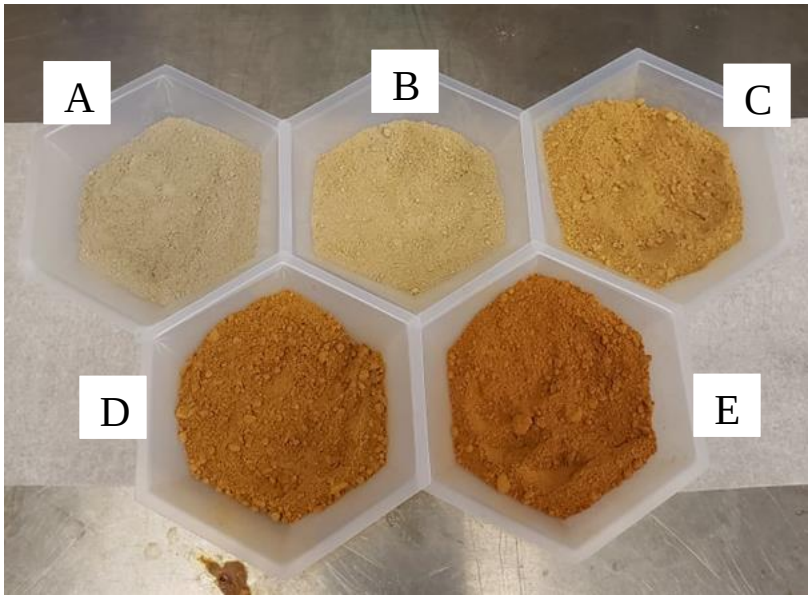

Figure 4.17: Colour change of the dry oxidized COREM samples of tests performed for 7 days, air supplied at 0.1 L/min and 500 rpm at varying temperatures. The experiments were conducted at 25 (A), 35 (B), 50 (C), 65 (D) and 80 °C (E).

Table 4.1: LPSA analysis of COREM oxidized at various temperatures

Test Temperature (°C)	Particle Size (µm)
Control	55
25	44
35	39
50	39
65	37
80	34

4.7.2 Complete Chemical Oxidation

The maximum oxidation of COREM was achieved in 11 days at 80 °C, air was supplied at 0.1 L/min and the solution was stirred at 500 rpm. As shown in Figure 4.18, the high oxidation was achieved in 24 h followed by slowing incremental increases. At 24, 72, 120, 168, 216, and 264 h, approximately 56, 64, 78, 89, 94 and 97 of the ore was oxidized, respectively. The difference in oxidation was only 5% and 3% for the last 3 kinetic samples.

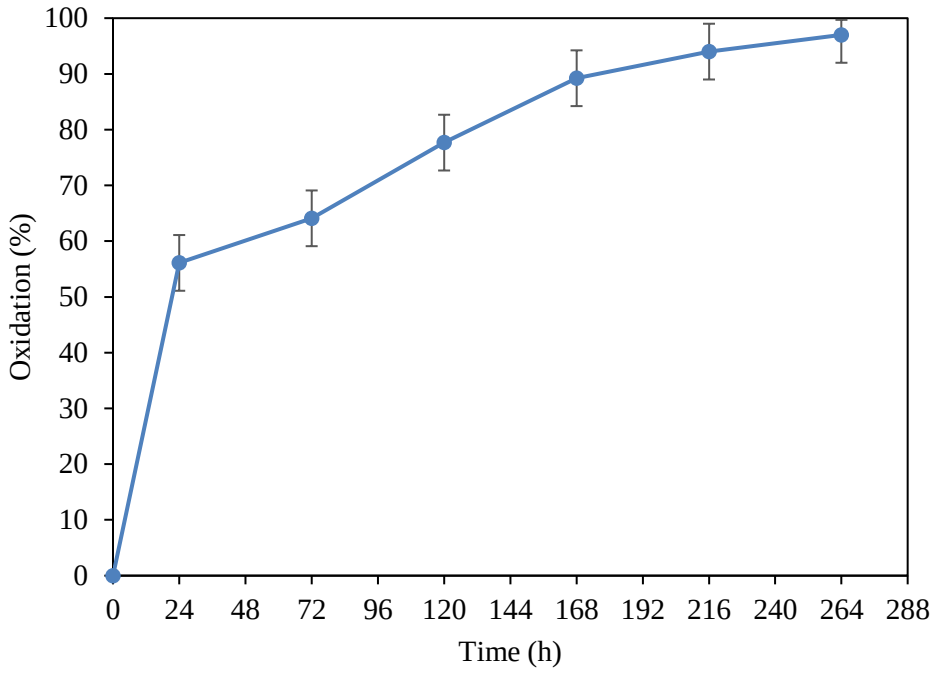

Figure 4.18: Complete oxidation test with COREM performed at 80 °C, 0.1 L/min air and 500 rpm for 11 days

4.7.3 Effect of Pulp Density

The pulp density was varied from 10 – 30% and the experiments were performed at 80 °C, air was supplied at 0.l L/min and the solution was stirred at 500 rpm for 3 days. Figure 4.19 exhibits the results at 10, 15, 20, 25, and 30% pulp density which oxidized approximately 78, 66, 58, 49 and 38% of COREM, respectively. The lowest pulp density, 10%, had the highest oxidation which was expected as increasing pulp density decreases iron solubility which negatively impacts the carbonate effect (Acevedo et al., 2004; Caldeira et al., 2010; Pathak et al., 2014). The oxidation pattern was similar to previous tests where initial oxidation was significant but diminished after 24 h. The experiments at 25 and 30% pulp density only had a 2% increase in oxidation from 48 to 72 h.

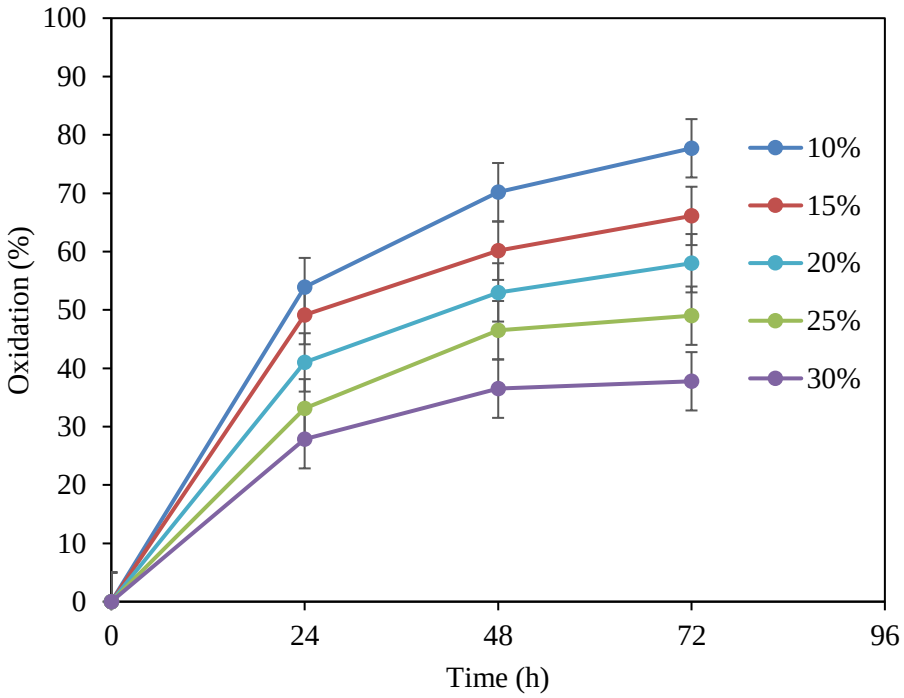

Figure 4.19: Pulp density tests with COREM at 80 °C, 0.1 L/min air and 500 rpm for 3 days

4.7.4 Investigations with other Media

To achieve higher oxidation, the media was altered in three ways. The experiments were conducted for 3 days, at ambient temperature, 500 rpm and 10% pulp density. The media was changed by doubling the concentration of carbonates/bicarbonates ("Media x2"), removing the bicarbonate ("Carbonate"), and removing the bicarbonate ("Carbonate x2") but doubling the carbonate concentration. These were compared against the "control" tests ("Media") which was the simplified media used for the previous chemical oxidation experiments. As shown in Figure 4.20, the regular media resulted in 23% oxidation which was enhanced to 31% by doubling the reagent concentration. The "Carbonate" and "Carbonate x2" experiments had 25 and 27% oxidation, respectively. These preliminary results indicated higher concentrations of carbonate/bicarbonate in solution increased oxidation, therefore this media was studied at 80 °C, 20% pulp density, 500 rpm, and air supplied at 0.1 L/min for 7 days (Figure 4.21). Experiments with no bicarbonates in the

media were not conducted with these parameters as the buffer could not be maintained from the acid produced during oxidation.

The results from Figure 4.21 revealed higher oxidation was achieved for the control media over the entire experiment. There was no indication as to why more oxidation was achieved as approximately 8% more oxidation occurred as shown in Figure 4.20. The reduced oxidation may be due to the higher temperature or excess formation of sodium chloride. Reimers and Franke (1991) studied the effects of additives on pyrite oxidation and reported that sodium bicarbonate reduced oxidation at higher temperatures and sodium chloride reduced oxidation by 20%.

Experiments with calcium hydroxide were performed, however, it could not chemically oxidize the ore as well as the carbonate/bicarbonate media. This can be explained by the passivation from the formation of calcite and dolomite reducing oxidation (Bidari and Aghazadeh, 2018b).

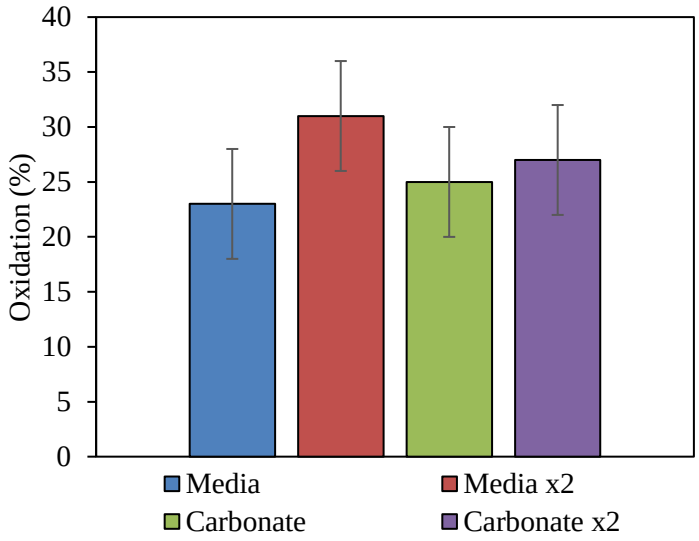

Figure 4.20: Oxidation with other media with COREM at ambient temperature for 3 days, 10% pulp density and 500 rpm.

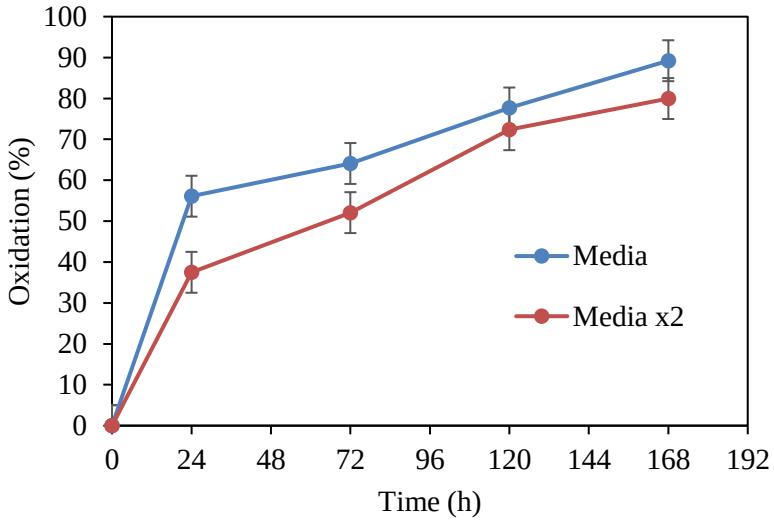

Figure 4.21: Oxidation of COREM comparing the original and altered media at 80 °C, 20% pulp density, air supplied at 0.1 L/min and 500 rpm for 7 days.

4.8 XRD and SEM Studies

The identification of materials in COREM were identified using XRD analysis before oxidation, after oxidation, and after acid washing of the completely oxidized ore as seen in Figure 4.22. The majority of initial minerals were quartz, pyrite and illite. After oxidation, the minerals were mostly composed of quartz and illite. The absence of pyrite in the analysis suggested all of the sulfide mineral was oxidized. After the ore was acid washed, only quartz, illite, and kaolinite were detected which suggested magnetite was removed during HCl leaching.

Figure 4.23 presents the surface morphology of COREM before oxidation, after oxidation, and after acid wash using SEM imaging. The unoxidized ore in Figure 4.23A had a relatively smooth surface with minimal indication of passivating elements. However, pyrite minerals were passivated with precipitates in the oxidized ore as seen in Figure 4.23B. Acid washing of the ore removed these precipitates and left the minerals with significant inclusion pits (Figure 4.23C).

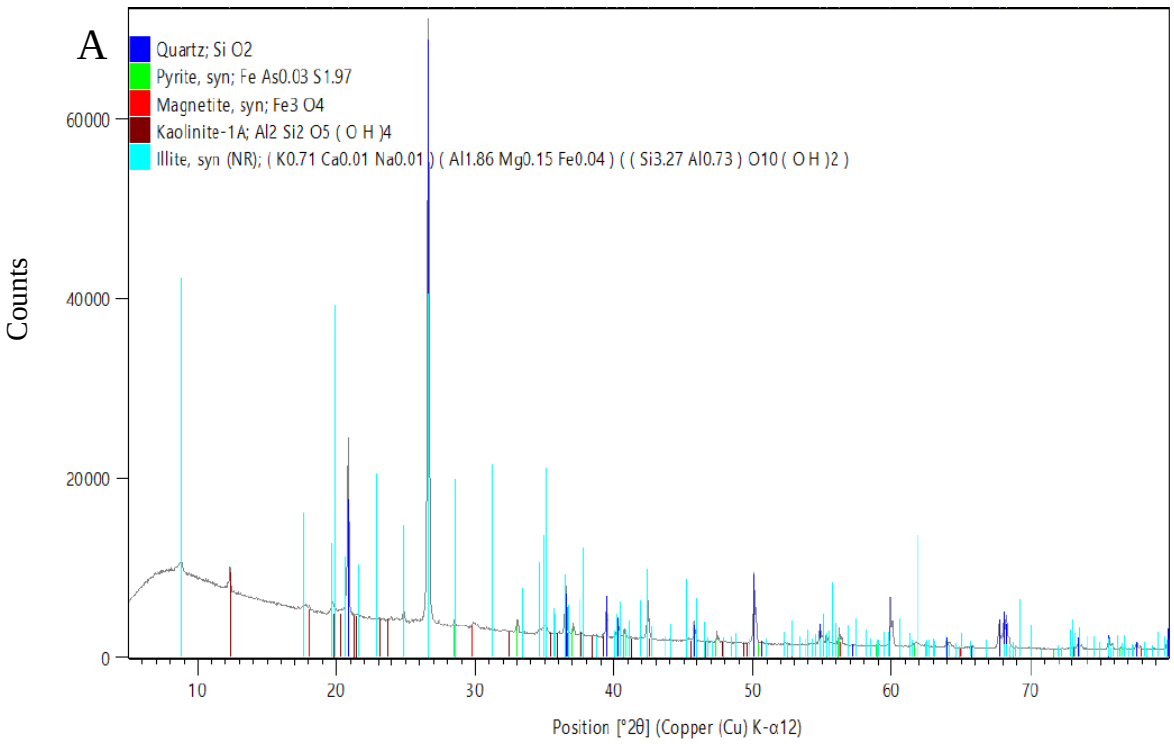
A
Quartz; Si O2
Pyrite, syn; Fe As0.03 S1.97
Magnetite, syn; Fe3 O4
Kaolinite-1A; Al2 Si2 O5 (O H)4
Illite, syn (NR); (K0.71 Ca0.01 Na0.01) (Al1.86 Mg0.15 Fe0.04) ((Si3.27 Al0.73) O10 (O H)2)
Counts
60000
40000
20000
0
10
20
30
40
50
60
70
Position [°2θ] (Copper (Cu) K-α12)

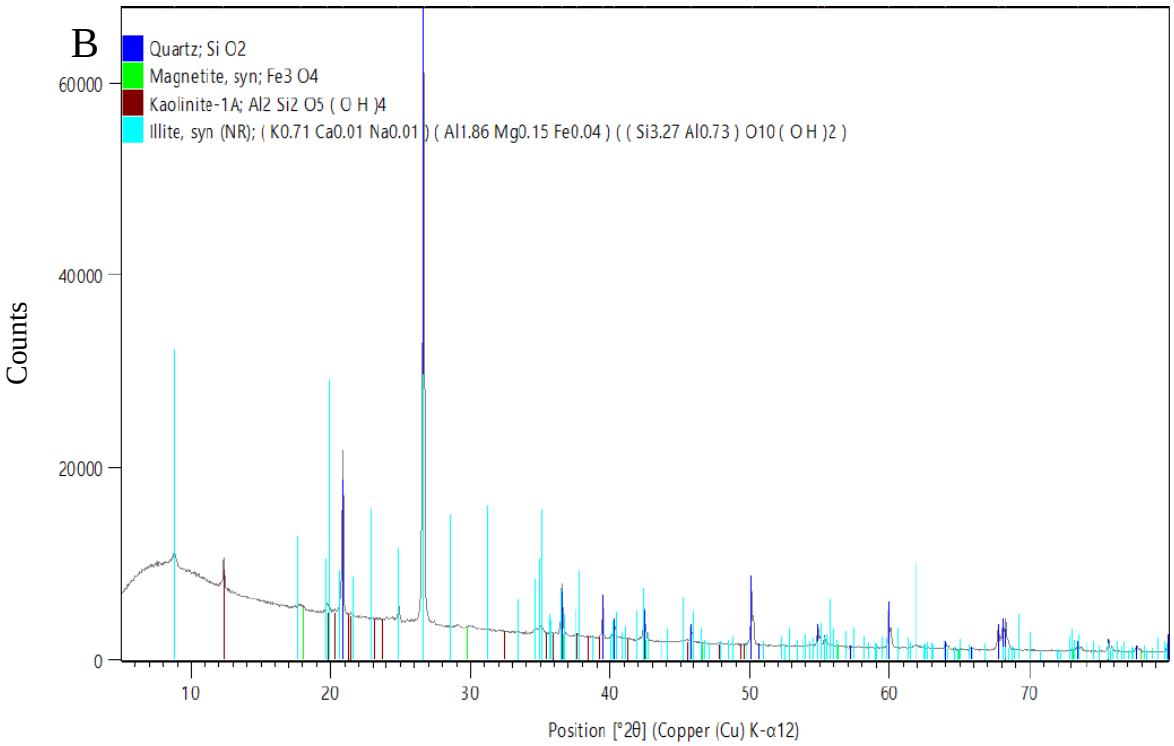
B
Quartz; Si O2
Magnetite, syn; Fe3 O4
Kaolinite-1A; Al2 Si2 O5 (O H)4
Illite, syn (NR); (K0.71 Ca0.01 Na0.01) (Al1.86 Mg0.15 Fe0.04) ((Si3.27 Al0.73) O10 (O H)2)
Counts
60000
40000
20000
0
10
20
30
40
50
60
70
Position [°2θ] (Copper (Cu) K-α12)

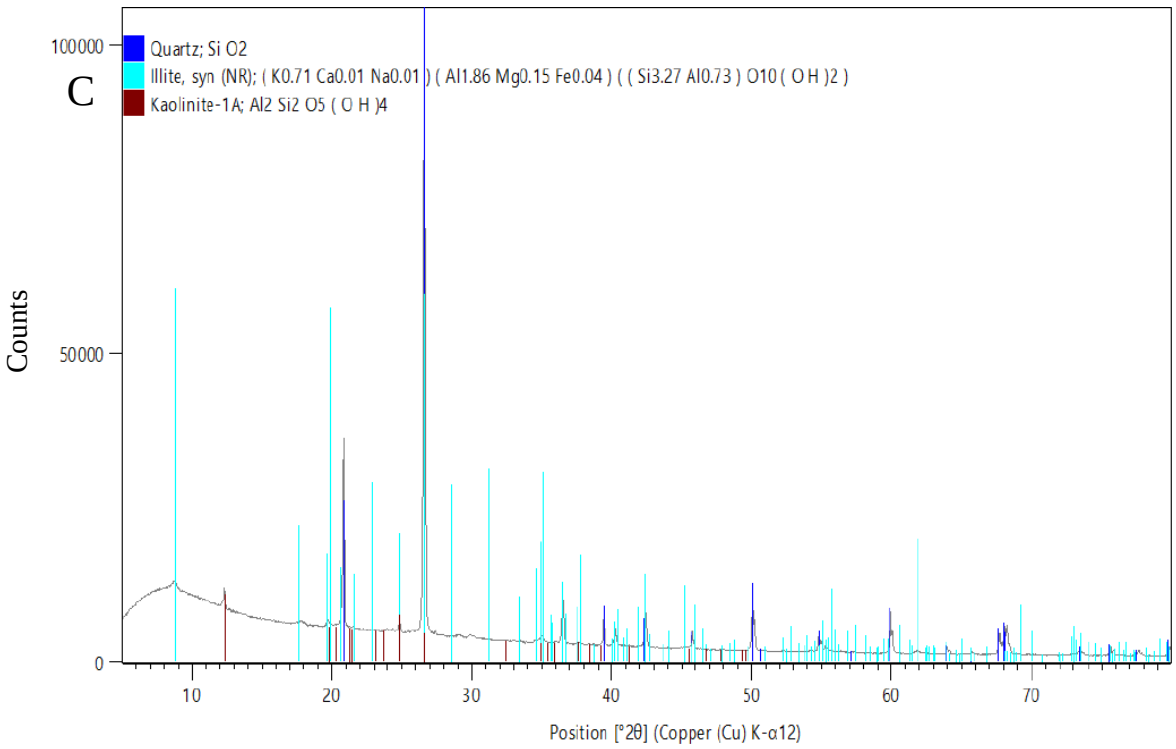

Figure 4.22: XRD analysis of COREM for the original ore (A), completely oxidized ore (B), and residue after HCl leaching (C).

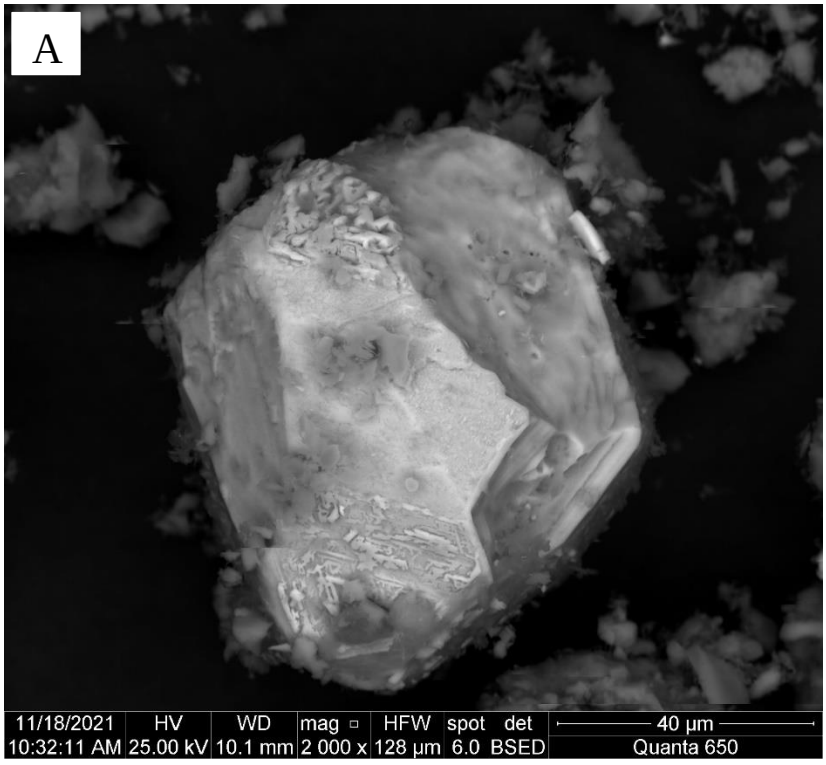
A
11/18/2021 HV WD mag HFW spot det 40 µm
10:32:11 AM 25.00 kV 10.1 mm 2 000 x 128 µm 6.0 BSED Quanta 650

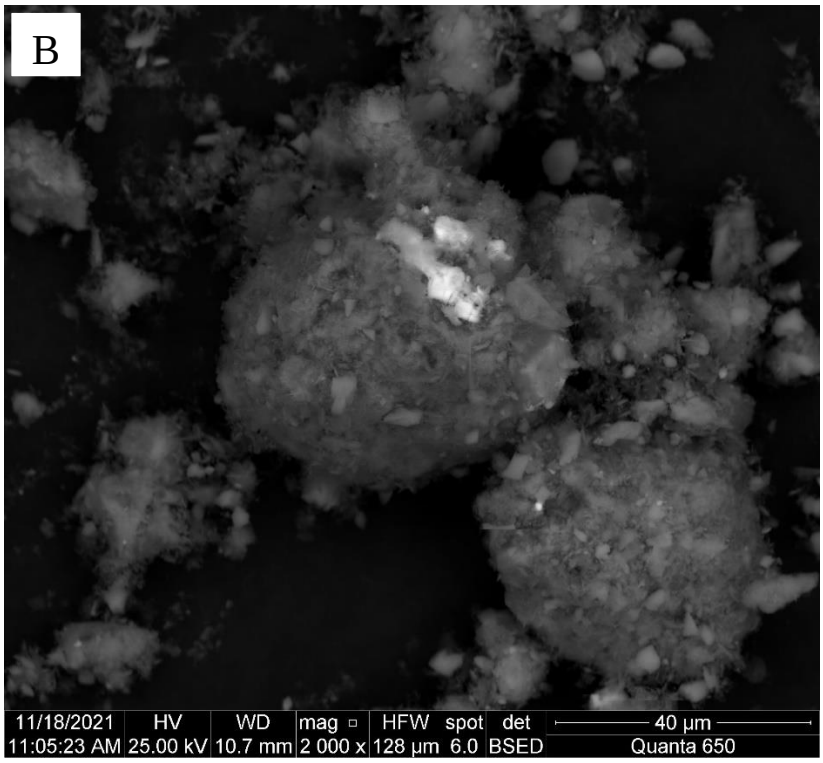
B
11/18/2021 HV WD mag HFW spot det 40 µm
11:05:23 AM 25.00 kV 10.7 mm 2 000 x 128 µm 6.0 BSED Quanta 650

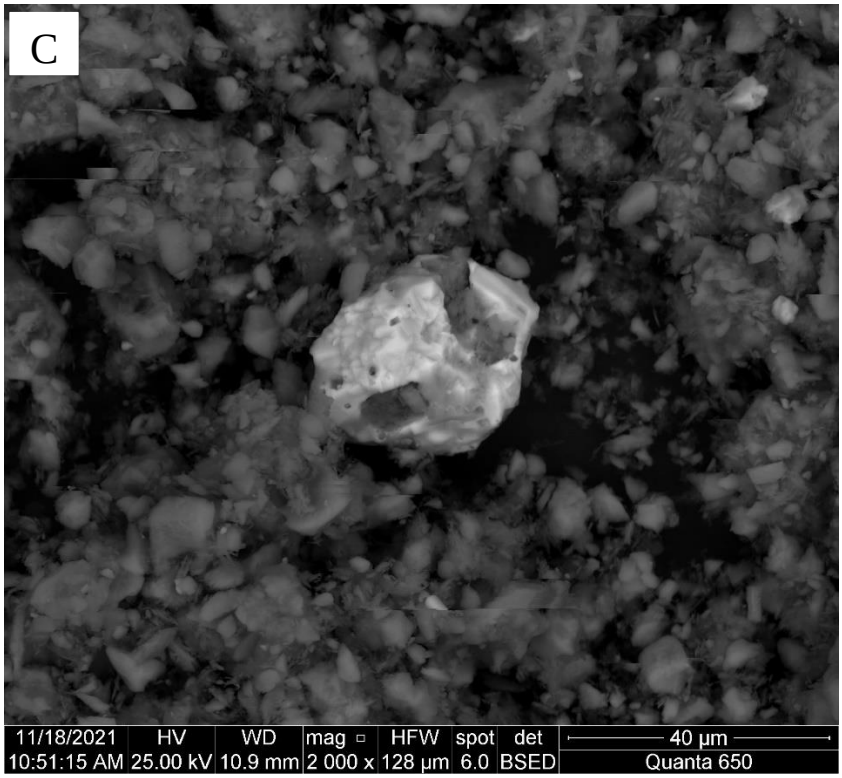

Figure 4.23: Surface morphology of COREM before oxidation (A), after oxidation (B), and after acid washing (C) of the completely oxidized ore.

4.9 Gold Recovery

The recovery of refractory gold from COREM was investigated by applying conventional cyanidation techniques to the oxidized ore. The results as displayed in Figure 4.24 which also includes a "control" experiment which was unoxidized ore. The control and samples oxidized at 25, 35, 50, 65, and 80 °C had gold recoveries of approximately 8, 21, 34, 66, 81 and 89%, respectively. High gold recovery was achieved without the use of NaOH, excessive oxygen supply or in a pressurized system (Bidari and Aghazadeh, 2018a; Li et al., 2006; Melashvili et al., 2016). Therefore, there was a positive correlation between chemical oxidation from the carbonate effect and gold recovery.

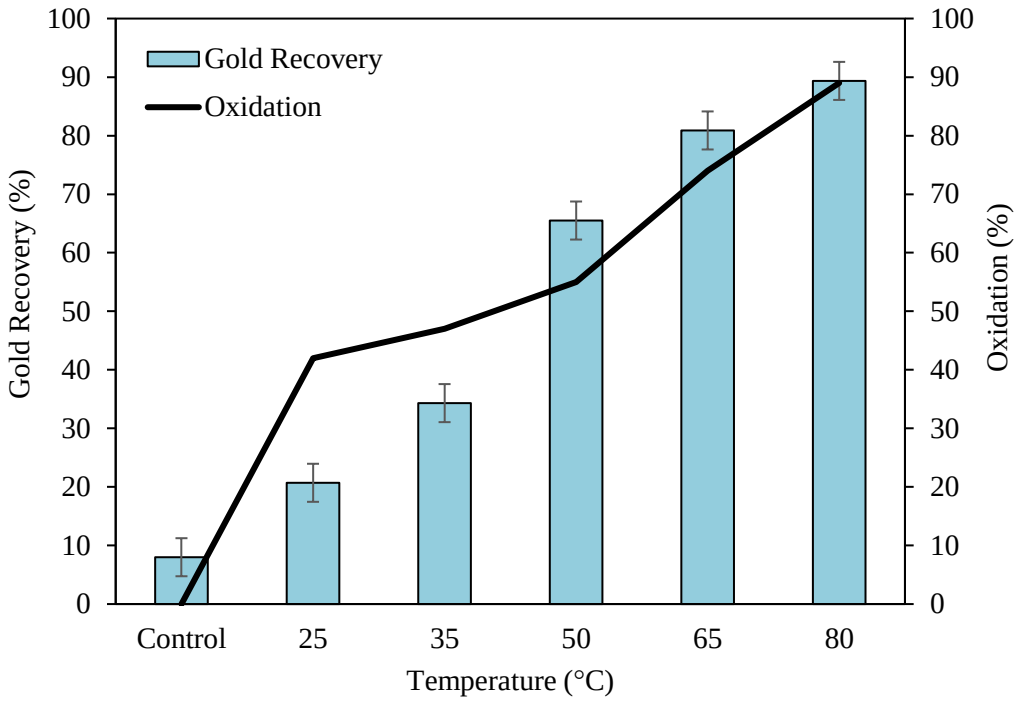

Figure 4.24: Gold recovery by cyanidation of COREM chemically oxidized at varying temperatures, 20% pulp density, air supplied at 0.1 L/min and 500 rpm for 7 days.

Chapter 5

Conclusion and Recommendations

Tm. aerophila and *Tv. versutus* are halo-tolerant and chemolithoautotroph bacteria previously used in desulfurization processes. They had optimal growth at pH 9.5 using DSMZ 925 media. Maximum growth was observed at 24 and 48 h for *Tv. versutus* and *Tm. aerophila*, respectively. Growth in media replacing carbonate/bicarbonate with phosphate, ammonium, and glycine-sodium hydroxide were attempted, however were unsuccessful. For future investigations, sodium salts are recommended as the bacteria require a certain concentration of sodium ions for growth.

Na_2S oxidation tests were effectively performed with both bacteria as approximately 96% was oxidized in 7 days starting with an initial sulfur concentration of 1000 mg/L. The control test (no bacteria) only oxidized 38% of the sulfur indicating the bacteria were responsible for 58% of the oxidation. To further understand the oxidative abilities of the bacteria in aqueous solutions, the concentration of sulfur can be increased or experiments to investigate the optimal residence time can be performed.

Oxidation tests with GSL (23.4% total sulfur content) were performed with *Tv. versutus* and *Tm. aerophila* oxidizing 34 and 23%, respectively. Comparatively, more oxidation occurred in the control test at 37% which was dissimilar to the patterns in the Na_2S experiments. The control test had a larger drop in pH and a more positive ORP which suggested more oxidation occurred. This may have been due to the toxic environment due to the high sulfur content in the sample or non-optimal parameters. Experiments were conducted to assess the effect of temperature and reduced thiosulfate concentration in the media, however the control test outperformed the tests with bacteria. No previous oxidation studies were performed with these bacteria on ore samples, therefore procedures such as adapting the bacteria to solids or altering the concentration of reagents in the media may increase oxidation.

Experiments with EQ2 (11.0% total sulfur content) were conducted as it had half the total sulfur content of GSL which reduced the extent of sulfur toxicity. Although the sulfur content was approximately half of GSL, the results were similar as the control, *Tv. versutus*, and *Tm. aerophila* oxidized 54, 44 and 42%, respectively. Further, the patterns in the pH, ORP and DO were similar to GSL. This suggests that the chemical reagents were outperforming the bacteria. Therefore, to reduce the toxic element and to increase the volume of the reactors, bottle roll tests were performed with COREM (5.7% total sulfur content). These experiments resulted in the same conclusion with the control test oxidizing more than the bacteria inoculated tests. The control, *Tv. versutus*, and *Tm. aerophila* oxidized the ore for 21, 16 and 19%, respectively. The only difference noted in these tests was that *Tm. aerophila* has better oxidation values than *Tv. versutus* which have not been observed previously. This may be due to their physiological nature as the bottle roll did not have an opening for air to freely pass through. The oxidation in the bacterial tests may be improved if the bacteria were put into their optimal temperature for growth at 30 °C, instead of the ambient temperature it was conducted at. Other strains of *Tv. versutus* and *Tm. aerophila* or species of *Thioalkalivibrio* and *Thiomicrospira* should be investigated as they have great oxidative capabilities. Further, alkaline microorganisms with the ability to utilize sulfur for growth may perform better than the *Tv. versutus* and *Tm. aerophila* used for this investigation.

The carbonate effect was evident as experimentation with three different pyrite concentrates all resulted in the same conclusion. Therefore, it was suggested that the carbonate effect hindered the oxidation of pyrite by preventing the bacteria from attaching to the surface of the particles. The formation of iron precipitates such as goethite and hematite are known to passivate on the surface during chemical oxidation.

Chemical oxidation tests were conducted with only carbonates and bicarbonates in solution as the other reagents were not necessary for the carbonate effect. Air was supplied at 0.1 L/min to provide oxygen to the experiments. The objective was to determine if more oxidation correlated with higher

gold recoveries. Initially, the effect of temperature was investigated by performing tests for 7 days at 25, 35, 50, 65, and 80 °C which resulted in 42, 47, 55, 74 and 89% oxidation, respectively. It was determined that 80 °C was the optimal temperature for chemical oxidation as higher temperatures were difficult to maintain due to the evaporation of water. Qualitative analysis was performed as the iron precipitates formed during oxidation turned the ore into a reddish orange colour which got darker as more oxidation occurred. The particle size of the ore was measured by LPSA analysis after oxidation. COREM ore had an initial particle size of 55 µm which was reduced to 44, 39, 39, 37, and 34 µm for experiments at 25, 35, 50, 65 and 80 °C, respectively. It was concluded that more oxidation led to smaller particle sizes as the sulfide matrices were degraded. Investigations on the complete oxidation of COREM were performed at 80 °C. After 11 days, 97% of the ore was oxidized.

The effect of pulp density was explored in case the experiments were scaled up. Tests with pulp densities of 10, 15, 20, 25, and 30% oxidized approximately 78, 66, 58, 49 and 38%, respectively. The pattern of decreasing oxidation with higher pulp densities has been previously noted in other studies.

Oxidation studies in altered media with various concentrations of carbonates and bicarbonates were performed. Doubling the concentration of carbonate/bicarbonate initially had more oxidation than at the original concentration at a smaller scale and at ambient temperature, therefore full-size tests were performed at 80 °C. However, the results exhibited lower oxidation for the double concentrated media although it achieved approximately 8% more oxidation at ambient temperature. This may be due to the high concentration of sodium bicarbonate which can reduce oxidation at higher temperatures. Chemical oxidation should be performed with other reagents (i.e. NaOH) for comparison and should be scaled-up to simulate a heap leach scenario.

The completely chemically oxidized COREM was analyzed quantitatively with XRD which indicated all pyrite was removed after oxidation. Further, qualitative analysis by SEM imaging

showed that the pyrite minerals passivated with precipitates after oxidation (due to the carbonate effect) and removal of sulfide matrices (inclusion pits on the ore surface) after acid wash.

Increased gold recovery was observed in all chemically oxidized samples compared to the unoxidized ore. Maximum gold recovery was recorded at 89% compared to the control test which had a gold recovery of only 8%.

References

AAT Bioquest Inc., 2020. Glycine-Sodium Hydroxide Buffer (0.08 M, pH 10) Preparation and Recipe [WWW Document]. URL https://www.aatbio.com/resources/buffer-preparations-and-recipes/glycine-sodium-hydroxide-buffer-ph-10 (accessed 9.29.20).

Acevedo, F., Gentina, J.C., Valencia, P., 2004. Optimization of pulp density and particle size in the biooxidation of a pyritic gold concentrate by Sulfolobus metallicus, in: World Journal of Microbiology and Biotechnology. pp. 865–869. https://doi.org/10.1007/s11274-004-1006-1

Adams, M.D., Swaney, S.J., Friedl, J., Wagner, F.E., 1996. Preg-robbing minerals in gold ores and residues, in: Johannesburg: South African Institute of Mining and Metallurgy. pp. 163–172.

Ahmaruzzaman, M., Gupta, V.K., 2011. Rice husk and its ash as low-cost adsorbents in water and wastewater treatment. Ind. Eng. Chem. Res. 50, 13589–13613. https://doi.org/10.1021/ie201477c

Ahn, A.-C., Cavalca, L., Colombo, M., Schuurmans, J.M., Sorokin, D.Y., Muyzer, G., 2019. Transcriptomic Analysis of Two Thioalkalivibrio Species Under Arsenite Stress Revealed a Potential Candidate Gene for an Alternative Arsenite Oxidation Pathway. Front. Microbiol. 10, 1–14. https://doi.org/10.3389/fmicb.2019.01514

Amankwah, R.K., Yen, W.T., Ramsay, J.A., 2005. A two-stage bacterial pretreatment process for double refractory gold ores. Miner. Eng. 18, 103–108. https://doi.org/10.1016/j.mineng.2004.05.009

Amils, R., 2011. Chemolithoautotroph, in: Encyclopedia of Astrobiology. Springer Berlin Heidelberg, pp. 289–289. https://doi.org/10.1007/978-3-642-11274-4_272

Ang, W.K., Mahbob, M., Dhouib, R., Kappler, U., 2017. Sulfur compound oxidation and carbon co-assimilation in the haloalkaliphilic sulfur oxidizers Thioalkalivibrio versutus and Thioalkalimicrobium aerophilum. Res. Microbiol. 168, 255–265. https://doi.org/10.1016/j.resmic.2016.12.004

Antón, J., 2011. Halophile, in: Encyclopedia of Astrobiology. Springer Berlin Heidelberg, pp. 725–727. https://doi.org/10.1007/978-3-642-11274-4_694

Asano, R., Hirooka, K., Nakai, Y., 2012. Middle-thermophilic sulfur-oxidizing bacteria Thiomonas sp. RAN5 strain for hydrogen sulfide removal. J. Air Waste Manag. Assoc. 62, 38–43. https://doi.org/10.1080/10473289.2011.617601

Astudillo, C., Acevedo, F., 2008. Adaptation of Sulfolobus metallicus to high pulp densities in the biooxidation of a flotation gold concentrate. Hydrometallurgy 92, 11–15. https://doi.org/10.1016/j.hydromet.2008.02.003

Bacelar-Nicolau, P., Johnson, D.B., 1999a. Leaching of pyrite by acidophilic heterotrophic iron-oxidizing bacteria in pure and mixed cultures. Appl. Environ. Microbiol. 65, 585–590. https://doi.org/10.1128/aem.65.2.585-590.1999

Bacelar-Nicolau, P., Johnson, D.B., 1999b. Leaching of Pyrite by Acidophilic Heterotrophic Iron-Oxidizing Bacteria in Pure and Mixed Cultures Downloaded from, APPLIED AND ENVIRONMENTAL MICROBIOLOGY.

Banciu, H., Sorokin, D.Y., Galinski, E.A., Muyzer, G., Kleerebezem, R., Kuenen, J.G., 2004. Thialkalivibrio halophilus sp. nov., a novel obligately chemolithoautotrophic, facultatively alkaliphilic, and extremely salt-tolerant, sulfur-oxidizing bacterium from a hypersaline alkaline lake. Extremophiles 8, 325–334. https://doi.org/10.1007/s00792-004-0391-6

Banciu, H.L., Sorokin, D.Y., Tourova, T.P., Galinski, E.A., Muntyan, M.S., Kuenen, J.G., Muyzer, G., 2008. Influence of salts and pH on growth and activity of a novel facultatively alkaliphilic, extremely salt-tolerant, obligately chemolithoautotrophic sufur-oxidizing Gammaproteobacterium Thioalkalibacter halophilus gen. nov., sp. nov. from South-Western Siber. Extremophiles 12, 391–404. https://doi.org/10.1007/s00792-008-0142-1

Belyi, A., Kondrat'eva, T.F., Bulaev, A., Solopova, N.V., Grigor'eva, N.V., Murav'yov, M.I., Panyushkina, A.E., Tsaplina, I.A., 2015a. Neutrophilic Microbial Community with High Rate of Elemental Sulfur Oxidation. Adv. Mater. Res. 1130, 59–62. https://doi.org/10.4028/www.scientific.net/amr.1130.59

Belyi, A., Solopova, N., Sekachev, V., Teleutov, A., Malashonok, A., Krasilnikov, G., 2015b. Biooxidation of a Gold-Arsenic Sulphide Concentrate by a Two-Stage Oxidation Using Consecutively Acidophilic and Neutrophilic Bacteria. Adv. Mater. Res. 1130, 329–332. https://doi.org/10.4028/www.scientific.net/amr.1130.329

Benson, D., 2019. Calvin-Benson-Bassham Cycle [WWW Document]. LibreTexts. URL https://chem.libretexts.org/Bookshelves/Biological_Chemistry/Supplemental_Modules_(Biological_Chemistry)/Metabolism/Catabolism/Calvin-Benson-Bassham_Cycle (accessed 5.16.20).

Berezowsky, M.G.S., Weir, D.R., 2013. Factors affecting the selection of pressure oxidation for the pretreatment of refractory gold ores, in: ALTA 2013. pp. 72–84.

Bidari, E., Aghazadeh, V., 2018a. Alkaline leaching pretreatment and cyanidation of arsenical gold ore from the Carlin-type Zarshuran deposit. Can. Metall. Q. 57, 283–293. https://doi.org/10.1080/00084433.2018.1444931

Bidari, E., Aghazadeh, V., 2018b. Pyrite oxidation in the presence of calcite and dolomite: Alkaline leaching, chemical modeling and surface characterization. Trans. Nonferrous Met. Soc. China (English Ed. 28, 1433–1443. https://doi.org/10.1016/S1003-6326(18)64782-X

Biselli, E., Schink, S.J., Gerland, U., 2020. Slower growth of Escherichia coli leads to longer survival in carbon starvation due to a decrease in the maintenance rate . Mol. Syst. Biol. 16. https://doi.org/10.15252/msb.20209478

Blais, J.F., Auclair, J.C., Tyagi, R.D., 1992. Cooperation between two Thiobacillus strains for heavy-metal removal from municipal sludge. Microbiology 38, 181–187.

Boden, R., 2017. Reclassification of Halothiobacillus hydrothermalis and Halothiobacillus halophilus to Guyparkeria gen. Nov. in the Thioalkalibacteraceae fam. nov., with emended

descriptions of the genus Halothiobacillus and family Halothiobacillaceae. Int. J. Syst. Evol. Microbiol. 67, 3919–3928. https://doi.org/10.1099/ijsem.0.002222

Boden, R., Hutt, L.P., Rae, A.W., 2017a. Reclassification of Thiobacillus aquaesulis (Wood & Kelly, 1995) as Annwoodia aquaesulis gen. nov., comb. nov., transfer of Thiobacillus (Beijerinck, 1904) from the Hydrogenophilales to the Nitrosomonadales, proposal of Hydrogenophilalia class. nov. withi. Int. J. Syst. Evol. Microbiol. 67, 1191–1205. https://doi.org/10.1099/ijsem.0.001927

Boden, R., Scott, K.M., Williams, J., Russel, S., Antonen, K., Rae, A.W., Hutt, L.P., 2017b. An evaluation of Thiomicrospira, Hydrogenovibrio and Thioalkalimicrobium: Reclassification of four species of Thiomicrospira to each Thiomicrorhabdus gen. nov. and Hydrogenovibrio, and reclassification of all four species of Thioalkalimicrobium to Thiomic. Int. J. Syst. Evol. Microbiol. 67, 1140–1151. https://doi.org/10.1099/ijsem.0.001855

Bosecker, K., 1997. Bioleaching: Metal solubilization by microorganisms, in: FEMS Microbiology Reviews. pp. 591–604. https://doi.org/10.1016/S0168-6445(97)00036-3

Bruslind, L., 2021. Microbial Growth, in: Microbiology. pp. 52–54.

Bruynesteyn, A., 1989. Mineral biotechnology. J. Biotechnol. https://doi.org/10.1016/0168-1656(89)90024-2

Bryantseva, I.A., Tourova, T.P., Kovaleva, O.L., Kostrikina, N.A., Gorlenko, V.M., 2010. Ectothiorhodospira magna sp. nov., a new large alkaliphilic purple sulfur bacterium. Microbiology 79, 780–790. https://doi.org/10.1134/S002626171006010X

Burakov, A.E., Galunin, E. V., Burakova, I. V., Kucherova, A.E., Agarwal, S., Tkachev, A.G., Gupta, V.K., 2018. Adsorption of heavy metals on conventional and nanostructured materials for wastewater treatment purposes: A review. Ecotoxicol. Environ. Saf. 148, 702–712. https://doi.org/10.1016/j.ecoenv.2017.11.034

Cai, J., Guan, · Y, Li, · F, Zhao, · Y, Feng, · C, Tang, · N, 2019. Biomass and pigments production of a newly isolated photosynthetic bacterium Ectothiorhodospira shaposhnikovii P2 from saline wastewater. Int. J. Environ. Sci. Technol. 16, 7487–7496. https://doi.org/10.1007/s13762-018-2141-9

Caldeira, C.L., Ciminelli, V.S.T., Dias, A., Osseo-Asare, K., 2003. Pyrite oxidation in alkaline solutions: Nature of the product layer. Int. J. Miner. Process. 72, 373–386. https://doi.org/10.1016/S0301-7516(03)00112-1

Caldeira, C.L., Ciminelli, V.S.T., Osseo-Asare, K., 2010. The role of carbonate ions in pyrite oxidation in aqueous systems. Geochim. Cosmochim. Acta 74, 1777–1789. https://doi.org/10.1016/j.gca.2009.12.014

Cardoso, R.B., Sierra-Alvarez, R., Rowlette, P., Flores, E.R., Gómez, J., Field, J.A., 2006. Sulfide oxidation under chemolithoautotrophic denitrifying conditions. Biotechnol. Bioeng. 95, 1148–1157. https://doi.org/10.1002/bit.21084

Cervantes, C., Ji, G., Ramirez, J., Silver, S., 1994. Resistance to arsenic compounds in microorganisms. FEMS Microbiol. Rev. 15, 355–367. https://doi.org/10.1111/j.1574-6976.1994.tb00145.x

Chandra, A.P., Gerson, A.R., 2010. The mechanisms of pyrite oxidation and leaching: A fundamental perspective. Surf. Sci. Rep. 65, 293–315. https://doi.org/10.1016/j.surfrep.2010.08.003

Chen, C.Y., Tsai, T.H., Chang, C.H., Tseng, C.F., Lin, S.Y., Chung, Y.C., 2018. Airlift bioreactor system for simultaneous removal of hydrogen sulfide and ammonia from synthetic and actual waste gases. J. Environ. Sci. Heal. - Part A Toxic/Hazardous Subst. Environ. Eng. 53, 694–701. https://doi.org/10.1080/10934529.2018.1439855

Chen, X.G., Geng, A.L., Yan, R., Gould, W.D., Ng, Y.L., Liang, D.T., 2004. Isolation and characterization of sulphur-oxidizing Thiomonas sp. and its potential application in biological deodorization. Lett. Appl. Microbiol. 39, 495–503. https://doi.org/10.1111/j.1472-765X.2004.01615.x

Chung, Y.C., Huang, C., Li, C.F., 1997. Removal Characteristics of H 2 S by Thiobacillus novellas CH 3 Biofilter in Autotrophic and Mixotrophic Environments. J. Environ. Sci. Heal. - Part A Toxic/Hazardous Subst. Environ. Eng. 32, 1435–1450. https://doi.org/10.1080/10934529709376619

Chung, Y.C., Huang, C., Tseng, C.P., 1996. Operation optimization of Thiobacillus thioparus CH11 biofilter for hydrogen sulfide removal. J. Biotechnol. 52, 31–38. https://doi.org/10.1016/S0168-1656(96)01622-7

Ciminelli, V.S.T., Osseo-Asare, K., 1995. Kinetics of pyrite oxidation in sodium hydroxide solutions. Metall. Mater. Trans. B 26, 677–685. https://doi.org/10.1007/BF02651713

Cline, C., Hoksberg, A., Abry, R., Janssen, A., 2003. Biological Process for H2S Removal from Gas Streams, in: Laurance Reid Gas Conditioning Conference. pp. 1–17.

Coram, N.J.N., Rawlings, D.E., 2002. Molecular relationship between two groups of the genus Leptospirillum and the finding that … Appl. Environ. Microbiol. 68, 838–845. https://doi.org/10.1128/AEM.68.2.838

Das, S., Jean, J.S., Kar, S., Chakraborty, S., 2013. Effect of arsenic contamination on bacterial and fungal biomass and enzyme activities in tropical arsenic-contaminated soils. Biol. Fertil. Soils 49, 757–765. https://doi.org/10.1007/s00374-012-0769-z

De Graaff, M., Klok, J.B.M., Bijmans, M.F.M., Muyzer, G., Janssen, A.J.H., 2012. Application of a 2-step process for the biological treatment of sulfidic spent caustics. Water Res. 46, 723–730. https://doi.org/10.1016/j.watres.2011.11.044

Descostes, M., Beaucaire, C., Mercier, F., Savoye, S., Sow, J., Zuddas, P., 2002. Effect of carbonate ions on pyrite (FeS2) dissolution. Bull. la Société Géologique Fr. 173, 265–270. https://doi.org/10.2113/173.3.265

Donati, E.R., Sand, W., 2007. Microbial processing of metal sulfides, Microbial Processing of

Metal Sulfides. https://doi.org/10.1007/1-4020-5589-7

Dong, B., Jia, Y., Tan, Q., Sun, H., Ruan, R., 2020. Contributions of microbial “contact leaching” to pyrite oxidation under different controlled redox potentials. Minerals 10, 1–16. https://doi.org/10.3390/min10100856

DSMZ, 2009. 925. Alkaliphilic Sulphur Respiring Strains Medium.

Evangelou, V.P.B., Zhang, Y.L., 1995. A Review : Pyrite Oxidation Mechanisms and Acid Mine Drainage Prevention. Crit. Rev. Environ. Sci. Technol. 25, 141–199. https://doi.org/10.1080/10643389509388477

Ewart, D.K., Hughes, M.N., 1991. The extraction of metals from ores using bacteria. Adv. Inorg. Chem. 36, 103–135. https://doi.org/10.1016/S0898-8838(08)60038-0

Fernández, R.R., Sohn, H.Y., LeVier, K.M., 2000. Process for treating refractory gold ores by roasting under oxidizing conditions. Miner. Metall. Process. 17, 1–6. https://doi.org/10.1007/bf03402822

Foti, M., Ma, S., Sorokin, D.Y., Rademaker, J.L.W., Kuenen, J.G., Muyzer, G., 2006. Genetic diversity and biogeography of haloalkaliphilic sulphur-oxidizing bacteria belonging to the genus Thioalkalivibrio. FEMS Microbiol. Ecol. 56, 95–101. https://doi.org/10.1111/j.1574-6941.2006.00068.x

Garrels, R.M., Thompson, M.E., 1960. Oxidation of Pyrite by Iron Sulfate Solutions. Am. J. Sci. 258-A, 57–67.

Gehrke, T., Telegdi, J., Thierry, D., Sand, W., 1998. Importance of extracellular polymeric substances from Thiobacillus ferrooxidans for bioleaching. Appl. Environ. Microbiol. 64, 2743–2747. https://doi.org/10.1128/aem.64.7.2743-2747.1998

Gonzalez-Sanchez, A., Revah, S., 2009. Biological sulfide removal under alkaline and aerobic conditions in a packed recycling reactor. Water Sci. Technol. 7.

Gründling, A., 2013. Potassium uptake systems in Staphylococcus aureus: New stories about ancient systems 4. https://doi.org/10.1128/mBio.00784-13

Gupta, V.K., Saleh, T.A., 2013. Sorption of pollutants by porous carbon, carbon nanotubes and fullerene- An overview. Environ. Sci. Pollut. Res. 20, 2828–2843. https://doi.org/10.1007/s11356-013-1524-1

Haghshenas, D.F., Keshavarz Alamdari, E., Amouei Torkmahalleh, M., Bonakdarpour, B., Nasernejad, B., 2009. Adaptation of Acidithiobacillus ferrooxidans to high grade sphalerite concentrate. Miner. Eng. 22, 1299–1306. https://doi.org/10.1016/j.mineng.2009.07.011

Hansen, M., Perner, M., 2015. A novel hydrogen oxidizer amidst the sulfur-oxidizing Thiomicrospira lineage. ISME J. 9, 696–707. https://doi.org/10.1038/ismej.2014.173

Hoeft, S.E., Blum, J.S., Stolz, J.F., Tabita, F.R., Witte, B., King, G.M., Santini, J.M., Oremland, R.S., 2007. Alkalilimnicola ehrlichii sp. nov., a novel, arsenite-oxidizing haloalkaliphilic

gammaproteobacterium capable of chemoautotrophic or heterotrophic growth with nitrate or oxygen as the electron acceptor. Int. J. Syst. Evol. Microbiol. 57, 504–512. https://doi.org/10.1099/ijs.0.64576-0

Holm, T.R., Fisher, R.P., Frant, M.S., Gagnon, C., Goodwin, L.R., 2000. 4500-S 2. Stand. methods 170–183.

Horikoshi, K., 1999. Alkaliphiles: some applications of their products for biotechnology. Microbiol. Mol. Biol. Rev. 63, 735–50, table of contents.

Hossner, L.R., Doolittle, J.J., 2003. Iron Sulfide Oxidation as Influenced by Calcium Carbonate Application. J. Environ. Qual. 32, 773–780. https://doi.org/10.2134/jeq2003.7730

Huminicki, D.M.C., Rimstidt, J.D., 2009. Iron oxyhydroxide coating of pyrite for acid mine drainage control. Appl. Geochemistry 24, 1626–1634.

Ichhpujani, R., Bhatia, R., Ichhpujani, R., 2008. Nutrition and Growth of Bacteria, in: Essentials of Medical Microbiology. pp. 22–22. https://doi.org/10.5005/jp/books/10281_4

ICMI, 2014. Cyanide Chemistry. International Cyanide Management Code (ICMI) For The Manufacture, Transport and Use of Cyanide In The Production of Gold [WWW Document]. URL https://www.cyanidecode.org/cyanide-facts/cyanide-chemistry (accessed 4.4.20).

Imhoff, J.F., 2006. Rhodopseudomonas Czurda and Maresch 1937, 119AL emend. Imhoff, Trüper and Pfennig 1984, 341, in: Bergey's Manual of Systematic Bacteriology. Springer, pp. 473–476. https://doi.org/10.1007/0-387-29298-5_115

Imhoff, J.F., Hiraishi, A., Süling, J., 2015. Anoxygenic Phototrophic Purple Bacteria, in: Bergey's Manual of Systematics of Archaea and Bacteria. John Wiley & Sons, Ltd, Chichester, UK, pp. 1–23. https://doi.org/10.1002/9781118960608.bm00002

Janssen, A.J.H., De Keizer, A., Lettinga, G., 1994. Colloidal properties of a microbiologically produced sulphur suspension in comparison to a LaMer sulphur sol. Colloids Surfaces B Biointerfaces 3, 111–117. https://doi.org/10.1016/0927-7765(93)01122-8

Jha, M.C., 1987. Refractoriness of certain gold ores to cyanidation - Probable causes and possible solutions. Miner. Process. Extr. Metall. Rev. 2, 331–352.

Kalantari, H., Nosrati, M., Shojaosadati, S.A., Shavandi, M., 2018. Investigation of transient forms of sulfur during biological treatment of spent caustic. Environ. Technol. (United Kingdom) 39, 1597–1606. https://doi.org/10.1080/09593330.2017.1334707

Kapoor, A., Viraraghavan, T., 1997. Nitrate Removal From Drinking Water—Review. J. Environ. Eng. 123, 371–380. https://doi.org/10.1061/(ASCE)0733-9372(1997)123:4(371)

Kelly, D.P., Uchino, Y., Huber, H., Amils, R., Wood, A.P., 2007. Reassessment of the phylogenetic relationships of Thiomonas cuprina. Int. J. Syst. Evol. Microbiol. 57, 2720–2724. https://doi.org/10.1099/ijs.0.65537-0

Kelly, D.P., Wood, A.P., 2000. Reclassification of some species of Thiobacillus to the newly

designated genera Acidithiobacillus gen. nov., Halothiobacillus gen. nov. and Thermithiobacillus gen. nov. Int. J. Syst. Evol. Microbiol. 50, 511–516. https://doi.org/10.1099/00207713-50-2-511

Kilbane, J.J., 2017. Biodesulfurization: How to Make it Work? Arab. J. Sci. Eng. https://doi.org/10.1007/s13369-016-2269-1

King, W.E., Lewis, J.A., 1980. Simultaneous Effects of Oxygen and Ferric Iron on Pyrite Oxidation in an Aqueous Slurry. Ind. Eng. Chem. Process Des. Dev. 19, 719–722. https://doi.org/10.1021/I260076A037

Kiragosyan, K., van Veelen, P., Gupta, S., Tomaszewska-Porada, A., Roman, P., Timmers, P.H.A., 2019. Development of quantitative PCR for the detection of Alkalilimnicola ehrlichii, Thioalkalivibrio sulfidiphilus and Thioalkalibacter halophilus in gas biodesulfurization processes. AMB Express 9. https://doi.org/10.1186/s13568-019-0826-1

Kumar, R., Dwivedi, V., Nayyar, N., Verma, H., Singh, A.K., Rani, P., Rao, D.L.N., Lal, R., 2015. Parapedobacter indicus sp. nov., isolated from hexachlorocyclohexane-contaminated soil. Int. J. Syst. Evol. Microbiol. 65, 129–134. https://doi.org/10.1099/ijs.0.069104-0

Kushner, D.J., Kamekura, M., 1988. Physiology of halophilic eubacteria. Halophilic Bact. 109–138.

Landis, T.D., Steenis, E. van, 2004. Macronutrients - Phosphorus 1–14.

Larsen, H., 1986. Halophilic and halotolerant microorganisms-an overview and historical perspective. FEMS Microbiol. Lett. 39, 3–7. https://doi.org/10.1111/j.1574-6968.1986.tb01835.x

Li, J., Dabrowski, B., Miller, J.D., Acar, S., Dietrich, M., LeVier, K.M., Wan, R.Y., 2006. The influence of pyrite pre-oxidation on gold recovery by cyanidation. Miner. Eng. 19, 883–895. https://doi.org/10.1016/j.mineng.2005.09.052

Liu, S.W., Xue, C.M., Li, F.N., Sun, C.H., 2020. Nocardioides vastitatis sp. Nov., isolated from Taklamakan desert soil. Int. J. Syst. Evol. Microbiol. 70, 77–82. https://doi.org/10.1099/ijsem.0.003718

Luther, G.W., 1987. Pyrite oxidation and reduction: Molecular orbital theory considerations. Geochim. Cosmochim. Acta 51, 3193–3199. https://doi.org/10.1016/0016-7037(87)90127-X

Luther, G.W., Kostka, J.E., Church, T.M., Sulzberger, B., Stumm, W., 1992. Seasonal iron cycling in the salt-marsh sedimentary environment: the importance of ligand complexes with Fe(II) and Fe(III) in the dissolution of Fe(III) minerals and pyrite, respectively. Mar. Chem. 40, 81–103. https://doi.org/10.1016/0304-4203(92)90049-G

Mahmoud, A., Cézac, P., Hoadley, A.F.A., Contamine, F., D'Hugues, P., 2017. A review of sulfide minerals microbially assisted leaching in stirred tank reactors. Int. Biodeterior. Biodegrad. 119, 118–146. https://doi.org/10.1016/j.ibiod.2016.09.015

McKibben, M.A., Barnes, H.L., 1986. Oxidation of pyrite in low temperature acidic solutions: Rate laws and surface textures. Geochim. Cosmochim. Acta 50, 1509–1520. https://doi.org/10.1016/0016-7037(86)90325-X

Melashvili, M., Fleming, C., Dymov, I., Matthews, D., Dreisinger, D., 2016. Dissolution of gold during pyrite oxidation reaction. Miner. Eng. 87, 2–9. https://doi.org/10.1016/j.mineng.2015.07.017

Millano, E.F., Sorber, C.A., 1986. Treatment of Thiosulfate-Containing Wastewater in Activated Sludge Systems. Water Pollut. Control Fed. 58, 917–923.

Mishra, K.K., Osseo-Asare, K., 1988. Aspects of the Interfacial Electrochemistry of Semiconductor Pyrite (FeS2) . J. Electrochem. Soc. 135, 2502–2509. https://doi.org/10.1149/1.2095366

Mohsenipour, M., Shahid, S., Ebrahimi, K., 2014. Removal techniques of nitrate from water. Asian J. Chem. https://doi.org/10.14233/ajchem.2014.17136

Moreira, D., Amils, R., 1997. Phylogeny of Thiobacillus cuprinus and other mixotrophic thiobacilli: Proposal for Thiomonas gen. nov. Int. J. Syst. Bacteriol. 47, 522–528. https://doi.org/10.1099/00207713-47-2-522

Moses, C.O., Herman, J.S., 1991. Pyrite oxidation at circumneutral pH. Geochim. Cosmochim. Acta 55, 471–482. https://doi.org/10.1016/0016-7037(91)90005-P

Moses, C.O., Kirk Nordstrom, D., Herman, J.S., Mills, A.L., 1987. Aqueous pyrite oxidation by dissolved oxygen and by ferric iron. Geochim. Cosmochim. Acta 51, 1561–1571. https://doi.org/10.1016/0016-7037(87)90337-1

Mubarok, M.Z., Winarko, R., Chaerun, S.K., Rizki, I.N., Ichlas, Z.T., 2017. Improving gold recovery from refractory gold ores through biooxidation using iron-sulfur-oxidizing/sulfur-oxidizing mixotrophic bacteria. Hydrometallurgy 168, 69–75. https://doi.org/10.1016/j.hydromet.2016.10.018

Myung Cha, J., Suk Cha, W., Lee, J.H., 1999. Removal of organo-sulphur odour compounds by Thiobacillus novellus SRM, sulphur-oxidizing microorganisms. Process Biochem. 34, 659–665. https://doi.org/10.1016/S0032-9592(98)00139-3

Nagadomi, H., Kitamura, T., Watanabe, M., Sasaki, K., 2000. Simultaneous removal of chemical oxygen demand (COD), phosphate, nitrate and H2S in the synthetic sewage wastewater using porous ceramic immobilized photosynthetic bacteria. Biotechnol. Lett. 22, 1369–1374. https://doi.org/10.1023/A:1005688229783

Nan, X.Y., Cai, X., Kong, J., 2014. Pretreatment process on refractory gold ores with as. ISIJ Int. 54, 543–547. https://doi.org/10.2355/isijinternational.54.543

NATCO Group, 1999. Environmental Technology Verification Report.

Ndlovu, S., 2008. Biohydrometallurgy for sustainable development in the African minerals industry. Hydrometallurgy 91, 20–27. https://doi.org/10.1016/j.hydromet.2007.11.007

Ofori-Sarpong, G., Tien, M., Osseo-Asare, K., 2010. Myco-hydrometallurgy: Coal model for potential reduction of preg-robbing capacity of carbonaceous gold ores using the fungus, Phanerochaete chrysosporium. Hydrometallurgy 102, 66–72. https://doi.org/10.1016/j.hydromet.2010.02.007

Oren, A., 2009. Chemolithotrophy, in: Encyclopedia of Life Sciences. John Wiley & Sons, Ltd. https://doi.org/10.1002/9780470015902.a0021153

Oyarzún, P., Arancibia, F., Canales, C., Aroca, G.E., 2003. Biofiltration of high concentration of hydrogen sulphide using Thiobacillus thioparus. Process Biochem. 39, 165–170. https://doi.org/10.1016/S0032-9592(03)00050-5

Özkaya, B., Nurmi, P., Sahinkaya, E., Kaksonen, A.H., Puhakka, J.A., 2007. Temperature Effects on the Iron Oxidation Kinetics of a Leptospirillum ferriphilum Dominated Culture at pH Below One. Adv. Mater. Res. 20–21, 465–468.

Padan, E., Bibi, E., Ito, M., Krulwich, T.A., 2005. Alkaline pH homeostasis in bacteria: New insights. Biochim. Biophys. Acta - Biomembr. https://doi.org/10.1016/j.bbamem.2005.09.010

Paques, 2014. Thiopaq [WWW Document]. URL https://en.paques.nl/products/featured/thiopaq (accessed 6.4.20).

Pathak, A., Kim, D., Kim, B., Sample, A., 2014. Effect of Pulp Density on Biodesulfurization of Mongolian Lignite Coal. Int. J. Environ. Ecol. Eng. 8, 618–621.

Pirieh, P., Naeimpoor, F., 2019. Discrimination of chemical and biological sulfide oxidation in a hybrid two-phase process. J. Environ. Chem. Eng. 7, 103027. https://doi.org/10.1016/j.jece.2019.103027

Podol'skaya, V.I., Gruzina, T.G., Ul'berg, Z.R., Sokolovskaya, A.S., Grishchenko, N.I., 2002. Effect of arsenic on bacterial growth and plasma membrane ATPase activity. Appl. Biochem. Microbiol. 38, 48–52. https://doi.org/10.1023/A:1013200605146

Poulain, A.J., Newman, D.K., 2009. Rhodobacter capsulatus catalyzes light-dependent Fe(II) oxidation under anaerobic conditions as a potential detoxification mechanism. Appl. Environ. Microbiol. 75, 6639–6646. https://doi.org/10.1128/AEM.00054-09

Purnomo, I., Chaerun, S.K., Mubarok, M.Z., 2019. Biooxidation pretreatment of low grade refractory gold tailings using a sulfur-oxidizing mixotrophic bacterium, in: IOP Conference Series: Materials Science and Engineering. https://doi.org/10.1088/1757-899X/478/1/012020

Raven, P., 2005. Biology. Twayne Publishers, Boston.

Rawlings, D.E., 2002. Heavy Metal Mining Using Microbes. Annu. Rev. Microbiol. 56, 65–91. https://doi.org/10.1146/annurev.micro.56.012302.161052

Rawlings, D.E., Johnson, D.B., 2007. Biomining. Springer-Verlag Berlin Heidelberg. https://doi.org/10.1007/978-3-540-34911-2_6

Reginald, G.H., Grisham, C., 2008. Biochemistry, Fourth. ed. Twayne Publishers, Boston.

Reimers, G.W., Franke, D.F., 1991. Effect of Additives on Pyrite Oxidation. https://doi.org/10.1021/bk-1994-0550.ch003

Rohwerder, T., Gehrke, T., Kinzler, K., Sand, W., 2003. Progress in bioleaching: Fundamentals and mechanisms of bacterial metal sulfide oxidation-part A. Appl. Microbiol. Biotechnol. 63, 239–248. https://doi.org/10.1007/s00253-003-1448-7

Sand, W., Gehrke, T., 2006. Extracellular polymeric substances mediate bioleaching/biocorrosion via interfacial processes involving iron(III) ions and acidophilic bacteria, in: Research in Microbiology. pp. 49–56. https://doi.org/10.1016/j.resmic.2005.07.012

Sand, W., Gehrke, T., Jozsa, P.G., Schippers, A., 2001. Biochemistry of bacterial leaching - direct vs. indirect bioleaching. Hydrometallurgy 59, 159–175. https://doi.org/10.1016/S0304-386X(00)00180-8

Schippers, A., 2004. Biogeochemistry of metal sulfide oxidation in mining environments, sediments, and soils.

Schippers, A., Hedrich, S., Vasters, J., Drobe, M., Sand, W., Willscher, S., 2014. Biomining: metal recovery from ores with microorganisms. Adv. Biochem. Eng. Biotechnol. https://doi.org/10.1007/10_2013_216

Schippers, A., Sand, W., 1999. Bacterial leaching of metal sulfides proceeds by two indirect mechanisms via thiosulfate or via polysulfides and sulfur. Appl. Environ. Microbiol. 65, 319–321. https://doi.org/10.1128/aem.65.1.319-321.1999

Schlumberger, 2016. THIOPAQ Biodesulfurization Process.

Schoonen, M., Elsetinow, A., Borda, M., Strongin, D., 2000. Effect of temperature and illumination on pyrite oxidation between pH 2 and 6. Geochem. Trans. 1. https://doi.org/10.1186/1467-4866-1-23

Senanayake, G., 2005. Role of copper(II), carbonate and sulphite in gold leaching and thiosulphate degradation by oxygenated alkaline non-ammoniacal solutions. Miner. Eng. 18, 409–426. https://doi.org/10.1016/j.mineng.2004.08.001

Singer, P.C., Stumm, W., 1970. Acidic mine drainage: The rate-determining step. Science (80-.). 167, 1121–1123. https://doi.org/10.1126/science.167.3921.1121

Sohrabi, M., Kamyab, H., Janalizadeh, N., Huyop, F.Z., 2012. Bacterial Desulfurization of Organic Sulfur Compounds Exist in Fossil Fuels. Pure Appl. Microbiol. 6, 717–729.

Sorokin, D.Y., Banciu, H., Robertson, L.A., Kuenen, J.G., 2006. Haloalkaliphilic Sulfur-Oxidizing Bacteria. The Prokaryotes 969–984. https://doi.org/10.1007/0-387-30742-7_30

Sorokin, D.Y., Gorlenko, V.M., Tourova, T.P., Tsapin, A.I., Nealson, K.H., Kuenen, G.J., 2002. Thioalkalimicrobium cyclicum sp. nov. and Thioalkalivibrio jannaschii sp. nov., novel

species of haloalkaliphilic, obligately chemolithoautotrophic sulfur-oxidizing bacteria from hypersaline alkaline Mono Lake (California). Int. J. Syst. Evol. Microbiol. 52, 913–920.

Sorokin, D.Y., Kuenen, J.G., Muyzer, G., 2011. The microbial sulfur cycle at extremely haloalkaline conditions of soda lakes. Front. Microbiol. 2. https://doi.org/10.3389/fmicb.2011.00044

Sorokin, D.Y., Lysenko, A.M., Mityushina, L., Tourova, T.P., Jones, B.E., Rainey, F.A., Robertson, L.A., Kuenen, G.J., 2001. Thioalkalimicrobium aerophilum gen. nov., sp. nov. and Thioalkalimicrobium sibericum sp. nov., and Thioalkalivibrio versutus gen. nov., sp. nov., Thioalkalivibrio nitratis sp. nov. and Thioalkalivibrio denitrificans sp. nov., novel obligately alkaliphilic, International Journal of Systematic and Evolutionary Microbiology.

Sorokin, D.Y., Muntyan, M.S., Panteleeva, A.N., Muyzer, G., 2012. Thioalkalivibrio sulfidiphilus sp. nov., a haloalkaliphilic, sulfur-oxidizing gammaproteobacterium from alkaline habitats. Int. J. Syst. Evol. Microbiol. 62, 1884–1889. https://doi.org/10.1099/ijs.0.034504-0

Sorokin, D.Y., Robertson, L.A., Kuenen, J.G., 2000. Isolation and characterization of alkaliphilic, chemolithoautotrophic, sulphur-oxidizing bacteria, Antonie van Leeuwenhoek.

Sorokin, D.Y., Van Den Bosch, P.L.F., Abbas, B., Janssen, A.J.H., Muyzer, G., 2008. Microbiological analysis of the population of extremely haloalkaliphilic sulfur-oxidizing bacteria dominating in lab-scale sulfide-removing bioreactors. Appl. Microbiol. Biotechnol. 80, 965–975. https://doi.org/10.1007/s00253-008-1598-8

Srinivas, T.N.R., Anil Kumar, P., Sasikala, C., Ramana, C. V., Imhoff, J.F., 2007. Rhodobacter vinaykumarii sp. nov., a marine phototrophic alphaproteobacterium from tidal waters, and emended description of the genus Rhodobacter. Int. J. Syst. Evol. Microbiol. 57, 1984–1987. https://doi.org/10.1099/ijs.0.65077-0

Takaichi, S., Maoka, T., Akimoto, N., Sorokin, D.Y., Banciu, H., Kuenen, J.G., 2004. Two novel yellow pigments natronochrome and chloronatronochrome from the natrono(alkali)philic sulfur-oxidizing bacterium Thialkalivibrio versutus strain ALJ 15. Tetrahedron Lett. 45, 8303–8305. https://doi.org/10.1016/j.tetlet.2004.09.073

Tributsch, H., 2001. Direct versus indirect bioleaching. Hydrometallurgy 59, 177–185. https://doi.org/10.1016/S0304-386X(00)00181-X

U.S. National Library of Medicine, 2107. Sulfur Dioxide [WWW Document]. URL https://toxtown.nlm.nih.gov/chemicals-and-contaminants/sulfur-dioxide (accessed 4.16.20).

Vainshtein, M.B., Gogotova, G.I., Heinritz, N.J., 1994. Removal of H2S by the purple sulphur bacterium Ectothiorhodospira shaposhnikovii. World J. Microbiol. Biotechnol. 10, 110–111. https://doi.org/10.1007/BF00357574

Van Den Bosch, P.L.F., Van Beusekom, O.C., Buisman, C.J.N., Janssen, A.J.H., 2007. Sulfide oxidation at halo-alkaline conditions in a fed-batch bioreactor. Biotechnol. Bioeng. 97, 1053–1063. https://doi.org/10.1002/bit.21326

Venkata Ramana, V., Chakravarthy, S., Raj, P., Kumar, B., Shobha, E., Ramaprasad, E.V.V., Sasikala, C., Ramana, C. V., 2012. Descriptions of rhodopseudomonas parapalustris sp. nov., rhodopseudomonas harwoodiae sp. nov. and rhodopseudomonas pseudopalustris sp. nov., and emended description of rhodopseudomonas palustris. Int. J. Syst. Evol. Microbiol. 62, 1790–1798. https://doi.org/10.1099/ijs.0.026815-0

Vera, M., Schippers, A., Sand, W., 2013a. Progress in bioleaching: Fundamentals and mechanisms of bacterial metal sulfide oxidation-part A. Appl. Microbiol. Biotechnol. https://doi.org/10.1007/s00253-013-4954-2

Vera, M., Schippers, A., Sand, W., 2013b. Progress in bioleaching: Fundamentals and mechanisms of bacterial metal sulfide oxidation-part A. Appl. Microbiol. Biotechnol. https://doi.org/10.1007/s00253-013-4954-2

Verron, H., Sterpenich, J., Bonnet, J., Mosser-Ruck, R., Bourdelle, F., Lorgeo, C., Randi, A., Michau, N., 2019. Experimental study of pyrite oxidation at 100 °c: implications for deep geological radwaste repository in claystone. Minerals 9. https://doi.org/10.3390/MIN9070427

Vikromvarasiri, N., Champreda, V., Boonyawanich, S., Pisutpaisal, N., 2017. Hydrogen sulfide removal from biogas by biotrickling filter inoculated with Halothiobacillus neapolitanus. Int. J. Hydrogen Energy 42, 18425–18433. https://doi.org/10.1016/j.ijhydene.2017.05.020

Vikromvarasiri, N., Pisutpaisal, N., 2016. Hydrogen sulfide removal in biotrickling filter system by Halothiobacillus neapolitanus. Int. J. Hydrogen Energy 41, 15682–15687. https://doi.org/10.1016/j.ijhydene.2016.04.180

Vlasceanu, L., Popa, R., Kinkle, B.K., 1997. Characterization of Thiobacillus thioparus LV43 and Its Distribution in a Chemoautotrophically Based Groundwater Ecosystem, APPLIED AND ENVIRONMENTAL MICROBIOLOGY.

Wagnar, S.C., 2011. Biological Nitrogen Fixation [WWW Document]. URL https://www.nature.com/scitable/knowledge/library/biological-nitrogen-fixation-23570419/ (accessed 4.19.20).

Wang, H., Dowd, P.A., Xu, C., 2019. A reaction rate model for pyrite oxidation considering the influence of water content and temperature. Miner. Eng. 134, 345–355. https://doi.org/10.1016/j.mineng.2019.02.002

Wang, L., Fan, D., Chen, W., Terentjev, E.M., 2015. Bacterial growth, detachment and cell size control on polyethylene terephthalate surfaces. Sci. Rep. 5. https://doi.org/10.1038/SREP15159

Wang, Y., Zeng, W., Qiu, G., Chen, X., Zhou, H., 2014. A Moderately Thermophilic Mixed Microbial Culture for Bioleaching of Chalcopyrite Concentrate at High Pulp Density. Appl. Environ. Microbiol. 80, 741–750. https://doi.org/10.1128/AEM.02907-13

Wei, D., Osseo-Asare, K., 1997. Semiconductor Electrochemistry of Particulate Pyrite: Mechanisms and Products of Dissolution. J. Electrochem. Soc. 144, 546–553. https://doi.org/10.1149/1.1837446

Willey, J., Sherwood, L., Woolverton, C.J., 2016. Prescott's Microbiology. McGraw-Hill Education.

Wood, A.P., Kelly, D.P., 1985. Physiological characteristics of a new thermophilic obligately chemolithotrophic Thiobacillus species, Thiobacillus tepidarius. Int. J. Syst. Bacteriol. 35, 434–437. https://doi.org/10.1099/00207713-35-4-434

Wu, H., Feng, Y., Li, Haoran, Li, Hailong, Ju, J., 2021. Effect of sodium carbonate on alkaline self-leaching of gold from flotation gold ore. Sep. Purif. Technol. 256, 117499. https://doi.org/10.1016/j.seppur.2020.117499

Xia, L., Liu, X., Zeng, J., Yin, C., Gao, J., Liu, J., Qiu, G., 2008. Mechanism of enhanced bioleaching efficiency of Acidithiobacillus ferrooxidans after adaptation with chalcopyrite. https://doi.org/10.1016/j.hydromet.2008.01.002

Yang, H., Gao, K., Feng, S., Zhang, L., Wang, W., 2015. Isolation of sulfide remover strain Thermithiobacillus tepidarius JNU-2, and scale-up bioreaction for sulfur regeneration. Ann. Microbiol. 65, 553–563. https://doi.org/10.1007/s13213-014-0891-2

Yoon, J.-H., Park, Y.-H., 2006. The Genus Nocardioides, in: The Prokaryotes. pp. 1099–1113. https://doi.org/10.1007/0-387-30743-5_44

Yoon, J.H., Cho, Y.G., Lee Taik, S., Suzuki, K.I., Nakase, T., Park, Y.H., 1999. Nocardioides nitrophenolicus sp. nov., a p-nitrophenol-degrading bacterium. Int. J. Syst. Bacteriol. 49, 675–680. https://doi.org/10.1099/00207713-49-2-675

Zhao, X., Li, X., Qi, N., Fu, Z., Chen, M., Jiang, B., Hu, X., 2018. Enhancement of COD, ammonia, phosphate and sulfide simultaneous removal by the anaerobic photosynthetic bacterium of Ectothiorhodospira magna in batch and sequencing batch culture. Water Sci. Technol. 78.